TENMAK BOREN BOR ARAŞTIRMA ENSTİTÜSÜ
TENMAK BOREN BORON RESEARCH INSTITUTE

ISSN: 2149-9020
e-ISSN: 2667-8438

BOR DERGİSİ
JOURNAL OF BORON

CİLT/VOL 09 SAYI/ISSUE 04 YIL/YEAR 2024

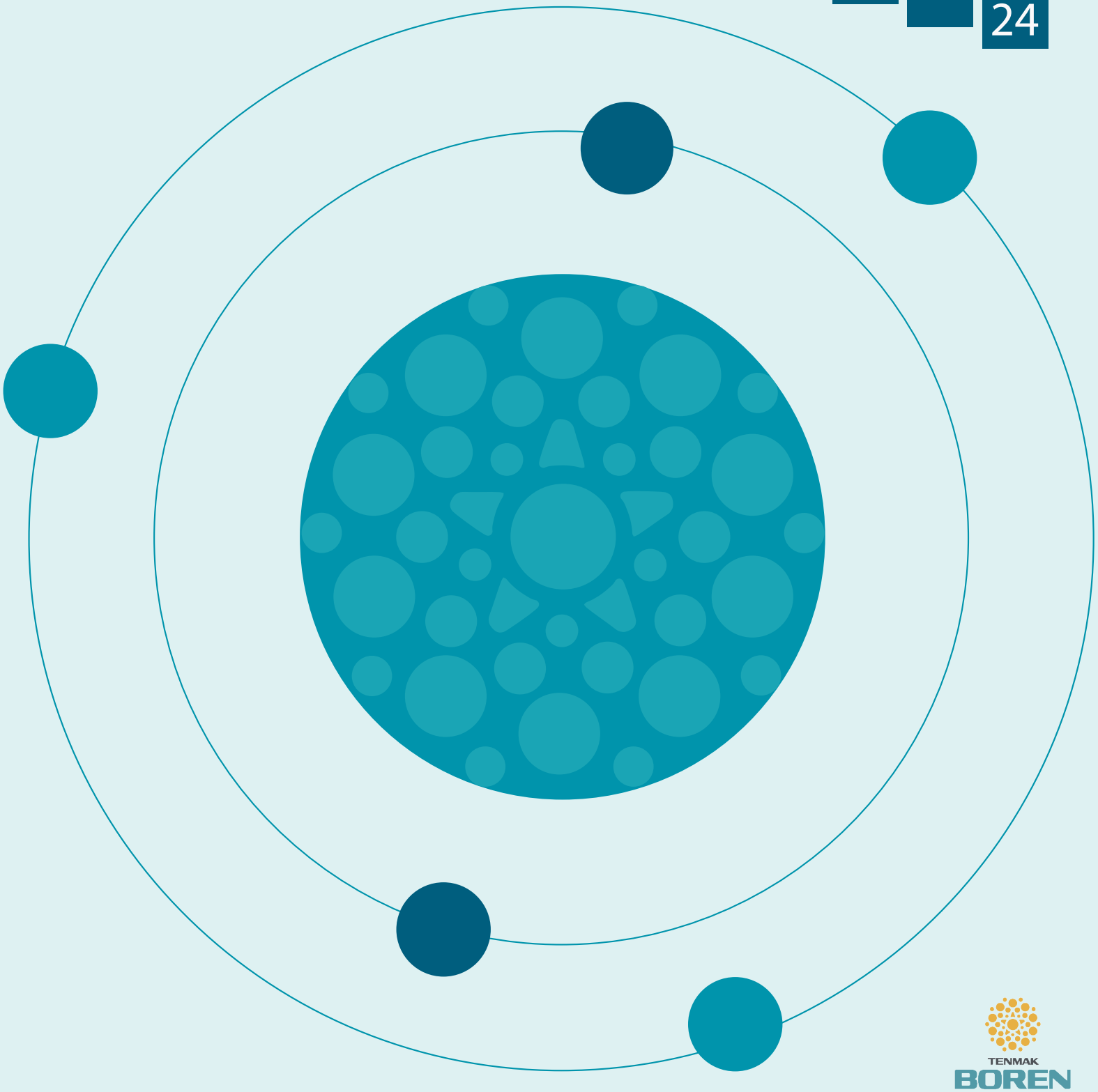

TENMAK BOREN

ISSN: 2149-9020
e-ISSN: 2667-8438

BOR DERGİSİ

JOURNAL OF BORON

CİLT VOL **09** **SAYI** ISSUE **04** **YIL** YEAR **2024**

Yayıncı/Publisher
TENMAK BOREN Bor Araştırma Enstitüsü

Yayın İdare Adresi/Adress of Publication Manager
Dumlupınar Bulvarı (Eskişehir Yolu 7. km), No:166, D Blok,
Ankara, 06530, Türkiye
Tel: (0312) 201 36 00
Fax: (0312) 219 80 55
E-posta: journalofboron@tenmak.gov.tr
Web: https://dergipark.org.tr/tr/pub/boron

Yayın Türü/Type of Publication: Yaygın süreli yayın
Yayın Aralığı/Range of Publication: 3 Aylık
Yayın Tarihi/Publication Date: 31/12/2024

ANKARA
ARALIK 2024 / DECEMBER 2024

TENMAK BOREN BOR ARAŞTIRMA ENSTİTÜSÜ

BOR DERGİSİ

JOURNAL OF BORON

https://dergipark.org.tr/boron

İÇİNDEKİLER/CONTENTS

BOR DERGİSİ
JOURNAL OF BORON
https://dergipark.org.tr/boron

Sürekli akış koşullarında sulu çözeltilerden bor giderimi için elektrokimyasal ayırma prosesi tasarlanması ve işletilmesi

Sevgi Polat [1,*]

[1]*Marmara Üniversitesi, Kimya Mühendisliği Bölümü, İstanbul 34854, Türkiye*

MAKALE BİLGİSİ

Makale Geçmişi:
İlk gönderi 29 Temmuz 2024
Kabul 30 Eylül 2024
Online 31 Aralık 2024

Araştırma Makalesi

DOI: 10.30728/boron.1524438

Anahtar kelimeler:
Akış hücresi tasarımı
Bor giderimi
Elektrokimyasal ayırma prosesi
Sürdürülebilirlik

ÖZET

Ülkemiz açısından stratejik öneme sahip olan bor minerali, uzay teknolojisinden savunma endüstrisine, cam sektöründen tekstil endüstrisine pek çok alanda yaygın olarak kullanılmaktadır. Doğada genel olarak borik asit ve borat iyonu olarak bulunan bor, yüzey ve yeraltı sularına karışarak kirlenmeye yol açabilmekte ve çevre kirliliğine sebep olmaktadır. Su kaynaklarının kısıtlı olması ve yakın gelecekte dünya nüfusunun su sıkıntısı yaşama olasılığının yüksek olduğu göz önüne alındığında, su arıtımında geleneksel yöntemlerin yanı sıra bor ve borat iyonu gibi kirleticilerin sularda bulunan diğer iyonlar arasından uzaklaştırılmasını sağlayan etkili ve yenilikçi teknolojilerin geliştirilmesi gerekmektedir. Bu çalışmada, sulu çözeltilerde bulunan borat iyonlarının elektrokimyasal ayırma yöntemi kullanılarak sürekli akış koşullarında ayrılması ve geri kazanımı incelenmiştir. Bu kapsamda, öncelikle aktif karbon ile kaplı elektrotlar hazırlanmış, elektrokimyasal ve morfolojik açıdan karakterizasyonu yapılmıştır. Daha sonra sürekli akış koşullarında bor iyon gideriminin yapılabilmesi için akış hücresi tasarlanmış ve elektrokimyasal ayırma prosesine entegrasyonu sağlanmıştır. +1,0/-1,0 V adsorpsiyon ve desorpsiyon koşullarında sistem en az 5 döngü olacak şekilde çalıştırılmış ve bor iyonu giderim verimi %90,3 olarak belirlenmiştir. Ayrıca, bu çalışmada farklı voltaj değerlerinde çalışılmış ve uygulanan potansiyel değerinin 0,75'ten 1,5 V'a artırılmasıyla tutunan bor iyonu miktarını 11,5 mg/g'dan 25,7 mg/g'a çıktığı tespit edilmiştir.

Design and operation of an electrochemical separation process for boron removal from aqueous solutions under continuous flow conditions

ARTICLE INFO

Article History:
Received July 29, 2024
Accepted September 30, 2024
Available online December 31, 2024

Research Article

DOI: 10.30728/boron.1524438

Keywords:
Cell design
Boron removal
Electrochemical separation process
Sustainability

ABSTRACT

Boron mineral which has strategic importance for Türkiye, is widely used in many fields from space technology to the defense industry, from the glass industry to the textile industry. Boron, which is generally found in nature as boric acid and borate ion, can cause pollution by mixing with surface and groundwater and cause environmental pollution. Considering the dwindling sources of water and the possibility of the world population experiencing water scarcity in the near future, effective and innovative technologies need to be developed to separate and to remove pollutants such as boron ions from other ions in the water stream as well as the conventional water treatment process. In this study, the removal and recovery of borate ions in aqueous solutions using the electrochemical separation technique under continuous flow conditions were investigated. In this context, firstly, electrodes coated with activated carbon were prepared and their electrochemical and morphological characterization was performed. Then, a flow cell was designed to perform boron ion removal under continuous flow conditions and its integration into the electrochemical separation system was provided. The system was operated for at least 5 cycles under +1.0/-1.0 V adsorption and desorption conditions and the boron ion removal efficiency was determined as 90.3%. In addition, different voltage values were studied in this study and it was determined that the amount of adsorbed boron ion increased from 11.5 mg/g to 25.7 mg/g by increasing the applied potential value from 0.75 to 1.5 V.

1. Giriş (Introduction)

Bor madeni, Türkiye için ekonomik değeri ve stratejik önemi çok büyük olan bir madendir. Ülkemiz Dünya toplam bor rezervinde yaklaşık olarak %73'lük bir paya sahiptir [1,2]. Günümüzde bor cevherleri ve türevleri, günlük yaşantının ve sanayinin her alanına girmiş olup ticari olarak çok geniş ve çeşitli alanlarda kullanılmaktadır. Kimya sanayinde en çok yararlanılan ara kimyasal maddelerden biri olarak kullanılmasının

*Corresponding author: sevgi.polat@marmara.edu.tr

yanı sıra, uzay teknolojisinden, bilişim sektörüne, nükleer teknolojiden savaş sanayine kadar pek çok alanda kullanılmaktadır. Ayrıca, cam ve seramik sanayi, temizleme ve beyazlatma endüstrisi, gübre, metalürji ve tekstil endüstrileri de borun yaygın olarak kullanıldığı başlıca sektörlerdir [3-5]. Bor doğada genel olarak borik asit ve borat iyonu olarak bulunur. Borik asit veya borat tuzları suda kolay çözündükleri için yüzey ve yeraltı sularına karışarak kirlenmeye yol açabilmekte ve atık olarak çevreye verildiklerinde yeraltı sularında birikerek toksik etki göstermektedirler. Bu nedenle, belirli konsantrasyon değerlerinin üzerinde çevresel olarak risk oluştururlar [6,7]. Örneğin, Dünya Sağlık Örgütü içme suları için bor limitini maksimum 2,4 mg/L olarak belirlemişken, bu değer Avrupa Birliği Mevzuatı'na göre 1 mg/L'dir [8]. Daha yüksek bor konsantrasyonu kardiyovasküler, koroner, sinir ve üreme sistemlerinde hasara sebep olmaktadır [5,8,9]. Türk Çevre Mevzuatı'na göre denize deşarj edilecek sudaki bor miktarının 500 mg/L'i geçmemesi gerekmektedir [10]. Ayrıca, kullanım alanına bağlı olarak bor konsantrasyonun belirli değerlerde olması gerektiği bilinmektedir. Örneğin, yarı iletken endüstrisinde, özellikle çip üretimi için yüksek miktarlarda saf su kullanılmakta olup, bu suyun içerdiği bor miktarının da (çiplerin yüzeylerinde kontaminasyon oluşmasını engellemek için) µg/L düzeyinde olması gerekmektedir [11]. Diğer bir kullanım alanı incelendiğinde ise bitkilerin sulama sularında bor konsantrasyonunun 1 mg/L'den yüksek olmamalıdır [12]. Özetle, belirli ve düşük konsantrasyonlarda borun ortamda bulunması insan ve çevre sağlığı açısından olumlu etkiler yaratsa da yüksek miktarlarda bulunması ciddi sorunlara neden olmaktadır. Ayrıca, su ihtiyacının artışı buna karşın su kaynaklarının giderek azalması ve kullanılabilir su kaynaklarının kirletilmeye devam edilmesinden dolayı dünya genelinde yaşanan su sıkıntısı günümüzde üzerinde durulması gereken önemli bir sorun haline gelmiştir. Özellikle su sistemlerinde kirleticilerin varlığı hem insan sağlığını olumsuz yönde etkilemekte hem de suda yaşayan canlı türleri ve ekosistem dengesi için ciddi sorunlar yaratarak suyun kullanılamaz hale gelmesine sebep olmaktadır [13,14]. Bu kapsamda, sulardaki bor kirliliği oldukça önemli bir çevre problemi haline gelmektedir. Bu nedenle, su sistemlerinde çözünmüş halde bulunan bor iyon derişiminin çevre açısından tehlike oluşturmayacak değerlere düşürülmesi ve geri kazanımın sağlanması gerekmektedir. Bor giderimi ile ilgili literatürde koagülasyon ve sedimentasyon [15], adsorpsiyon [16,17], evaporasyon, ekstraksiyon [18], kristalizasyon [19], iyon değiştirme [20], membran prosesleri [21-24] ve elektrokoagülasyon [25,26] gibi farklı arıtım yöntemleri kullanılan birçok sayıda çalışma mevcuttur. Bu yöntemlerden bazıları bor giderimi alanında başarılı sonuçlar vermekte ve günümüzde halen sıklıkla kullanılmalarına rağmen, adsorbentlerin rejenerasyon süreçlerindeki zorluk ve maliyet, iyon değiştirici reçine ihtiyaçları, membran maliyetlerinin pahalı olması, sürekli bakım gerektirmeleri gibi nedenlerle çeşitli dezavantajlara da sahip olabilmektedirler [15-26]. Bu nedenle, alternatif ve yenilikçi proseslerin geliştirilmesine ihtiyaç duyulmaktadır. Sulu çözeltilerden bor iyonlarının ekonomik ve yüksek verimle ayrılması/geri kazanımındaki gelişmeler hem ekonomik fayda açısından hem de insan sağlığı ve çevre açısından oldukça önemlidir [27]. Borun yüksek verimle ayrılması işlemi hızlı dönüşüm, elektriksel potansiyel ile kontrol ve tekrar kullanılabilirlik sağlaması açısından elektrokimyasal ayırma yöntemiyle yapılabilir. Ayrıca, elektrokimyasal ayırma işlemi rejenerasyon prosesi sırasında ilave kimyasallara ihtiyaç duyulmaması nedeniyle su ekonomisi ve atık sürdürülebilirliği açısından diğer yöntemlerle kıyaslandığında son derece avantajlıdır [28-31]. Elektrokimyasal ayırma kapsamında bulunan kapasitif deiyonizasyon (KDI) teknolojisi, düşük basınç gerektiren kapasitörlerin kullanılması ile iyonların ayrılması esası üzerine çalışan önemli bir prosestir [32,33]. KDI prosesi, düşük elektrik potansiyelinin aralarında su akışı olan iki paralel elektrot plakasına uygulanması sonucu suda bulunan iyonların zıt yüklü elektrotların yüzeyinde oluşan elektrik çift tabakanın içine adsorbe olması prensibiyle çalışmaktadır. Bu prosesin en önemli avantajı oldukça düşük enerji tüketimidir [34]. Bu kapsamda bu çalışmada, ülkemiz açısından stratejik öneme sahip borun sürekli akış koşullarında tasarlanan akış hücresi ve kurulan yenilikçi elektrokimyasal ayırma prosesi kullanılarak adsorpsiyon ve desorpsiyon süreci incelenmiştir.

2. Yöntemler (Methods)

2.1. Elektrotların Hazırlanması ve Karakterizasyonu (Preparation and Characterization of Electrodes)

Bu çalışma kapsamında, 1×2 cm (aktif yüzey alanı olarak 1×1 cm^2) ve 8×8 cm (aktif yüzey alanı 5×5 cm^2)'lik olmak üzere iki farklı ölçekte elektrotlar hazırlanmıştır. Elektrotların hazırlanmasında Toray karbon kağıdı (TGP-H-60, Toray, Japonya), aktif karbon (Merck, ABD), karbon siyahı (Nanografi, Türkiye), polivinilidin florür (PVDF, Nanografi, Türkiye) ve çözücü olarak da aseton (Merck, ABD) kullanılmıştır. Besleme çözeltisinin hazırlanmasında ise Merck firmasından temin edilen sodyum tetraborat dekahidrat kullanılmıştır. Ağırlıkça aktif karbon: karbon siyahı: PVDF oranı 85:10:5 olacak şekilde tartılmış ve 20 ml aseton eklenerek hazırlanan karışımın 2 saat karıştırılması sağlanmıştır. Daha sonra elde edilen bu süspansiyon daldırmalı ultrasonik prob kullanılarak 1 saat ultrasonikasyon işlemine tabi tutulmuştur. Damlatma (drop casting) yöntemi kullanılarak elektrotlar hazırlanmıştır. Hazırlanan elektrotlar döngüsel voltametri, yüzey alanı ölçümü (BET) ve taramalı elektron mikroskopu (SEM, Zeiss EVO LS 10, Almanya) analiz yöntemleri kullanılarak karakterize edilmiştir. Elektrokimyasal karakterizasyon işlemi döngüsel voltametre kullanılarak gerçekleştirilmiştir. Döngüsel voltammogramlar üç elektrotlu sistem kullanılarak 5 mV/s tarama hızında 5 döngü olacak şekilde kaydedilmiştir. Referans elektrot olarak Ag/

AgCl ve karşıt elektrot olarak da platinyum plaka kullanılmıştır.

Elektrotların morfolojik özellikleri SEM, yüzey alanı ise Quantachrome marka Quadrosorb SI cihazı (ABD) kullanılarak belirlenmiştir. Elektrotların yüzeyini kaplayan aktif karbon numunesine ilk olarak 8 saat boyunca 120°C'de gaz giderme işlemi uygulanmış, ardından örneklerin 77 K'de azot adsorpsiyon-desorpsiyon izotermleri alınmıştır. Yüzey alanı hesaplamasında Brunauer-Emmett-Teller (BET) eşitliği kullanılmıştır.

2.2. Elektrokimyasal Hücre Tasarımı (Electrochemical Cell Design)

Bu çalışmada, sürekli akış koşullarında borat iyonu giderimi deneyleri için Rhinoceros 3D (Robert McNeel & Associates, ABD) yazılımı kullanılarak elektrokimyasal akış hücre tasarımı yapılmıştır. Şekil 1'de deneylerde kullanılan akış hücresinin temel parçalarını gösteren 3 boyutlu çizimi verilmiştir. Elektrokimyasal hücre (8×8 cm) 2 adet akrilikten oluşan plaka, 2 adet simetrik aktif karbon ile kaplı elektrot, 2 adet titanyum kollektör, 1 adet akrilikten yapılmış ayırıcı plaka ve 1 adet akışın hücre içerisinden homojen ve etkin olarak geçişini sağlayacak polimer dağıtıcıdan (spacer) oluşmaktadır.

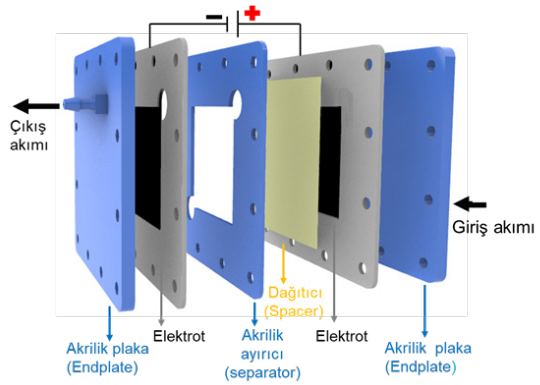

Şekil 1. Elektrokimyasal akış hücrenin 3 boyutlu görseli (3-dimensional image of the electrochemical flow cell)

2.3. Elektrokimyasal Proses/Deney Düzeneği (Electrochemical Process/Experimental Setup)

Proses besleme tankı, besleme çözeltisini elektrokimyasal hücreye farklı akış hızlarında besleyecek peristaltik pompa, elektrokimyasal hücre, güç kaynağı, iletkenlik sensörü (eDAQ, Avustralya), pH probu (eDAQ, Avustralya) ve kaydedicileri ve çıkış tankından oluşmaktadır. Şekil 2'de deney düzeneğinin şematik gösterimi verilmiştir.

Deneylerde beş döngü olacak şekilde adsorpsiyon ve desorpsiyon çalışmaları yürütülmüştür. Bor çözeltisi hücreye peristaltik pompa aracılığıyla 1 ml/dk akış hızında beslenmiş ve 0,75, 1,0, 1,25 ve 1,5 V olmak üzere dört farklı voltaj değerinde çalışılmıştır. Öncelikle besleme çözeltisi prosese beslenmiş ve bu çözelti elektrokimyasal hücreye girdiği an itibariyle sisteme voltaj uygulanarak iyonların elektrot yüzeylerine tutunması sağlanmıştır. Elektrokimyasal hücreyi terk eden çözeltinin inline olarak iletkenlik ve pH değerleri sürekli olarak kaydedilmiştir. Adsorpsiyon ve desorpsiyon prosesi boyunca, belirli zaman aralıklarında çıkış akımından numuneler alınmış, iyon derişimi indüktif eşleşmiş plazma atomik emisyon spektroskopisi (ICP-OES, Spectro Analytical Instruments, Almanya) kullanılarak belirlenmiş ve verim hesaplanmıştır.

Elektrot yüzeyine kaplanan aktif karbonun birim kütlesi başına tutunan borat iyonu miktarı (q_e) ve adsorplanan borat iyonu yüzdesi (verim) Eşitlik 1 ve 2 kullanılarak hesaplanmıştır. C_i başlangıç konsantrasyonunu, C_t çıkış akımındaki borat konsantrasyonunu (mg/L), V çözeltinin hacmini (L), w ise aktif karbon elektrotun kütlesini (g) göstermektedir.

$$q_e = \frac{(C_i - C_t) \times V}{w} \quad (1)$$

$$\text{Verim } (\%) = \frac{(C_i - C_t)}{C_i} \times 100 \quad (2)$$

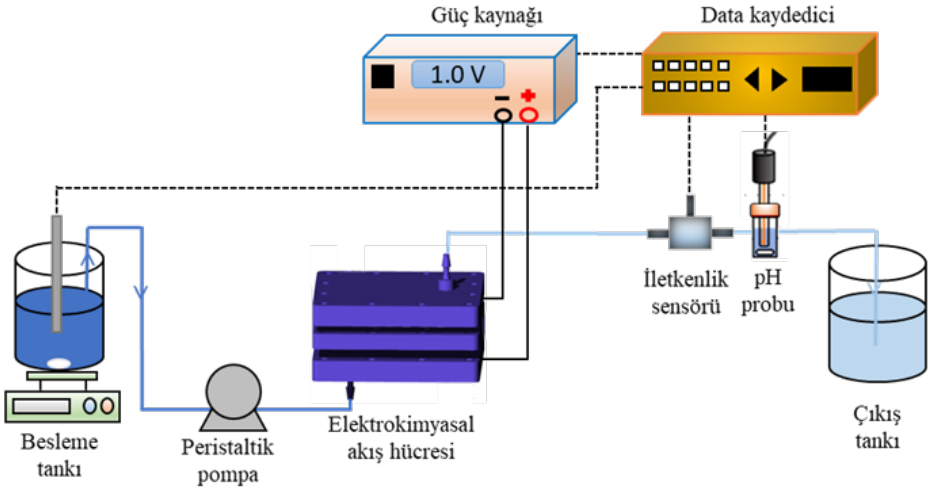

Şekil 2. Elektrokimyasal ayırma sistemi düzeneğinin şematik gösterimi (Schematic representation of electrochemical separation system's setup)

3. Sonuçlar ve Tartışma (Results and Discussion)

3.1. Elektrot Karakterizasyonu (Electrode Characterization)

Bu çalışmada aktif karbon ile kaplanmış elektrotların elektrokimyasal olarak karakterizasyonu için döngüsel voltametriden (CV) yararlanılmıştır. Ölçümlerde Şekil 3a'da verilen üç elektrot konfigürasyonu kullanılmış, yüzeyi aktif karbon ile kaplanmış Toray karbon kâğıdı, platin plaka ve Ag/AgCl sırasıyla çalışma, karşıt ve referans elektrot olarak kullanılmıştır. CV ölçümleri için potansiyel aralığı -1V ile +1V arasında seçilmiş olup, en az 5 döngü olacak şekilde 5 mV/s tarama hızında 0,1M potasyum sülfat (K_2SO_4) çözeltisi kullanarak analiz yapılmış ve elde edilen CV eğrisi Şekil 3b'de verilmiştir. Ayrıca, çalışma elektrodunun borat iyonunu adsorpsiyonu açısından performansı kronoamperometri kullanarak belirlenmiş, ölçümler 900 saniye 0,8 V potansiyel uygulanarak alınmış ve elde edilen sonuç Şekil 3c'de verilmiştir.

Şekil 3'te verilen elektrokimyasal karakterizasyon sonuçları incelendiğinde, CV eğrisinin beş döngü için de aynı eğilimi gösterdiği yani elektrokimyasal olarak kararlı olduğu ve literatürdeki çalışmalarla [35,36] da uyumlu olarak dikdörtgensel davranış gösterdiği belirlenmiştir. Şekil 3d-f'de verilen SEM analiz görüntüleri incelendiğinde Toray karbon kağıdının yüzeyinin yaklaşık 10 µm çapa sahip karbon fiber yapılarından oluştuğu belirlenmiştir. Yüzeyin aktif karbon ile kaplanmasından sonra elektrot yüzeyi tamamen değişerek, homojen olmayan daha gözenekli yapıya sahip bir morfolojiye sahip olduğu belirlenmiştir. Ayrıca, aktif karbon ile kaplanmış yüzeydeki BET spesifik yüzey alanı 694 m^2/g olarak ölçülmüştür. Borat iyonlarının adsorpsiyonu sonucunda elektrot yüzeyinin değiştiği, boşlukların azaldığı ve daha homojen yüzeye sahip olduğu tespit edilmiştir.

3.2. Sürekli Akış Koşullarında Bor Adsorpsiyon ve Desorpsiyon Sonuçları (Boron Adsorption and Desorption Results under Continuous Flow Conditions)

Aktif yüzey alanı 1×1 cm^2 olan çalışma elektrodunun elektrokimyasal ve morfolojik karakterizasyon işleminin tamamlanmasından sonra, aktif yüzey alanı 5×5 cm^2 olan elektrotlar hazırlanmış ve elektrokimyasal akış hücresine yerleştirilmiştir. 10 mg/L boraks dekahidrat çözeltisi 1,0 ml/dakika akış hızında peristaltik pompa aracılığıyla ayırma sistemine 5 döngü adsorpsiyon-desorpsiyon olacak şekilde sürekli olarak beslenmiştir. Her bir döngü için 10 ml besleme çözeltisi kullanılmıştır. Çıkış akımının iletkenlik ve pH değerleri inline olarak ölçülmüş, adsorpsiyon deneylerinde +1,0 V, desorpsiyon deneylerinde ise -1,0 V potansiyel sürekli olarak uygulanmıştır. Şekil 4a ve 4b'de zamana bağlı olarak değişen akım değerleri ve akış hücresini terk eden çözeltinin iletkenliğe bağlı olarak hesaplanan konsantrasyon ve pH değerleri verilmiştir.

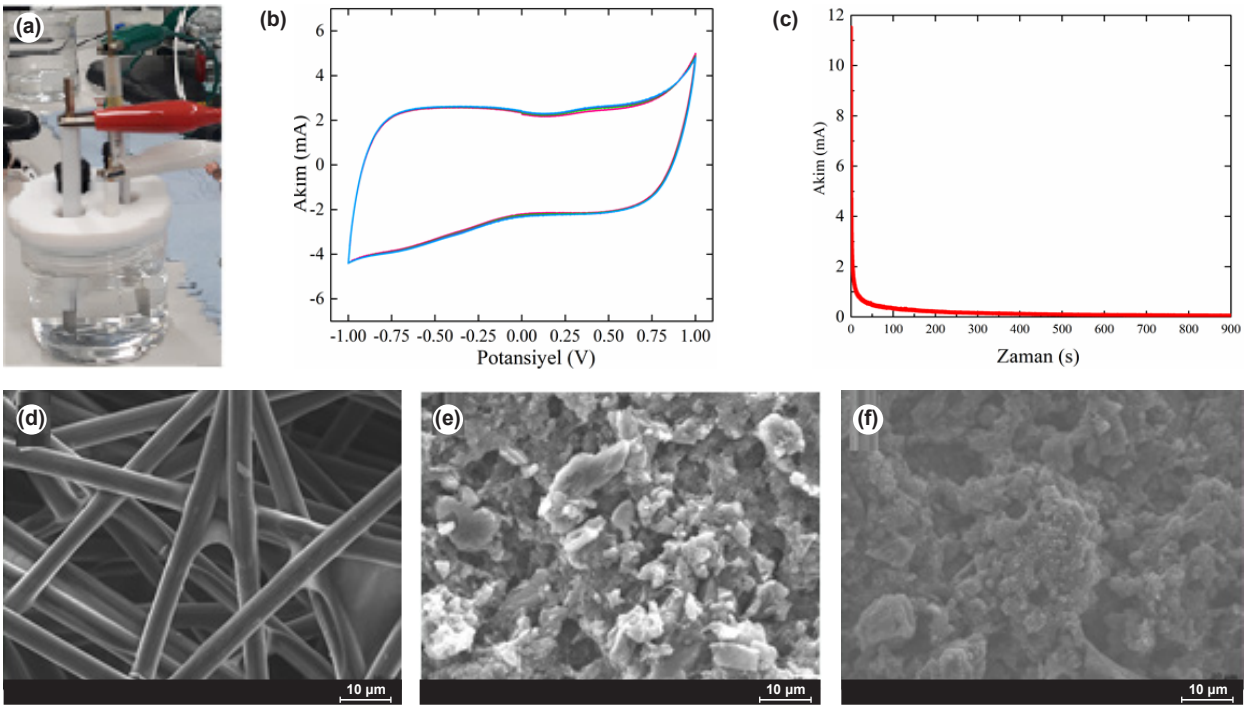

Şekil 3. a) Elektrokimyasal karakterizasyon işleminde kullanılan elektrot hücresi, çalışma elektrotunun b) dönüşümlü voltametri (CV) eğrisi ve c) kronoamperometrik (CA) eğrisi, d) Toray karbon kağıdı, e) aktif karbon ile kaplanmış çalışma elektrodu, f) bor adsorpsiyonu sonrasında çalışma elektrodunun 1000X büyütmede elde edilen SEM görüntüleri (Ölçek çubuğu: 10 µm) (a) Electrode cell used in the electrochemical characterization process, b) cyclic voltammetry (CV) curve and c) chronoamperometric (CA) curve of the working electrode, SEM images obtained at 1000X magnification of d)Toray carbon paper electrode, e) working electrode coated with activated carbon, f) working electrode after boron adsorption (Scale bar: 10 µm))

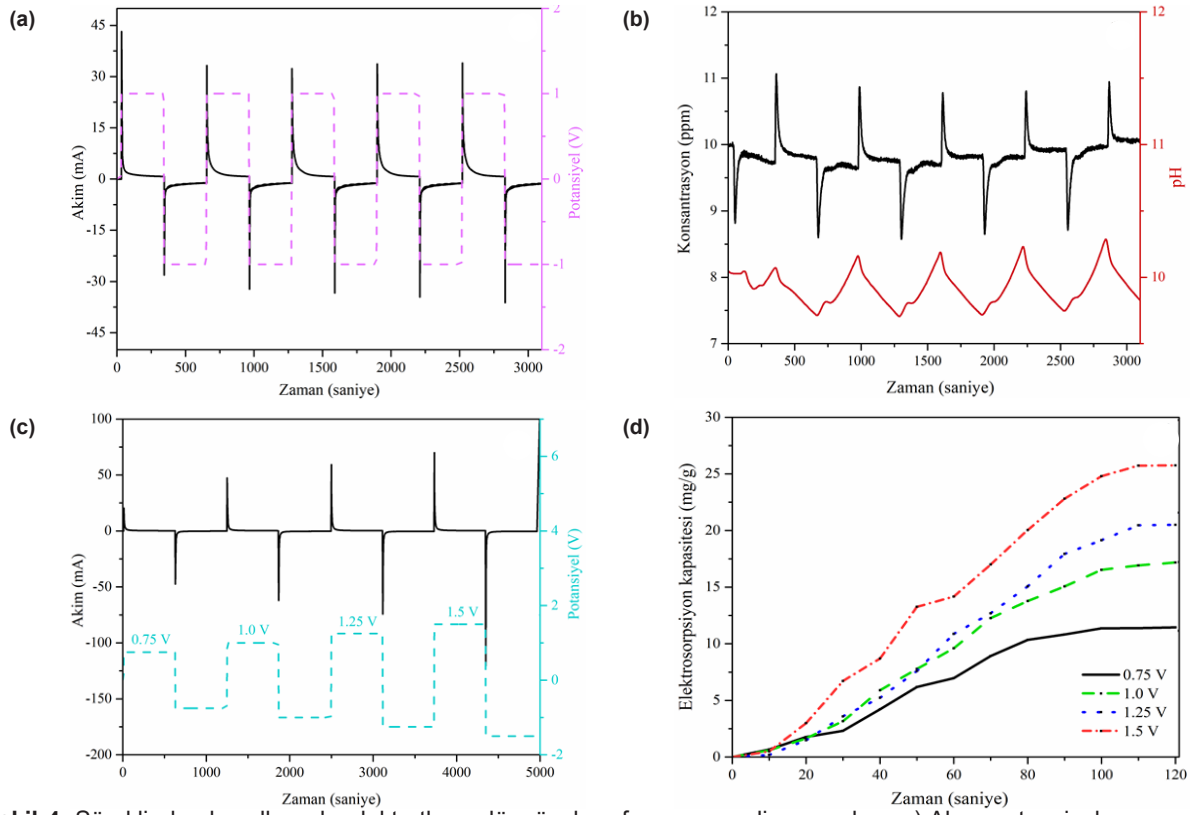

Şekil 4. Sürekli akış koşullarında elektrotların döngüsel performans analiz sonuçları. a) Akım-potansiyel-zaman grafiği, b) zamana bağlı olarak konsantrasyon ve pH değişim grafikleri, c) farklı potansiyel değerlerinde zamana bağlı akım değişimi grafiği d) farklı potansiyel değerleri için zamana bağlı olarak hesaplanan elektrosorpsiyon kapasitesi değerleri (Cyclic performance analysis results of electrodes under continuous flow conditions. a) Current-voltage-time profiles, b) Concentration and pH change profiles with time, c) current change profile with time at different applied potentials, d) electrosorption capacity values calculated as a function of time for different applied potentials)

Şekil 4a'da verilen sonuçlar incelendiğinde, her bir adsorpsion-desorpsiyon döngüsü için benzer akım değişimi eğilimi belirlenmiştir. Şekil 4b'de verilen zamana bağlı konsantrasyon değişimi grafiği incelendiğinde, başlangıçta çözelti derişimi 10 mg/L olarak ölçülmüştür. 5 döngü olacak şekilde elektrotlara 5 dakika 1,0 V ve 5 dakika -1,0 V uygulanmıştır. Sistem +1,0 V koşullarında çalıştırıldığında, çıkış akımındaki borat iyonu konsantrasyonunun besleme çözeltisine göre düştüğü tespit edilmiştir. Elektrotlara gerilim uygulanmasıyla besleme akımında bulunan borat iyonları aktif karbon ile kaplanmış elektrot yüzeylerine adsorbe olmuştur (Şekil 4a). Yüzeye tutunan bu iyonlar çözeltideki iyon miktarının düşmesine ve buna bağlı olarak da çıkış akımında ölçülen iletkenlik değerinin yani iyon konsantrasyonun azalmasına sebep olmuştur. Daha sonra aktif karbonla kaplanmış elektrotlar doygunluk seviyesine ulaşmış ve çıkış akımında ölçülen konsantrasyon, başlangıç besleme çözeltisi konsantrasyonun değerine geri dönmüştür. Hem elektrotların rejenerasyonu hem de borat iyonlarının geri kazanılması için sisteme adsorpsiyon işleminde uygulanan gerilime eşit ancak negatif değeri olan -1,0 V uygulanmıştır. Desorpsiyon sürecinde, elektrot yüzeyine adsorplanmış olan borat iyonları çözeltiye geri dönmüş ve bu durum da çıkış akımında ölçülen konsantrasyon değerinin artışına neden olmuştur (Şekil 4b). Bu süreç 5 döngü olacak şekilde yapılmış ve tüm döngüler için benzer sonuçlar elde edilmiştir. Bu çalışmada ayrıca 0,75, 1,0, 1,25 ve 1,5 V olmak üzere dört farklı voltaj değerinde çalışılmış ve sonuçlar Şekil 4c ve 4d'de verilmiştir. Sonuçlar incelendiğinde uygulanan potansiyel değerinin 0,75'ten 1,5 V'a artırılmasıyla tutunan bor iyonu miktarı 11,5 mg/g'dan 25,7 mg/g'a çıkmıştır. Ayrıca, Şekil 4d incelendiğinde, zamana bağlı olarak adsorbe edilen bor iyonu konsantrasyonu artığı belirlenmiştir. Literatürde aktif karbon kullanılarak KDI prosesi ile bor iyon giderimi üzerine yapılan çalışmalar incelendiğinde, Kluczka ve arkadaşları [37] tarafından modifiye edilmiş aktif karbon kullanıldığında adsorpsiyon kapasitesi 1,5 mg/g, Halim ve arkadaşları [38] tarafından ise maksimum adsorpsiyon kapasitesi 5,0 mg/g olarak hesaplanmıştır.

Adsorpsiyon ve desorpsiyon süresince çıkış çözeltisinin pH'ı 10,29 ile 9,71 arasında değişmiş, adsorpsiyon aşamasında pH değeri artarken desorpsiyon aşamasında ise bu değer azalmıştır. Ayrıca, adsorplanan ve geri kazanılan iyon miktarının kantitatif olarak belirlenmesi için belirli zaman aralıklarında çıkış akımından numuneler alınmış ve analiz edilmiştir. Adsorpsiyon ve desorpsiyon sürecinde akış hücresinin şematik gösterimi Şekil 5'de verilmiştir. 5. döngü sonunda adsorsiyon ve desorpsiyon verimi %90,3 ve %88,7 olarak hesaplanmıştır.

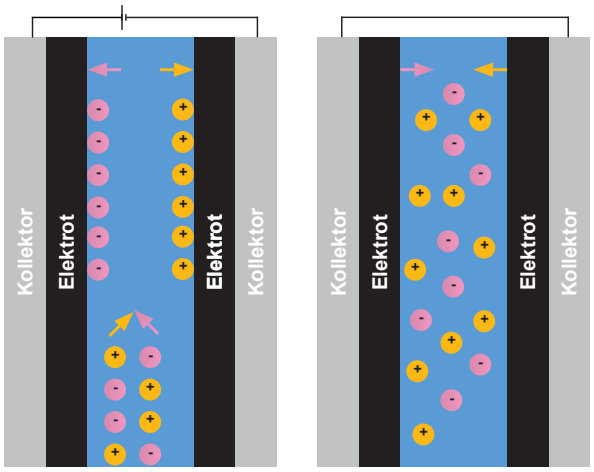

Şekil 5. Adsorpsiyon ve desorpsiyon sürecinde akış hücresinin şematik gösterimi (Schematic representation of the flow cell during adsorption and desorption)

Bu çalışmada ayrıca akış hızının adsorpisyon ve desorpsiyon verimine etkisi incelemiştir. Bu kapsamda, sabit potansiyel değerinde (+1,0/-1,0 V) 4 ve 10 ml/dk akış hızı olmak üzere iki farklı akış hızında ölçümler alınmış ve sonuçlar Şekil 6'da verilmiştir. 5. döngü sonunda elde edilen bor giderim verimi 4 ve 10 ml/dk akış hızı için sırasıyla %81,6 ve %67,1 olarak hesaplanmıştır.

4. Sonuçlar (Conclusions)

Bu çalışmada, sürekli akış koşullarında bor iyonlarının sulu çözeltilerden elektrokimyasal ayırma yöntemi ile giderilmesi ve geri kazanımı incelenmiştir. Bu kapsamda, ilk olarak aktif karbon ile kaplanmış elektrotlar hazırlanmış ve karakterize edilmiştir. Dönüşümlü voltametri sonuçları elektrokimyasal açıdan kararlı elektrotların elde edildiği ve SEM görüntüleri elektrot yüzeylerinin gözenekli bir yapıya sahip olduğunu göstermiştir. Ayrıca, elektrotların BET spesifik yüzey alanı 694 m^2/g olarak ölçülmüştür. Daha sonra akış ortamında adsorpsiyon ve desorpsiyon çalışmalarının yürütülebilmesi için akış hücresi tasarlanmıştır. Sürekli akış koşullarında, 0,75, 1,0, 1,25 ve 1,5 V voltaj değerlerinde tutunan bor iyonu miktarı sırasıyla 11,5, 17,2, 20,5 ve 25,7 mg/g olarak hesaplanmıştır. Tasarlanan elektrokimyasal ayırma prosesi sulu çözeltilerde bulunan bor iyonlarının hem adsorpsiyon hem de desorpsiyonunun başarıyla gerçekleştirilmesini sağlamıştır. Bu proses kullanılarak sürekli akış koşullarında %90'nın üzerinde bor giderimi sağlanmıştır. Bu çalışmadan elde edilen sonuçların hem bor iyonlarının giderimi ve geri kazanımı açısından yenilikçi teknolojiler geliştirmesine hem de su kirliği, çevrenin korunumu ve su sürdürülebilirliğine katkı sağlayacağı düşünülmektedir.

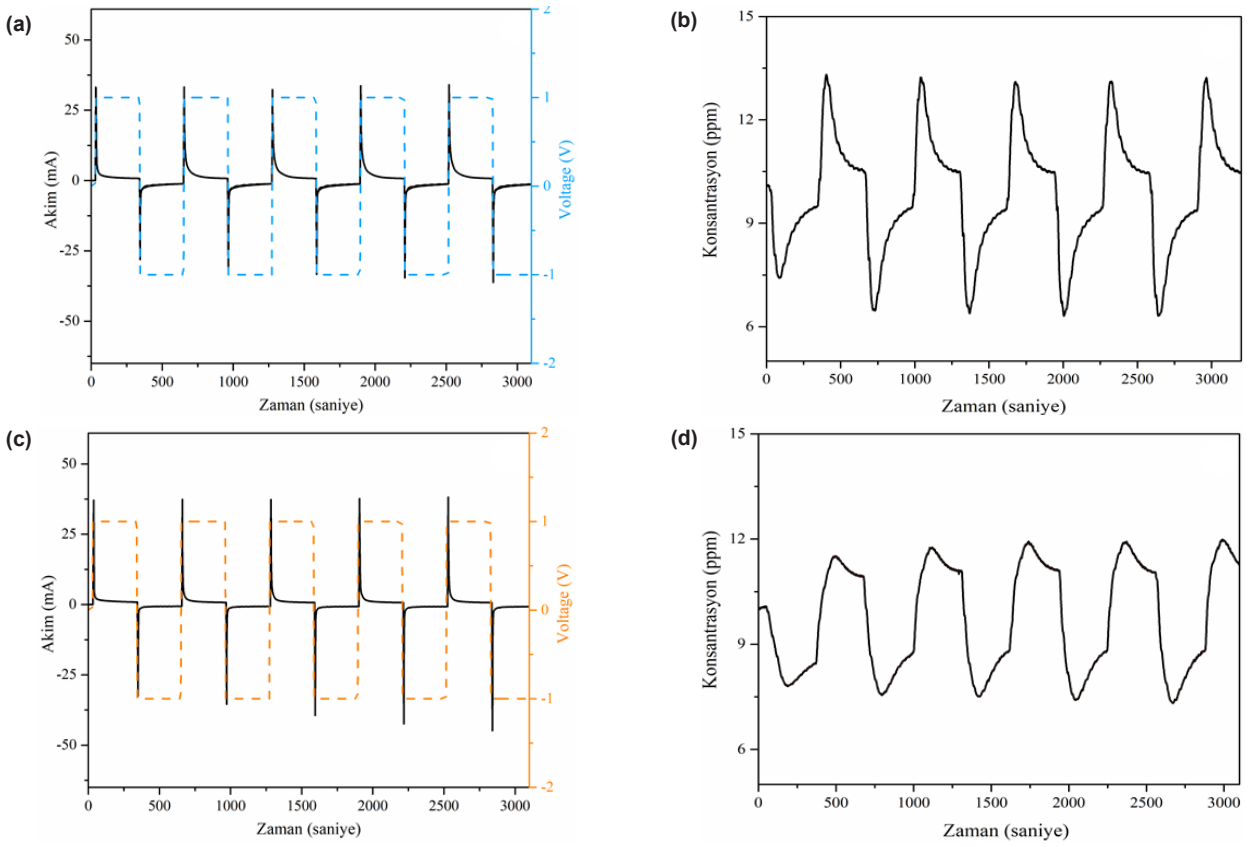

Şekil 6. Farklı akış hızlarında elektrotların döngüsel performans analiz sonuçları. 4 ml/dk akış hızı için a) akım-potansiyel-zaman ve b) konsantrasyon-zaman grafiği, 10 ml/dk akış hızı için c) akım-potansiyel-zaman ve d) konsantrasyon-zaman grafiği (Cyclic performance of analysis results of electrodes at different flow rates. a) Current-voltage-time profiles and b) concentration-time profiles for 4 ml/min, c) current-voltage-time profiles and d) concentration-time profiles for 10 ml/min)

5. Teşekkürler (Acknowledgements)

Bu çalışma, Türkiye Bilimsel ve Teknolojik Araştırma Kurumu (TÜBİTAK) tarafından 123M952 numaralı proje ile desteklenmiştir. Projeye verdiği destekten ötürü TÜBİTAK'a teşekkürlerimi sunarım.

Kaynaklar (References)

[1] Çelen, Y. Y., Evcin, A., Akkurt, I., Bezir, N. Ç., Günoğlu, K., & Kutu, N. (2019). Evaluation of boron waste and barite against radiation. *International Journal of Environmental Science and Technology*, *16*, 5267-5274. https://doi.org/10.1007/s13762-019-02333-3

[2] Eti Maden. (2024, October). *Boron as the rising value of Turkey*. https://www.etimaden.gov.tr/en/boron-in-turkey

[3] Yu, N., Jiang, H., Luo, Z., Geng, W., & Zhu, J. (2023). Boron adsorption using NMDG-modified polypropylene melt-blown fibers induced by ultraviolet grafting. *Polymers*, *15*(10), 2252. https://doi.org/10.3390/polym15102252

[4] Altınbaş, B. F., & Yüksel, A. (2024). Synthesis of a novel cellulose-based adsorbent from olive tree pruning waste for removal of boron from aqueous solution. *Biomass Conversion and Biorefinery*, *14*, 20117-20127. https://doi.org/10.1007/s13399-023-04147-3

[5] Kim, K. C., Kim, N., Jiang, T., Kim, J. C., & Kang, C. I. (2023). Boron recovery from saltlake brine, seawater, and wastewater-A review. *Hydrometallurgy*, *218*, 106062. https://doi.org/10.1016/j.hydromet.2023.106062

[6] Vasudevan, S. & Lakshmi, J. (2012). Electrochemical removal of boron from water: Adsorption and thermodynamic studies. *The Canadian Journal of Chemical Engineering*, *90*(4), 1017-1026. https://doi.org/10.1002/cjce.20585

[7] Avraham, E., Noked, M., Soffer, A., & Aurbach, D. (2011). The feasibility of boron removal from water by capacitive deionization. *Electrochimica Acta*, *56*(18), 6312-6317. https://doi.org/10.1016/j.electacta.2011.05.037

[8] Goren, A. Y., Recepoglu, Y. K., Karagunduz, A., Khataee, A., & Yoon, Y. (2022). A review of boron removal from aqueous solution using carbon-based materials: An assessment of health risks. *Chemosphere*, *293*, 133587. https://doi.org/10.1016/j.chemosphere.2022.133587

[9] Bryjak, M., Wolska, J., & Kabay, N. (2008). Removal of boron from seawater by adsorption-membrane hybrid process: Implementation and challenges. *Desalination*, *223*(1-3), 57-62. https://doi.org/10.1016/j.desal.2007.01.202

[10] Bilen, M., Ateş, Ç., & Bayraktar, B. (2018). Determination of optimal conditions in boron factory wastewater chemical treatment process via response surface methodology. *Journal of the Faculty of Engineering and Architecture of Gazi University*, *33*(1), 267-278. https://doi.org/10.17341/gazimmfd.406798

[11] Tanaka, Y. (2007). Electro-deionization. *Membrane Science and Technology*, *12*, 437-460. https://doi.org/10.1016/S0927-5193(07)12018-0

[12] Meng, X., Luo, R., Guo, G., Li, Y., Fang, H., Bai, P., … & Guo, X. (2022). Boron adsorption and isotopic separation from water by isostructural metal-organic frameworks MIL-100(M). *Desalination*, *541*, 116038. https://doi.org/10.1016/j.desal.2022.116038

[13] Guo, Z., Wang, R., Ren, W., Cheng, M., Wang, Z., Li, W., & Zhang, M. (2022). Synthesis of distorted octahedral C-doped nickel nanocrystals encapsulated in CNTs: A highly active and stable catalyst for water pollutions treatment. *Chemical Engineering Journal*, *446*, 136805. https://doi.org/10.1016/j.cej.2022.136805

[14] Zhu, W., Li, Y., Dai, L., Li, J., Li, X., Li, W., … & Chen, T. (2018). Bioassembly of fungal hyphae/carbon nanotubes composite as a versatile adsorbent for water pollution control. *Chemical Engineering Journal*, *339*, 214-222. https://doi.org/10.1016/j.cej.2018.01.134

[15] Lin, J. Y., Mahasti, N. N., & Huang, Y. H. (2021). Recent advances in adsorption and coagulation for boron removal from wastewater: A comprehensive review. *Journal of Hazardous Materials*, *407*, 124401. https://doi.org/10.1016/j.jhazmat.2020.124401

[16] Xia, N. N., Zhang, H. Y., Hu, Z. H., Kong, F., & He, F. (2021). A functionalized bio-based material with abundant mesopores and catechol groups for efficient removal of boron. *Chemosphere*, *263*, 12820. https://doi.org/10.1016/j.chemosphere.2020.128202

[17] Qiu, X., Sasaki, K., Hirajima, T., Ideta, K., & Miyawaki, J. (2014). One-step synthesis of layered double hydroxide-intercalated gluconate for removal of borate. *Separation and Purification Technology*, *123*, 114-123. https://doi.org/10.1016/j.seppur.2013.12.031

[18] Wolska, J., & Bryjak, M. (2013). Methods for boron removal from aqueous solutions-A review. *Desalination*, *310*, 18-24. https://doi.org/10.1016/j.desal.2012.08.003

[19] Lin, J. Y., Mahasti, N. N. N., & Huan, Y. H. (2021). Fluidized-bed crystallization of barium perborate for continuous boron removal from concentrated solution: Supersaturation as a master variable. *Separation and Purification Technology*, *278*, 119588. https://doi.org/10.1016/j.seppur.2021.119588

[20] Biçak, N. Bulutçu, N. Şenkal, B. F. & Gazi, M. (2001). Modification of crosslinked glycidyl methacrylate-based polymers for boron-specific column extraction. *Reactive & Functional Polymers*, *47*(3), 175-184. https://doi.org/10.1016/S1381-5148(01)00025-6

[21] Wang, S., Bing, S., Zhang, H., Zhou, Y., Zhang, L., & Gao, C. (2022). Surface engineering design of polyamide membranes for enhanced boron removal in seawater desalination. *Journal of Membrane Science*, *651*, 120425. https://doi.org/10.1016/j.memsci.2022.120425

[22] Ghiasi, S., Mohammadi, T., & Tofighy, M. A. (2022). Hybrid nanofiltration thin film hollow fiber membranes with adsorptive supports containing bentonite and LDH nanoclays for boron removal. *Journal of Membrane Science*, *655*, 120576. https://doi.org/10.1016/j.memsci.2022.120576

[23] Tang, Y. P., Luo, L., Thong, Z., & Chung, T. S. (2017). Recent advances in membrane materials and technologies for boron removal. *Journal of Membrane Science*, *541*, 434-446. https://doi.org/10.1016/j.memsci.2017.07.015

[24] Guesmi, F., Louati, I., Hannachi, C., & Hamrouni, B. (2020). Optimization of boron removal from water by electrodialysis using response surface methodology. *Water Science and Technology*, *81*(2), 293-300. https://doi.org/10.2166/wst.2020.105

[25] Isa, M. H., Ezechi, E. H., Ahmed, Z., Magram, S. F., & Kutty, S. R. M. (2014). Boron removal by electrocoagulation and recovery. *Water Research*, *51*, 113-123. https://doi.org/10.1016/j.watres.2013.12.024

[26] Ezechi, E. H., Isa, M. H., Kutty, S. R. M., & Yaqub, A. (2014). Boron removal from produced water using electrocoagulation. *Process Safety and Environmental Protection*, *92*(6), 509-514. https://doi.org/10.1016/j.psep.2014.08.003

[27] Haddadi, E., Gujar, J. G., & Sonawane, S. S. (2023). Kinetics and isotherm studies for the adsorption of boron from water using titanium dioxide. *The Canadian Journal of Chemical Engineering*, *101*(3), 1335-1344. https://doi.org/10.1002/cjce.24429

[28] Su, X., Kushima, A., Halliday, C., Zhou, J., Li, J., & Hatton, T. A. (2018). Electrochemically-mediated selective capture of heavy metal chromium and arsenic oxyanions from water. *Nature Communications*, *9*, 4701. https://doi.org/10.1038/s41467-018-07159-0

[29] Dash, A., & Chakravarty, R. (2014). Electrochemical separation: Promises, opportunities, and challenges to develop next-generation radionuclide generators to meet clinical demands. *Industrial & Engineering Chemistry Research*, *53*, 3766-3777. https://doi.org/10.1021/ie404369y

[30] Su, X. (2020). Electrochemical interfaces for chemical and biomolecular separations. *Current Opinion in Colloid and Interface Science*, *46*, 77-93. https://doi.org/10.1016/j.cocis.2020.04.005

[31] Su, X., & Hatton, T. A. (2017). Redox-electrodes for selective electrochemical separations. *Advances in Colloid and Interface Science*, *244*, 6-20. https://doi.org/10.1016/j.cis.2016.09.001

[32] Porada, S., Zhao, R., Van der Wal, A., Presser, V., & Biesheuvel, P. M. (2013). Review on the science and technology of water desalination by capacitive deionization. *Progress in Materials Science*, *58*(8), 1388-1442. https://doi.org/10.1016/j.pmatsci.2013.03.005

[33] Anderson, M. A., Cudero, A. L. & Palma, J. (2010). Capacitive deionization as an electrochemical means of saving energy and delivering clean water. Comparison to present desalination practices: Will it compete? *Electrochimica Acta*, *55*(12), 3845-3856. https://doi.org/10.1016/j.electacta.2010.02.012

[34] Subramani, A., Badruzzaman, M., Oppenheimer, J., & Jacangelo, J. G. (2011). Energy minimization strategies and renewable energy utilization for desalination: a review. *Water Research*, *45*(5), 1907-1920. https://doi.org/10.1016/j.watres.2010.12.032

[35] Shabeebaa, P., Thayyila, M. S., Pillaic, M. P., Soufeenaa, P. P., & Niveditha, C. V. (2018). Electrochemical investigation of activated carbon electrode supercapacitors. *Russian Journal of Electrochemistry*, *54*, 302-308. https://doi.org/10.1134/S1023193517120096

[36] Gurten Inal, I. I., & Aktas, Z. (2020). Enhancing the performance of activated carbon based scalable supercapacitors by heat treatment. *Applied Surface Science*, *514*, 145895. https://doi.org/10.1016/j.apsusc.2020.145895

[37] Kluczka, J., Pudło, W., & Krukiewicz, K. (2019). Boron adsorption removal by commercial and modified activated carbons. *Chemical Engineering Research and Design*, *147*, 30-42. https://doi.org/10.1016/j.cherd.2019.04.021

[38] Halim, A. A., Roslan, N. A., Yaacub, N. S., & Latif, M. T. (2013). Boron removal from aqueous solution using curcumin-impregnated activated carbon. *Sains Malaysiana*, *42*(9), 1293-1300. Retrieved from https://www.ukm.my/jsm/pdf_files/SM-PDF-42-9-2013/13%20Azhar%20Abdul%20Halim.pdf

BOR DERGİSİ
JOURNAL OF BORON
https://dergipark.org.tr/boron

Development of PCL/PVA/PCL scaffold for local delivery of calcium fructoborate for bone tissue engineering

Ali Deniz Dalgic [1,*]

[1]*İstanbul Bilgi University, Faculty of Engineering and Natural Sciences, Department of Genetics and Bioengineering, İstanbul, 34060, Türkiye*

ARTICLE INFO

Article history:
Received September 13, 2024
Accepted October 14, 2024
Available online December 31, 2024

Research Article

DOI: 10.30728/boron.1549809

Keywords:
Bone tissue engineering
Boron
Calcium fructoborate
Polycaprolactone
Polyvinyl alcohol

ABSTRACT

Calcium fructoborate (CaFB) has gathered attention due to its boron and calcium content, both of which are known to support bone health, deposition and regeneration. Previous studies have shown that CaFB has a positive effect on bone health and has been proven to promote bone-like properties. In light of this information, a local CaFB delivering scaffold could improve bone regeneration in cases of bone tissue loss. This study aimed to design a layer-by-layer polymeric sponge capable of achieving controlled local delivery of CaFB to improve bone tissue healing. The dose-dependent effect of CaFB on the cell viability of the Saos-2 cell line was investigated *in vitro*. Layer-by-layer structure of the polymeric scaffold supported controlled release of CaFB, with 33.9±7.4% released after 7 days of incubation. CaFB at 31.25 µg/mL concentration was able to improve Saos-2 cell viability up to 174.7±24.1% and 127.7±8.7% after 1 and 4 days of incubation. After 7 days of incubation CaFB treatment at concentrations of 250, 125, 62.5 and 31.25 µg/mL improved cell viability up to 194.3±47.7, 155.3±17.7, 149.4±5.4 and 132.5±13.3%. The polycaprolactone/polyvinyl alcohol/polycaprolactone (PCL/PVA/PCL) scaffold supported the viability of cells for 7 days and was shown to be biocompatible. The results of this study showed that CaFB is a potential compound that can be locally delivered within a scaffold system to improve bone tissue regeneration.

1. Introduction

Boron is a trace element that exhibits both metal and non-metal properties and has several beneficial effects on human health such as influencing calcium metabolism, enhancing bone growth, and affecting nutrient and hormone metabolism. The main source of boron for humans is diet. Only plants can directly metabolize boric acid and borate compounds, converting them into monoester or diester forms, which are then consumed by humans and animals. Boron is essential for enhancing bone growth and strength. Boron is also known for its ability to regulate vitamin D metabolism, which has been shown to positively affect bone growth and differentiation [1,2]. Also, increased boron supplementation has been attributed to improved serum levels of vitamin D in deficient subjects [3]. Previous *in vitro* and *in vivo* studies have reported that boron can improve bone regeneration and strength [4-9]. When interacted with osteoblast cells, even at low doses, boron has been reported to activate cell proliferation and differentiation [10]. Similarly, low doses of boron have been shown to promote the expression of osteogenic markers, like collagen type I, osteopontin, bone sialoprotein, osteocalcin and runX2 while increasing levels of bone morphogenetic proteins (BMP-4, -6, -7) [9]. *In vivo* studies have shown a strong relation between increased bone strength and boron supplementation in Weanling pigs [5] and Sprague Dawley rats [6]. The positive effects of boron containing biomaterials on bone tissue healing are well defined in the literature. Boron bearing materials like bone cement, boron-doped hydroxyapatite (HAp), bioactive glasses, nanofibers and 3D-printed polymeric matrixes have been fabricated and shown to improve structural properties as well as bioactivity for bone regeneration [11-13].

Fructoborates are organic compounds consisting of boron and fructose and are naturally found in several fruits like apples, pears, and grapes [1]. Fructoborates exhibit no toxicity and accumulation and show better absorption than other boron compounds. Among fructoborates, calcium fructoborate (CaFB) has drawn attention for human health due to its calcium content [14]. CaFB can also be synthetically produced by allowing boric acid to form complexes with organic compounds like d-fructose [15]. Calcium, the other key component of CaFB, is a well-known ion that has been proven to support bone growth and strength by benefiting bone metabolism [16-18]. *In vivo* studies with CaFB have shown that CaFB can be systemically absorbed by the body [14,19]. When CaFB is taken via

*Corresponding author: deniz.dalgic@bilgi.edu.tr

diet, low pH in the stomach and enzymes can catalyze the hydrolysis of ester bonds to form fructose and boric acid which can be readily absorbed [20].

CaFB supplementation has been reported to stimulate osteoblast for mineralization when introduced along with dexamethasone [21]. In a pilot study, CaFB, when supplemented for six months, was reported to improve bone density in subjects with osteoporosis [22]. CaFB has also been incorporated into the surface coating of hydroxyapatite-coated titanium samples where its rapid release was reported to promote osteointegration [23]. CaFB can also improve bone health by regulating vitamin D metabolism. A previous pilot clinical trial has shown that boron supplementation in the form of CaFB can increase serum vitamin D and can be effective in improving bone and joint health in elderly patients [3]. Inflammation is another factor that is associated with bone loss due to increased osteoclastogenesis by proinflammatory cytokines and bone resorption. CaFB has been shown to lower inflammation by interacting with inflammatory molecules at cellular and enzymatic level, modulating the serum levels of reactive protein C (CRP) and other cytokines [19,24]. Today, as an alternative boron source, CaFB supplement products are available. Study by Marone et al. has evaluated the safety of CaFB supplements with an *in vivo* study and demonstrated that CaFB products have no mutagenic or genotoxic potential while no adverse toxicologic effects were found after a 90-day sub-chronic toxicology study [25].

These findings support the idea that a controlled local delivery system for CaFB could improve bone tissue regeneration by enhancing osteogenesis and osteoconduction. CaFB is a water-soluble molecule, that is why CaFB release from a traditional hydrogel is expected to be fast by water diffusion. If a CaFB-loaded hydrogel is implanted into the body, CaFB could be lost in a very short period and cannot sustain a therapeutic dose over bone tissue healing time. This reveals the need for a novel biodegradable scaffold that can control the local release of CaFB and sustain steady release over healing time. In light of previous literature, this study hypothesizes that local CaFB delivery can improve bone tissue regeneration, and a biodegradable polymeric scaffold can sustain a controlled release of CaFB. To achieve controlled release of CaFB, this study aimed to design a layer-by-layer polymeric scaffold (PCL/PVA/PCL) as a local delivery system. CaFB-loaded PCL/PVA/PCL scaffold was prepared from poly(ε-caprolactone) (PCL) and polyvinyl alcohol (PVA) polymers using consecutive freeze-drying steps.

Layer-by-layer scaffold fabrication for PCL and PVA has previously been reported for technologies like 3D printing and electrospinning [26,27]. The layered formation has enabled composites of polymers with different chemistry to be fabricated into the same scaffold which allows to tailor drug release and degradation rate [26]. PVA is a hydrophilic polymer that can be degraded in a short time in the body which causes the loss of mechanical strength. To support the mechanical strength of the scaffold, a synthetic polymer like PCL that has slower biodegradation should be used to form a composite [28,29]. In this study, freeze-drying technique was used to produce PCL/PVA/PCL composite scaffold which will carry CaFB in the core PVA layer. PCL layer was formed around the PVA to control the release rate and support the tissue mechanically through healing.

The fabricated scaffold was analyzed in terms of micro- and nano-morphology, time-dependent weight loss, and the capacity of PCL/PVA/PCL scaffold to controlling the release of CaFB. *In vitro* cell viability studies were conducted using Saos-2 (Human osteosarcoma cell line) cells which exhibit an osteoblast phenotype and have shown to be successful in replicating primary human osteoblast interaction with biomaterials [30]. Initially, the effect of CaFB on bone cells was analyzed in detail using i*n vitro* cell culture techniques to assess Saos-2 cell viability under varying concentrations of CaFB. Then, the effect of CaFB-loaded PCL/PVA/PCL scaffold was analyzed via direct incubation of cells on the scaffold surface via an *in vitro* cell viability test.

2. Materials and Methods

2.1. Fabrication of Layer-by-Layer Scaffold

The tri-layered scaffold was fabricated using PCL (Mw: 70.000-90.000 g/mol, Sigma-Aldrich, USA) and PVA (Mw: 72.000 g/mol, Sigma-Aldrich, USA) polymers. Compositions of experimental groups are presented in Table 1 and the steps of scaffold fabrication are presented in Figure 1a.

Table 1. Percent weight composition of experimental groups PVA and PCL/PVA/PCL

Sample ID	Materials					
	PVA		PCL		CaFB	
	wt (mg)	wt (%)	wt (mg)	wt (%)	wt (mg)	wt (%)
PVA	50	95.2	-	-	2.5	4.8
PCL/PVA/PCL	50	18.7	215	80.4	2.5	0.9

Cross-section and schematic representation of the PCL/PVA/PCL scaffold is presented in Figure 1b. PCL solution (10% wt/v) was prepared in glacial acetic acid (Sigma-Aldrich, USA.), which has a freezing temperature around 17°C. To form the bottom layer of the scaffold, 0.7 mL of PCL solution was poured into a 24-well plate and incubated at -80°C overnight. To prepare the PVA layer, 0.5 mL of 10% PVA solution (10% wt/v, dH2O), containing 5 mg/mL of CaFB (Via-Bor, Türkiye) was freeze-dried in a 48-well plate. The PVA sponge was then extracted from the well and placed onto the frozen PCL layer in the 24-well plate. To fill the space surrounding the PVA layer and to achieve the same PCL layer thickness above, 1.4 mL

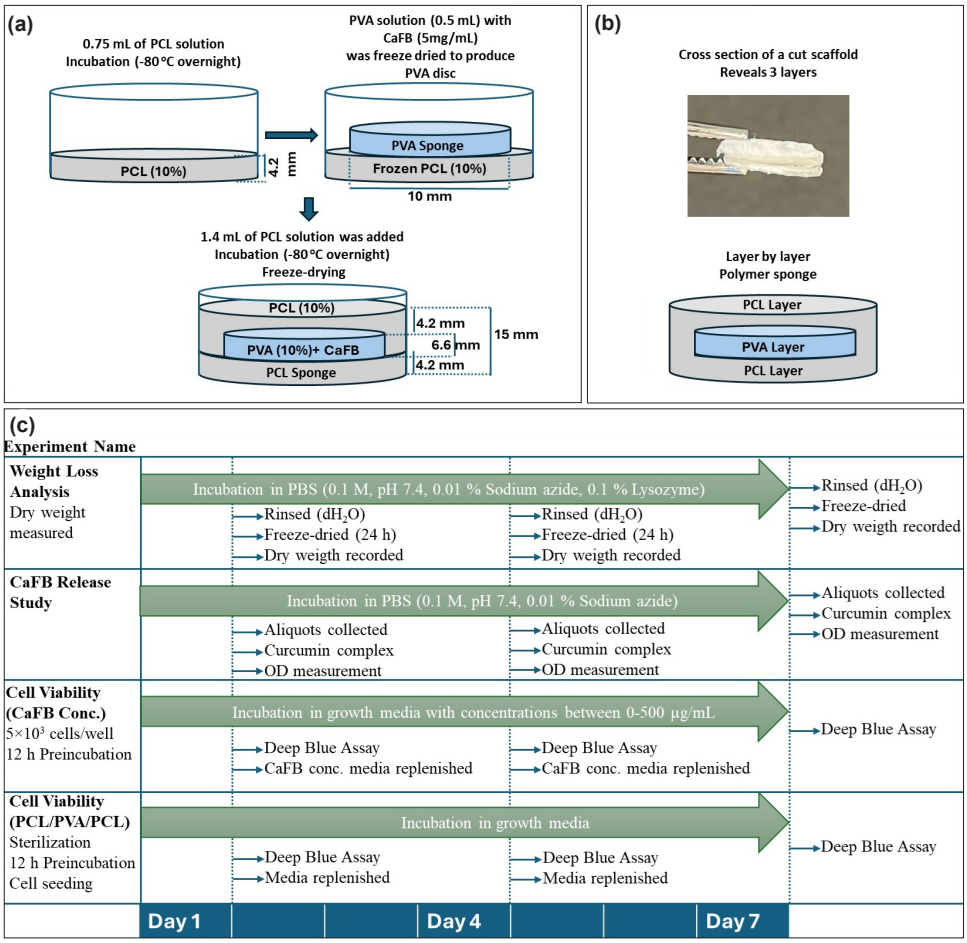

Figure 1. a) Schematic representation of the layer-by-layer scaffold fabrication via freeze drying method. b) Cross section of the PCL/PVA/PCL scaffold and schematic representation of the final form of the layer-by-layer scaffold. c) Diagram showing the experimental steps performed at incubation time points

of PCL solution was added on top of the PVA to form the third layer. The amount of PCL solution needed was calculated according to the volume that will fill the space at the edges of the PVA disc and achieve the same thickness for the top PCL layer. After incubation at -80°C overnight, the plate was freeze-dried to obtain the final layer-by-layer scaffold. The diagram showing the following experiments and incubation time points is presented in Figure 1c.

2.2. Morphological Analysis via Scanning Electron Microscopy

The surface morphology of PCL and PVA layers was characterized via high-resolution field emission scanning electron microscopy (FE-SEM, SU7000, HITACHI, Japan). The surfaces of the samples were coated with a 5 nm gold layer prior to analysis using a vacuum sputter coater (EM ACE 600, Leica, Germany).

2.3. Fourier Transform Infrared (FTIR) Spectroscopy Analysis

Attenuated total reflectance Fourier transform infrared spectroscopy (ATR-FTIR) was used to confirm the chemical structure of CaFB. The IR spectra were recorded using a Spectrum 100 FTIR spectrometer equipped with an ATR accessory (Perkin Elmer, USA). The samples were positioned on the ATR crystal plate and scanned at room temperature across the mid-infrared region (650-4000 cm^{-1}) with a resolution of 4 cm^{-1} in absorbance mode.

2.4. Weight Loss Analysis

After fabricating the layer-by-layer scaffold with freeze-drying, samples were taken out from the wells in which they were cast, and their initial dry weight was measured. To determine the overall hydrolytic and enzymatic degradation rate of the samples over 7 days, they were incubated in a shaking incubator at 37°C (JSR JSSI-300C, Korea), in phosphate buffer solution (PBS) (0.1 M, pH 7.4, 4 mL) containing 0.01 % sodium azide and 0.1 % lysozyme enzyme. A single-layer PVA hydrogel was also tested as the control group for comparison. At each incubation time point, samples were gently rinsed with dH_2O and freeze-dried for 24 h before their weights were recorded. The *in vitro* degradation rate was calculated according to Equ 1.

$$\text{Weight loss } (\%) = \frac{(W_0 - W_t)}{(W_0)} \times 100 \qquad (1)$$

2.5. Study of CaFB Release

To detect CaFB dose-dependent optical density by ultraviolet (UV) absorption, a complex between curcumin and CaFB was formed, and a dose-dependent calibration curve was plotted. Curcumin was initially extracted from turmeric by ethanol extraction method. Briefly, 20 g of turmeric was incubated in an ethanol solution (80%) for 3 h and the solution was filtered through filter paper to remove solid particles from ethanol. Then ethanol was removed under vacuum to obtain the curcumin-bearing extract. Then the weighted extract was resuspended in methanol (10 mg/mL). To study CaFB release, CaFB-loaded PCL/PVA/PCL scaffolds were incubated in 4 mL of PBS (0.1 M, pH 7.4, 0.01 % sodium azide) and aliquots from the release media were collected over 7 days for optical density measurement. For comparison, CaFB release from the single-layer PVA hydrogel was also tested as a control. To detect CaFB in the release media, 1 mL release media and 50 µL of curcumin extract solution were added to an Eppendorf tube and the suspension was vortexed for 1 min. The PBS phase was then removed for optical density measurement at 410 nm wavelength via UV spectrophotometer (PG Instruments Ltd., UK). The amount of CaFB released was calculated from a calibration curve prepared with known concentrations of CaFB.

2.6. In Vitro Cell Viability Analysis

In vitro cell viability tests were conducted using the Saos-2 cell line (ATCC, USA) to determine the effect of different CaFB concentrations on cell metabolism. Dulbecco's Modified Eagle Medium (DMEM) with high glucose, supplemented with 10% fetal bovine serum (FBS) and %1 Penicillin/Streptomycin was used as the growth media. Cell cultures were maintained in a CO_2 incubator (New Brunswick, Galaxy 170 S, Eppendorf, Germany) at 37°C. For the viability experiments to determine concentration-dependent cell viability, 5×10^3 cells/well were seeded in 96-well plate and left for incubation overnight. CaFB was dissolved in the cell media at concentrations ranging between 0-500 µg/mL and introduced to the wells. The Deep Blue cell viability kit (Biolegend, USA) was used to measure cell viability after 1, 4, and 7 days of incubation. Briefly, the Deep Blue solution was added to the wells to achieve a final concentration of 10% (v/v) and the plate was incubated for 4 h at 37°C. Deep Blue solutions were then transferred to a new 96-well plate to measure fluorescence at 535 nm excitation and 590 nm emission with a microplate reader (Varioskan Lux, Thermo Scientific, USA). The media in all the wells were replaced with fresh media, maintaining the same CaFB concentrations and incubation continued. Results were compared to the control group, which did not contain CaFB.

The effect of direct contact with CaFB releasing scaffold on cell viability was analyzed by direct seeding of cells on the surface of the scaffold. After the scaffold was fabricated via freeze-drying, each surface of the samples was sterilized with UV light for 30 min in a well plate. The samples were then incubated in cell media overnight and the wet scaffolds were used for cell seeding after the media was removed. Cells (2.5×10^4 cells/scaffold) were transferred to the scaffold surface in a 20 µL drop of media and incubated for 2 h in a humidified CO_2 incubator to ensure that the cells attached to the scaffold. Each well was then filled with media to cover the scaffolds. Deep Blue tests were conducted on days 1, 4, and 7. Media for each scaffold was changed to fresh DMEM media on the test days.

2.7. Statistical Analysis

Statistically significant differences between experimental groups were calculated using SPSS software (Version 22, IBM, USA). Independent samples t-tests and One-Way Analysis of Variance (ANOVA) were used to compare mean values and measure statistically significant differences between groups. The level of significance was set at $P<0.05$.

3. Results and Discussion

The surface micro-nano morphology of the layered scaffold was observed by FE-SEM analyses and the morphology of the inner PVA layer was observed after separating the scaffold layers (Figure 2).

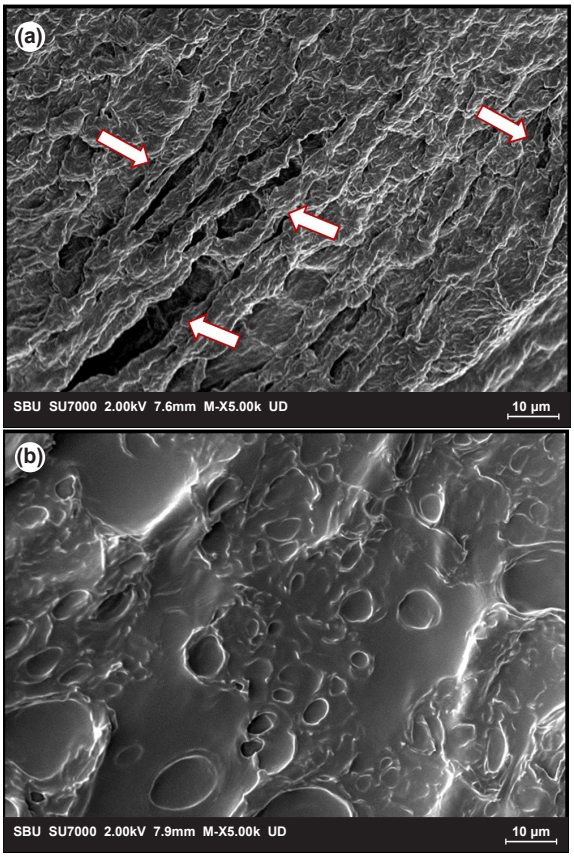

Figure 2. FE-SEM images of scaffold layers, PCL (a) and PVA (b). Arrows show the pores that have been created on the surface. Images were taken at 5000X magnification and scale bars show 10 µm length

PCL layer was designed to surround the surface of the inner PVA layer of the scaffold to control the release of CaFB from the inner PVA layer. FE-SEM images of the PCL layer present a rough surface with pores that connect to the depths of the layer (Figure 2a). Pore size is one of the factors that determines the interaction of bone cells with the scaffold which will determine cell fate and tissue regeneration [31]. Porous structure and interconnectivity in scaffolds have been reported to be essential for osteoconduction. A minimum pore size of 100 µm has been reported to be essential for osteointegration and pores larger than 300 µm have been reported to be needed for the vascularization of the healing bone tissue [32]. Surface with a smaller pore size of around 62 µm has been reported to promote osteogenic gene expression (RUNX2, ALP, BSP, COL, and OPN) while viability and proliferation of osteoblast cells were reported to be improved on surfaces with larger pores [33]. A study of Lee et al. has evaluated the interaction of MG63 osteoblast-like cells with PCL membrane surfaces that have pore sizes between 0.2 to 8 µm. Studies have revealed that as the pore size increases and gets closer to 8 µm, cell differentiation and matrix production are increased which was observed by higher total protein synthesis and ALP specific activity [34]. These results have shown that the effect of porosity on osteoblast-like cells can vary on different surfaces and has no strict boundaries. The outermost surface of the PCL/PVA/PCL scaffold is the PCL layer and SEM images of the PCL surface have revealed micropores between 2 to 10 µm. The observed pore diameter has previously been associated with enhanced cell differentiation, and matrix production in osteoblast-like cells [34]. Also, after implantation, the polymer surface is expected to biodegrade over time, and this biodegradation could open new pores and increase the diameter of the existing pores which will support better osteointegration. The presence of surface roughness is known to enhance osteoblasts attachment and adhesion while improving osteogenic activity and mineralization [35,36]. Therefore, roughness is expected to support a better interaction with bone tissue and create an osteoconductive scaffold. Surface roughness is also known to increase protein adhesion which will improve cell adhesion and differentiation of bone cells was reported to be enhanced on rough surfaces compared to smooth surfaces [37]. On the other hand, the inner layer of the scaffold, the PVA layer, has shown a smoother micro-nano surface topography with close pore structures. The main role of the PVA layer is to carry CaFB in the core of the scaffold and support the controlled release of CaFB over time. Therefore, the PVA layer is not expected to have direct contact with regenerating tissue as PVA polymer will also leave the scaffold over time by degradation.

FTIR analysis was performed to verify the chemical structure of CaFB (Figure 3). The broad band centered at 3247 cm^{-1} was observed in the IR spectrum of metal complexes of saccharides and can be attributed to the

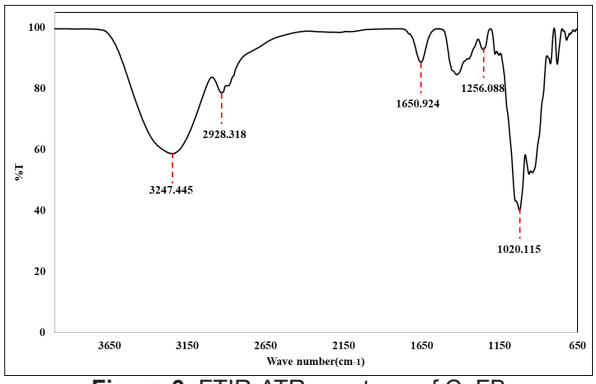

Figure 3. FTIR-ATR spectrum of CaFB

B-O bond. The stretching of the CH_2 group creates a band at 2928 cm^{-1} with a shoulder around 2880 cm^{-1}. The band at 1650 cm^{-1} is attributed to the stretching motion of the terminal B-O linkage of fructoborate [15]. The IR spectrum formed by chemical groups CH, OH, COH, CH_2OH, and CH_2 in the CaFB structure can be observed in the bands around 1421 cm^{-1} and a band created by water crystallization can be seen at 1256 cm^{-1}. Vibrational bands of characteristics groups to fructose and CaFB, CO, CH_2OH, C-CH, CH_2, C-C, and C-O-C, can be observed between 1200 to 650 cm^{-1} [38].

Weight loss analysis of the scaffold was conducted in PBS solution that contains lysozyme enzyme (Figure 4a). Lysozyme was added to mimic physiologic conditions since lysozyme is a common enzyme that exists in blood and serum. The use of the enzyme also mimics the wound site since the natural level

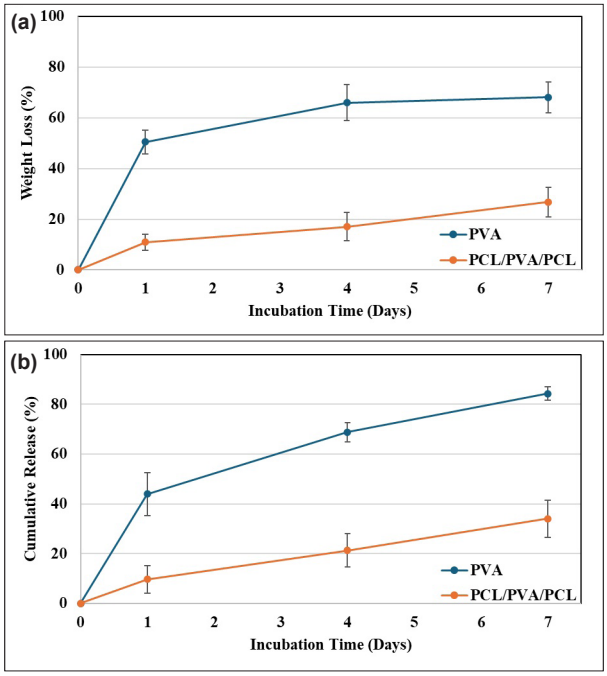

Figure 4. Percent weight loss of single-layered PVA hydrogel and PCL/PVA/PCL scaffold through 7 days of incubation in PBS supplemented with lysozyme (a) and percent CaFB cumulative release of single-layered PVA hydrogel and PCL/PVA/PCL scaffold through 7 days of incubation in PBS (b)

of this enzyme increases in tissues when there is an inflammation or infection [39]. PCL is a hydrophobic biodegradable polymer that has long-term stability in the body and is expected to remain structurally stable *in vitro* with little to no degradation in several weeks [40]. The tri-layered scaffold was produced by freeze-drying and during the freezing step, PVA polymer chains form intermolecular and intramolecular hydrogen bonds and crystalline regions which achieve physical crosslinking [41]. Although PVA is a water-soluble polymer, the ability of PVA to form physical crosslinking has previously been reported to decrease its degradation rate and weight loss in aqueous environment. Previous studies have applied several freeze and thaw cycles to improve physical crosslinking and achieved slower degradation [42-44]. On the other hand, in this study PVA layer was produced via freeze dryer, directly after freezing in order to avoid further delaying PVA degradation, thereby promoting CaFB release. Also, a hydrophobic PCL layer was fabricated to cover the PVA surface to control CaFB release. When PVA as a single layer was incubated for 24 h, 50.41±4.7% of the hydrogel was lost. After 3 and 7 days in PBS, weight loss of the single-layer PVA scaffold has increased to 65.9±7.1% and 68.03±6.1% (Figure 4a). The initial fast degradation can be attributed to polymer chains that did not form entanglement and physical crosslinking. After initial mass loss, the weight of the hydrogel remained stable. Weight loss of the tri-layered scaffold was lower compared to the single-layer PVA scaffold (26.8±5.7% at 7 days of incubation). Also, initial weight loss was only at 10.8±3.1% after one day of incubation. This is due to the hydrophobic PCL layer covering the PVA surface and slowing down the water diffusion into the PVA layer [45]. Since the PCL layer covering the PVA will decrease the diffusion of aqueous media, the weight loss of the PVA layer will be lower in the same incubation period. The same reason also created a control mechanism for CaFB release from the scaffold groups and achieved long-term release (Figure 4b). The single-layer PVA hydrogel created a burst CaFB release of 43.9±8.6% on day one and achieved a cumulative release of 84.2±2.6% after 7 days of release. On the other hand, the PCL layer surrounding the tri-layered scaffold was able to control and prevent the bust release of CaFB achieving a steady increase in cumulative release with a 33.9±7.4% release after 7 days. Tri-layered design of the scaffold has proven to be successful in controlling the release of CaFB.

The effect of CaFB dose on Saos-2 cell viability was analyzed with CaFB concentrations between 1.95 to 500 µg/ml after 1, 4, and 7 days of incubation (Figure 5a). Results have shown that, even at concentrations as high as 500 µg/ml, CaFB has not shown a negative effect on cells, and viability was preserved through 7 days. After 1 and 4 days of incubation cells treated with 31.25 µg/ml CaFB have shown improved cell viability. After 7 days of incubation, cell viability was higher in groups treated with 250, 125, 62.5, and 31.25 µg/ml CaFB concentrations. In the second trial for cell viability, Saos-2 cells were directly seeded onto the PCL/PVA/PCL scaffold with CaFB loaded inside the PVA layer at the core (Figure 5b). The results of cell viability under different CaFB doses and CaFB release studies were considered to decide the amount of CaFB that will be loaded into the PCL/PVA/PCL scaffold. The CaFB dose study has shown that CaFB concentration between 62.5 and 250 µg/mL has supported the highest cell viability after 7 days of incubation. According to the results of the release study, after 1, 4, and 7 days of incubation, the cumulative release of CaFB was expected to be roughly around 9.7, 21.2, and 33.9%. With an initial CaFB loading of 2.5 mg, the scaffold was expected to release, 60.6, 71.9, and 79.3 µg/mL CaFB between incubation time points in 4 mL of media when media replenishment was also considered. To obtain a steady CaFB release within the effective dose, 2.5 mg of CaFB was loaded into the scaffold. Results showed that the PCL/PVA/PCL scaffold has supported the viability of cells through 7 days when compared to a monolayer of cells seeded in a well. After 7 days of incubation, the viability of cells on the scaffold was slightly higher as compared to the control group. The CaFB release from the tri-layered scaffold was shown to be at a slow rate and reaching 33.9±7.4% after 7 days and the CaFB dose study revealed that CaFB treatment starts to improve cell viability after 7 days of incubation at certain concentrations. This could explain why the CaFB-releasing scaffold improved

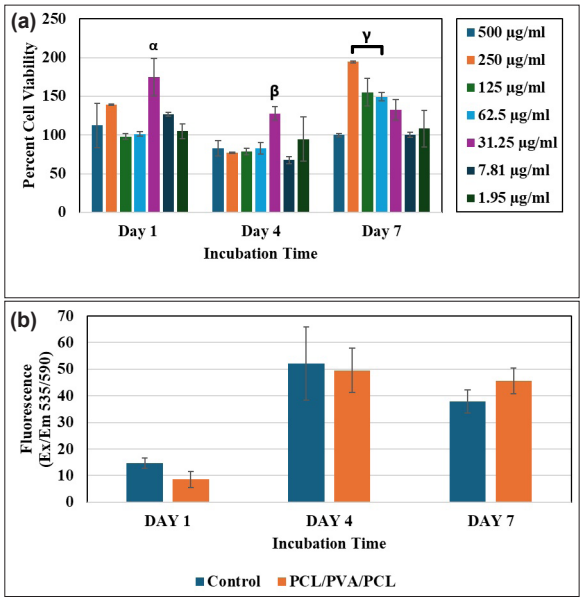

Figure 5. The effect of CaFB concentrations on Saos-2 cell viability through 7 days of incubation. The percent cell viability was calculated with respect to cells incubated with only growth media without CaFB as the control (a). Saos-2 cell viability through 7 days of incubation on control well and PCL/PVA/PCL scaffold (b). α: Statistically significant difference of 31.25 µg/ml group from other groups at day 1 of incubation ($P<0.05$). β: Statistically significant difference of 31.25 µg/ml group from other groups except group 1.95 µg/ml at day 4 ($P<0.05$). γ: Statistically significant difference of 250, 125 and 62.5 µg/ml groups from 500, 7.81, 1.95 µg/ml groups at day 7 ($P<0.05$)

viability after 7 days when compared to the control. The calcium and boron ions in CaFB were responsible for enhanced viability of Saos-2 cells which are known to promote osteogenic activities and enhance bone cell viability [46,47]. The study of Capati et al. analyzed the effects of boron on osteoblastic activity in NOS-1 cells i*n vitro* and reported that even in low concentrations, boron promotes proliferation and differentiation [10]. Another study showed that boron is able to improve bone health and strength *in vivo* in rabbits [4]. CaFB was previously reported to increase osteopontin and osteocalcin expression in bone tissue and the boron that it contains has a role in increasing the expression of genes responsible for mineralization and hormones like 17β-estradiol (E2) and testosterone) [12,48]. A pilot study that treats 13 middle-aged subjects who are deficient in vitamin D with CaFB supplementation for 60 days, has reported a significant increase in 25 (OH) vitamin D levels [3]. This shows that CaFB can also improve bone health by regulating Vitamin D metabolism. Several previous studies have also adapted PCL/PVA/PCL layered scaffold structure and used different fabrication techniques to achieve this layered formation. Study of Harmanci et al. used 3D printing to achieve PCL/PVA/PCL layered scaffold for diabetic wound healing and evaluated scaffolds' biocompatibility by testing viability of human fibroblast cell line (HFF-1) *in vitro*. HFF-1 cell viability on PCL/PVA/PCL scaffold was reported to be biocompatible with around 89.2% viability after 7 days [26]. Another study has also produced a PCL/PVA/PCL layered scaffold by electrospinning to assess the wound-healing potential of the scaffold. Biocompatibility of the scaffold was evaluated on the L929 mouse fibroblast cell line and the PCL/PVA/PCL scaffold was found to be compatible with over 80% viability after 2 days [27]. PCL and PVA polymers have also been used in bone tissue engineering studies in fiber forms which were produced by layers or blends [49-53]. Previously, co-axial fibers have been fabricated by PCL shell and PVA core, and fabricated scaffold has shown to support the viability and osteogenic differentiation of mesenchymal stem cells [49]. Pattanashetti et al., demonstrated biocompatibility of multilayered PCL/PVA scaffolds by showing the proliferation of MG-63 bone osteosarcoma cells [53]. Ebrahimi et al. reported the biocompatibility of PCL/PVA nanofibrous membranes and showed that membranes support the differentiation of human endometrial stem cells to osteogenic linage [51]. Similarly, Maheshwari et al. reported enhanced adhesion and proliferation of MG-63 osteoblast cells on PVA/HAp/PCL scaffolds [52]. These studies have shown the potential of PCL/PVA composite scaffold used for bone tissue engineering. This study demonstrated the fabrication of a PCL/PVA/PCL scaffold via freeze-drying method and proved that the PCL/PVA/PCL scaffold supports the viability of Saos-2 cells.

The results of this study have shown that local release of CaFB from a bone scaffold can improve bone tissue regeneration by controlled release of CaFB. The results showed that a designed layered scaffold was able to control the release of CaFB and loading of CaFB into a biodegradable scaffold was found to be a promising approach for local delivery. Additionally, CaFB has shown to increase cell viability while CaFB-loaded scaffold was successfully supported cell viability. These results have supported the hypothesis of the study by proving control of the PCL/PVA/PCL scaffold on CaFB release and the ability of the scaffold to support cell viability.

4. Conclusions

This study has demonstrated the production of a CaFB-releasing polymeric scaffold system for bone tissue regeneration. A tri-layered PCL/PVA/PCL scaffold was designed to carry CaFB within the hydrophilic PVA core and the core was surrounded by hydrophobic PCL polymer. The presence of the PCL layer has been shown to successfully control PVA weight loss, achieving a stable scaffold structure. The hydrophobic PCL layer was also successful in slowing down the CaFB release rate by limiting the rate of water diffusion. An *in vitro* study has shown that CaFB has dose dependent effect on Saos-2 cell viability and the highest improvement in viability was recorded after 7 days of CaFB treatment. The fabricated CaFB-releasing tri-layered PCL/PVA/PCL scaffold has supported cell viability through 7 days and was shown to be biocompatible. This study has shown that controlled release of CaFB can be achieved with polymeric scaffolds and scaffolds carrying CaFB are promising as biomaterials to improve bone tissue regeneration.

5. Acknowledgements

CaFB was a kind gift from Via-Bor (Türkiye). The FTIR-ATR analysis was performed by Yıldız Technical University, Application and Research Center for Science and Technology (BİTUAM).

References

[1] Rondanelli, M., Faliva, M. A., Peroni, G., Infantino, V., Gasparri, C., Iannello, G., … & Tartara, A. (2020). Pivotal role of boron supplementation on bone health: A narrative review. *Journal of Trace Elements in Medicine and Biology*, *62*, 126577. https://doi.org/10.1016/J.JTEMB.2020.126577

[2] Mahdavi, R., Belgheisi, G., Haghbin-Nazarpak, M., Omidi, M., Khojasteh, A., & Solati-Hashjin, M. (2020). Bone tissue engineering gelatin-hydroxyapatite/graphene oxide scaffolds with the ability to release vitamin D: fabrication, characterization, and in vitro study. *Journal of Materials Science: Materials in Medicine*, *31*(11), 97. https://doi.org/10.1007/s10856-020-06430-5

[3] Miljkovic, D., Miljkovic, N., & McCarty, M. F. (2004). Up-regulatory impact of boron on vitamin D function-Does it reflect inhibition of 24-hydroxylase? *Medical Hypotheses*, *63*(6), 1054-1056. https://doi.org/10.1016/j.mehy.2003.12.053

[4] Hakki, S. S., Dundar, N., Kayis, S. A., Hakki, E. E., Hamurcu, M., Kerimoglu, U., … & Nielsen, F. H. (2013). Boron enhances strength and alters mineral composition of bone in rabbits fed a high energy diet. *Journal of Trace Elements in Medicine and Biology*, *27*(2), 148-153. https://doi.org/10.1016/J.JTEMB.2012.07.001

[5] Armstrong, T. A., Spears, J. W., Crenshaw, T. D., & Nielsen, F. H. (2000). Boron supplementation of a semipurified diet for weanling pigs improves feed efficiency and bone strength characteristics and alters plasma lipid metabolites. *The Journal of Nutrition*, *130*(10), 2575-2581. https://doi.org/10.1093/jn/130.10.2575

[6] Naghii, M. R., Torkaman, G., & Mofid, M. (2006). Effects of boron and calcium supplementation on mechanical properties of bone in rats. *BioFactors*, *28*(3-4), 195-201. https://doi.org/10.1002/biof.5520280306

[7] Nielsen, F. H., & Stoecker, B. J. (2009). Boron and fish oil have different beneficial effects on strength and trabecular microarchitecture of bone. *Journal of Trace Elements in Medicine and Biology*, *23*(3), 195-203. https://doi.org/10.1016/j.jtemb.2009.03.003

[8] Ying, X., Cheng, S., Wang, W., Lin, Z., Chen, Q., Zhang, W., … & Lu, C. Z. (2011). Effect of boron on osteogenic differentiation of human bone marrow stromal cells. *Biological Trace Element Research*, *144*(1-3), 306-315. https://doi.org/10.1007/s12011-011-9094-x

[9] Hakki, S. S., Bozkurt, B. S., & Hakki, E. E. (2010). Boron regulates mineralized tissue-associated proteins in osteoblasts (MC3T3-E1). *Journal of Trace Elements in Medicine and Biology*, *24*(4), 243-250. https://doi.org/10.1016/j.jtemb.2010.03.003

[10] Capati, M. L. F., Nakazono, A., Igawa, K., Ookubo, K., Yamamoto, Y., Yanagiguchi, K., … & Hayashi, Y. (2016). Boron accelerates cultured osteoblastic cell activity through calcium flux. *Biological Trace Element Research*, *174*(2), 300-308. https://doi.org/10.1007/s12011-016-0719-y

[11] Seydibeyoğlu, M. Ö., Caka, M., Ulucan-Karnak, F., Onak, G., Uzel, A., Ozyildiz, F., & Karaman, O. (2021). Bone cement formulation with reduced heating of bone cement resin. *Journal of Boron*, *6*(2), 274-282. https://doi.org/10.30728/BORON.835919

[12] Uysal, İ., Yılmaz, B., & Evis, Z. (2020). Boron doped hydroxapatites in biomedical applications. *Journal of Boron*, *5*(4), 199-208. https://doi.org/10.30728/BORON.734804

[13] Aki, D., Ulag, S., Unal, S., Sengor, M., Ekren, N., Lin, C. C., … & Gunduz, O. (2020). 3D printing of PVA/hexagonal boron nitride/bacterial cellulose composite scaffolds for bone tissue engineering. *Materials & Design*, *196*, 109094. https://doi.org/10.1016/J.MATDES.2020.109094

[14] Butan, S., Filimon, V., & Bounegru, A. V. (2024). Human health impact and advanced chemical analysis of fructoborates: A comprehensive review. *Chemical Papers*, *78*(9), 5151-5167. https://doi.org/10.1007/S11696-024-03428-Z/FIGURES/6

[15] Wagner, C. C., Ferraresi Curotto, V., Pis Diez, R., & Baran, E. J. (2008). Experimental and theoretical studies of calcium fructoborate. *Biological Trace Element Research*, *122*(1), 64-72. https://doi.org/10.1007/s12011-007-8060-0

[16] Capozzi, A., Scambia, G., & Lello, S. (2020). Calcium, vitamin D, vitamin K2, and magnesium supplementation and skeletal health. *Maturitas*, *140*, 55-63. https://doi.org/10.1016/J.MATURITAS.2020.05.020

[17] Marie, P. J. (2010). The calcium-sensing receptor in bone cells: A potential therapeutic target in osteoporosis. *Bone*, *46*(3), 571-576. https://doi.org/10.1016/j.bone.2009.07.082

[18] Chai, Y. C., Carlier, A., Bolander, J., Roberts, S. J., Geris, L., Schrooten, J., … & Luyten, F. P. (2012). Current views on calcium phosphate osteogenicity and the translation into effective bone regeneration strategies. *Acta Biomaterialia*, *8*(11), 3876-3887. https://doi.org/10.1016/j.actbio.2012.07.002

[19] Mogoşanu, G. D., Biţă, A., Bejenaru, L. E., Bejenaru, C., Croitoru, O., Rău, G., … & Scorei, R. I. (2016). Calcium fructoborate for bone and cardiovascular health. *Biological Trace Element Research*, *172*(2), 277-281. https://doi.org/10.1007/s12011-015-0590-2

[20] Turck, D., Castenmiller, J., De Henauw, S., Hirsch-Ernst, K. I., Kearney, J., Maciuk, A., … & Knutsen, H. K. (2021). Safety of calcium fructoborate as a novel food pursuant to Regulation (EU) 2015/2283. *EFSA Journal*, *19*(7). https://doi.org/10.2903/j.efsa.2021.6661

[21] Manda, D., Popa, O., Vladoiu, S., & Dumitrache, C. (2009). Calcium fructoborate effect on osteoblast mineralization in vitro. *Bone*, *44*, S298-S299. https://doi.org/10.1016/J.BONE.2009.03.545

[22] Scorei, R. I., & Rotaru, P. (2011). Calcium fructoborate-Potential anti-inflammatory agent. *Biological Trace Element Research*, *143*(3), 1223-1238. https://doi.org/10.1007/s12011-011-8972-6

[23] Văruţ, R. M., Melinte, P. R., Pîrvu, A. S., Gîngu, O., Sima, G., Oancea, C. N., … & Neamţu, J. (2020). Calcium fructoborate coating of titanium-hydroxyapatite implants by chemisorption deposition improves implant osseointegration in the femur of New Zealand White rabbit experimental model. *Romanian Journal of Morphology and Embryology*, *61*(4), 1235-1247. https://doi.org/10.47162/RJME.61.4.25

[24] Scorei, I. D., & Scorei, R. I. (2013). Calcium fructoborate helps control inflammation associated with diminished bone health. *Biological Trace Element Research*, *155*(3), 315-321. https://doi.org/10.1007/s12011-013-9800-y

[25] Marone, P. A., Heimbach, J. T., Nemzer, B., & Hunter, J. M. (2016). Subchronic and genetic safety evaluation of a calcium fructoborate in rats. *Food and Chemical Toxicology*, *95*, 75-88. https://doi.org/10.1016/j.fct.2016.06.021

[26] Harmanci, S., Dutta, A., Cesur, S., Sahin, A., Gunduz, O., Kalaskar, D. M., & Ustundag, C. B. (2022). Production of 3D printed bi-layer and tri-layer sandwich scaffolds with polycaprolactone and poly (vinyl alcohol)-metformin towards diabetic wound healing. *Polymers*, *14*(23), 5306. https://doi.org/10.3390/polym14235306

[27] Saeed, S. M., Mirzadeh, H., Zandi, M., & Barzin, J. (2017). Designing and fabrication of curcumin loaded

PCL/PVA multi-layer nanofibrous electrospun structures as active wound dressing. *Progress in Biomaterials*, *6*(1-2), 39-48. https://doi.org/10.1007/s40204-017-0062-1

[28] Ghiyasi, Y., Salahi, E., & Esfahani, H. (2021). Synergy effect of Urtica dioica and ZnO NPs on microstructure, antibacterial activity and cytotoxicity of electrospun PCL scaffold for wound dressing application. *Materials Today Communications*, *26*, 102163. https://doi.org/10.1016/j.mtcomm.2021.102163

[29] Govender, M., Indermun, S., Kumar, P., Choonara, Y. E., & Pillay, V. (2018). 3D printed, PVA-PAA hydrogel loaded-polycaprolactone scaffold for the delivery of hydrophilic in-situ formed sodium indomethacin. *Materials*, *11*(6), 1006. https://doi.org/10.3390/ma11061006

[30] Dvorakova, J., Wiesnerova, L., Chocholata, P., Kulda, V., Landsmann, L., Cedikova, M., … & Babuska, V. (2023). Human cells with osteogenic potential in bone tissue research. *BioMedical Engineering OnLine*, *22*(1), 33. https://doi.org/10.1186/s12938-023-01096-w

[31] Arpornmaeklong, P., Suwatwirote, N., Pripatnanont, P., & Oungbho, K. (2007). Growth and differentiation of mouse osteoblasts on chitosan-collagen sponges. *International Journal of Oral and Maxillofacial Surgery*, *36*(4), 328-337. https://doi.org/10.1016/j.ijom.2006.09.023

[32] Ratnayake, J. T. B., Gould, M. L., Shavandi, A., Mucalo, M., & Dias, G. J. (2017). Development and characterization of a xenograft material from New Zealand sourced bovine cancellous bone. *Journal of Biomedical Materials Research Part B: Applied Biomaterials*, *105*(5), 1054-1062. https://doi.org/10.1002/jbm.b.33644

[33] Teixeira, L. N., Crippa, G. E., Lefebvre, L.-P., De Oliveira, P. T., Rosa, A. L., & Beloti, M. M. (2012). The influence of pore size on osteoblast phenotype expression in cultures grown on porous titanium. *International Journal of Oral and Maxillofacial Surgery*, *41*(9), 1097-1101. https://doi.org/10.1016/j.ijom.2012.02.020

[34] Lee, S. J., Choi, J. S., Park, K. S., Khang, G., Lee, Y. M., & Lee, H. B. (2004). Response of MG63 osteoblast-like cells onto polycarbonate membrane surfaces with different micropore sizes. *Biomaterials*, *25*(19), 4699-4707. https://doi.org/10.1016/j.biomaterials.2003.11.034

[35] Dwivedi, R., Kumar, S., Pandey, R., Mahajan, A., Nandana, D., Katti, D. S., & Mehrotra, D. (2020). Polycaprolactone as biomaterial for bone scaffolds: Review of literature. *Journal of Oral Biology and Craniofacial Research*, *10*(1), 381-388. https://doi.org/10.1016/j.jobcr.2019.10.003

[36] Filipov, E., Angelova, L., Vig, S., Fernandes, M. H., Moreau, G., Lasgorceix, M., … & Daskalova, A. (2022). Investigating potential effects of ultra-short laser-textured porous poly-ε-caprolactone scaffolds on bacterial adhesion and bone cell metabolism. *Polymers*, *14*(12), 2382. https://doi.org/10.3390/polym14122382

[37] Melčová, V., Krobot, Š., Šindelář, J., Šebová, E., Rampichová, M. K., & Přikryl, R. (2024). The effect of surface roughness and wettability on the adhesion and proliferation of Saos-2 cells seeded on 3D printed poly(3-hydroxybutyrate)/polylactide (PHB/PLA) surfaces. *Results in Surfaces and Interfaces*, *16*, 100271. https://doi.org/10.1016/j.rsurfi.2024.100271

[38] Rotaru, P., Scorei, R., Hărăbor, A., & Dumitru, M. D. (2010). Thermal analysis of a calcium fructoborate sample. *Thermochimica Acta*, *506*(1-2), 8-13. https://doi.org/10.1016/j.tca.2010.04.006

[39] Lan, W., Zhang, X., Xu, M., Zhao, L., Huang, D., Wei, X., & Chen, W. (2019). Carbon nanotube reinforced polyvinyl alcohol/biphasic calcium phosphate scaffold for bone tissue engineering. *RSC Advances*, *9*(67), 38998-39010. https://doi.org/10.1039/C9RA08569F

[40] Yoshioka, T., Kamada, F., Kawazoe, N., Tateishi, T., & Chen, G. (2010). Structural changes and biodegradation of PLLA, PCL, and PLGA sponges during in vitro incubation. *Polymer Engineering & Science*, *50*(10), 1895-1903. https://doi.org/10.1002/pen.21714

[41] Waresindo, W. X., Luthfianti, H. R., Edikresnha, D., Suciati, T., Noor, F. A., & Khairurrijal, K. (2021). A freeze-thaw PVA hydrogel loaded with guava leaf extract: physical and antibacterial properties. *RSC Advances*, *11*(48), 30156-30171. https://doi.org/10.1039/D1RA04092H

[42] Wu, F., Gao, J., Xiang, Y., & Yang, J. (2023). Enhanced mechanical properties of PVA hydrogel by low-temperature segment self-assembly vs. freeze-thaw cycles. *Polymers*, *15*(18), 3782. https://doi.org/10.3390/polym15183782

[43] Lotfipour, F., Alami-Milani, M., Salatin, S., Hadavi, A., & Jelvehgari, M. (2019). Freeze-thaw-induced cross-linked PVA/chitosan for oxytetracycline-loaded wound dressing: The experimental design and optimization. *Research in Pharmaceutical Sciences*, *14*(2), 175. https://doi.org/10.4103/1735-5362.253365

[44] Adelnia, H., Ensandoost, R., Shebbrin Moonshi, S., Gavgani, J. N., Vasafi, E. I., & Ta, H. T. (2022). Freeze/thawed polyvinyl alcohol hydrogels: Present, past and future. *European Polymer Journal*, *164*, 110974. https://doi.org/10.1016/j.eurpolymj.2021.110974

[45] Zhou, X., Hou, C., Chang, T.-L., Zhang, Q., & Liang, J. F. (2020). Controlled released of drug from doubled-walled PVA hydrogel/PCL microspheres prepared by single needle electrospraying method. *Colloids and Surfaces B: Biointerfaces*, *187*, 110645. https://doi.org/10.1016/j.colsurfb.2019.110645

[46] Della Pepa, G. (2016). Microelements for bone boost: the last but not the least. *Clinical Cases in Mineral and Bone Metabolism*. https://doi.org/10.11138/ccmbm/2016.13.3.181

[47] Decker, S., Arango-Ospina, M., Rehder, F., Moghaddam, A., Simon, R., Merle, C., … & Westhauser, F. (2022). In vitro and in ovo impact of the ionic dissolution products of boron-doped bioactive silicate glasses on cell viability, osteogenesis and angiogenesis. *Scientific Reports*, *12*(1), 8510. https://doi.org/10.1038/s41598-022-12430-y

[48] Uzunçakmak, S. K. (2023). Sıçanlarda borik asit, kalsiyum fruktoborat ve potasyum bor sitratın kemik sağlığı ve sistemik inflamatuvar belirteçler üzerine etkisi. *Bor Dergisi*, *8*(1), 9-15. https://doi.org/10.30728/BORON.1142574

[49] Prosecká, E., Buzgo, M., Rampichová, M., Kocourek, T., Kochová, P., Vysloužilová, L., … & Amler, E. (2012).

Thin-layer hydroxyapatite deposition on a nanofiber surface stimulates mesenchymal stem cell proliferation and their differentiation into osteoblasts. *Journal of Biomedicine and Biotechnology*, 2012, 1-10. https://doi.org/10.1155/2012/428503

[50] Mahalingam, S., Bayram, C., Gultekinoglu, M., Ulubayram, K., Homer-Vanniasinkam, S., & Edirisinghe, M. (2021). Co-axial gyro-spinning of PCL/PVA/ha core-sheath fibrous scaffolds for bone tissue engineering. *Macromolecular Bioscience*, *21*(10). https://doi.org/10.1002/mabi.202100177

[51] Ebrahimi, L., Farzin, A., Ghasemi, Y., Alizadeh, A., Goodarzi, A., Basiri, A., … & Ai, J. (2021). Metformin-loaded PCL/PVA fibrous scaffold preseeded with human endometrial stem cells for effective guided bone regeneration membranes. *ACS Biomaterials Science & Engineering*, *7*(1), 222-231. https://doi.org/10.1021/acsbiomaterials.0c00958

[52] Uma Maheshwari, S., Samuel, V. K., & Nagiah, N. (2014). Fabrication and evaluation of (PVA/HAp/PCL) bilayer composites as potential scaffolds for bone tissue regeneration application. *Ceramics International*, *40*(6), 8469-8477. https://doi.org/10.1016/j.ceramint.2014.01.058

[53] Pattanashetti, N. A., Achari, D. D., Torvi, A. I., Doddamani, R. V., & Kariduraganavar, M. Y. (2020). Development of multilayered nanofibrous scaffolds with PCL and PVA:NaAlg using electrospinning technique for bone tissue regeneration. *Materialia*, *12*, 100826. https://doi.org/10.1016/j.mtla.2020.100826

TENMAK BOREN BOR ARAŞTIRMA ENSTİTÜSÜ

BOR DERGİSİ
JOURNAL OF BORON
https://dergipark.org.tr/boron

Bor katkılı BNT-6BT piezoseramik toz takviyeli PVDF kompozitlerin üretimi ve karakterizasyonu

Serhat Tıkız [1,2], **Metin Özgül** [1,2,*]

[1]*Afyon Kocatepe Üniversitesi, Mühendislik Fakültesi, Malzeme Bilimi ve Mühendisliği Bölümü, Afyonkarahisar, 03200, Türkiye*
[2]*Afyon Kocatepe Üniversitesi, Teknoloji Uygulama ve Araştırma Merkezi (TUAM) Müdürlüğü, Afyonkarahisar, 03200, Türkiye*

MAKALE BİLGİSİ

Makale Geçmişi:
İlk gönderi 10 Eylül 2024
Kabul 25 Ekim 2024
Online 31 Aralık 2024

Araştırma Makalesi

DOI: 10.30728/boron.1547636

Anahtar kelimeler:
Bor katkılı BNT-6BT
Elektroeğirme
Hidrotermal yöntem
Kurşunsuz piezoseramikler
PVDF polimer

ÖZET

Piezoelektrik malzemeler, mekanik enerjiyi elektrik enerjisine ve tersinir olarak da elektrik enerjisini mekanik enerjiye dönüştürme kabiliyetleri sayesinde otomotivden sağlığa kadar pek çok sektörde; sensör, aktüatör ve transdüser gibi uygulamalar için yoğun ilgi görmektedir. Çevreci ve yenilenebilir enerji üretiminin büyük önem kazandığı günümüzde, yeni geliştirilen piezoelektrik malzemeler pek çok alanda ideal çözümler sunmaktadırlar. Nanomalzemeler ve karakterizasyon tekniklerinde yaşanan ilerlemeler de araştırmacılara yenilikçi yaklaşımlar geliştirme imkânları sunmaktadır. Son yıllarda artan çevre duyarlılığı ile birlikte Pb içerikli malzeme kompozisyonlarına alternatif benzer üstün özellikli malzeme geliştirilmesi araştırmaları önemli çıktılar ortaya koymuştur. Bu çerçevede bu çalışmada, en yaygın kullanılan Pb içerikli kurşun zirkonat titanat (PZT) seramiklere benzer yapı ve özellikler sunan $0,94(Bi_{0,5}Na_{0,5})TiO_3$-$0,06BaTiO_3$ BNT-6BT piezoseramiklerin bor (B^{+3}) katkılı tozlarının üretimi ve bu tozların polivinilidin florür (PVDF) polimerinde kullanımı ile üstün özellikli hafif ve esnek kompozitlerin üretimi amaçlanmıştır. Hidrotermal yöntemle üretilen piezoseramik tozların karakterizasyonu x-ışını difraksyonu (XRD) ve taramalı elektron mikroskobu (SEM-EDX) analizleri ile gerçekleştirilmiştir. Piezoseramik tozlar, PVDF polimerine katkı maddesi olarak eklendikten sonra elektroeğirme yöntemiyle fiber yapılar oluşturulmuştur. Fiberlerin morfolojisi SEM-EDX teknikleri, piezoelektrik özellikleri sağlayan β fazındaki değişim ise Fourier dönüşümlü kızılötesi spektroskopisi (FT-IR) gibi detaylı analizlerle incelenmiştir. Elde edilen sonuçlar, bor katkılı piezoseramik tozların PVDF polimerine eklenmesiyle piezoelektrik özelliklerde iyileşmeler sağlandığını göstermektedir.

Production and characterization of boron-doped BNT-6BT piezoceramic powder-reinforced PVDF composites

ARTICLE INFO

Article History:
Received September 10, 2024
Accepted October 25, 2024
Available online December 31, 2024

Research Article

DOI: 10.30728/boron.1547636

Keywords:
Boron doped BNT-6BT
Electrospinning
Hydrothermal method
Lead-free piezoceramics
PVDF polymer

ABSTRACT

Piezoelectric materials attract intensive attention from the automotive to health industries for such applications as sensors, actuators, and transducers due to their ability to convert mechanical energy to electrical energy and also, as a reversible effect, electrical energy to mechanical energy. Since eco-friendly and renewable energy generation has gained crucial importance, piezoelectric materials offer ideal solutions in many fields. The improvements in nanomaterials and characterization techniques also offer the possibility of creating novel approaches for researchers. Along with the rising environmental awareness in recent years, studies on developing alternative materials to Pb containing compositions with similar superior properties present important outputs. In this context, this study aims to produce light and flexible composites with superior characteristics by synthesizing boron (B^{3+}) doped $0,94(Bi_{0,5}Na_{0,5})TiO_3$-$0,06BaTiO_3$ BNT-6BT piezoceramics, which offer similar structure and properties as the most commonly used Pb-containing Lead zirconate titanate (PZT) ceramics, and used in polyvinylidene fluoride (PVDF) polymers. Characterization of the piezoceramic powders synthesized by hydrothermal method was performed using x-ray diffraction (XRD) and scanning electron microscopy (SEM-EDX) analyses. After the addition of the piezoceramic powders into PVDF polymer as filler material, fiber structure was obtained using the electrospinning method. The morphology of the fibers was investigated using SEM-EDX techniques, while a detailed analysis as Fourier-transform infrared spectroscopy (FT-IR) was used for observing the alteration in β phase, which provides the piezoelectric properties. The obtained results indicate that substantial improvements in the piezoelectric properties were observed by adding boron-doped piezoceramics into the PVDF polymers.

*Corresponding author: metinozgul@aku.edu.tr

1. Giriş (Introduction)

Günümüzde enerji ihtiyacı yeni teknolojik gelişmelerle birlikte farklı uygulama alanlarında çeşitlenerek sürekli bir artış göstermektedir. Kullanım alanlarının gerektirdiği tür ve miktara göre enerji ihtiyacının karşılanması için yenilikçi ve yüksek performanslı malzemelerin geliştirilmesine yönelik bilimsel araştırmalar da yoğunlaşmaktadır. Piezoelektrik malzemeler enerjiyi, mekanik ile elektrik enerjisi arasında iki yönlü dönüştürebilme kabiliyeti nedeniyle yoğun ilgi görmektedir ve otomotivden (yakıt enjeksiyonu) sağlık (ultrasonik görüntüleme) alanına kadar pek çok sektörde kullanılmaktadır [1]. Son yıllarda, tükenmeden ve çevreye zarar vermeden enerji üretimine olanak tanıyan malzemeler ile bu malzemelerden üretilen yapılar, yenilenebilir veya yeşil enerji olarak adlandırılmakta ve birçok mühendislik dalında önemli bir araştırma alanı haline gelmiştir. Piezoelektrik malzemeler, akıllı malzeme kategorisine giren, yapı ve çalışma prensipleri sayesinde yenilenebilir enerji üretimini mümkün kılan malzemeler olarak değerlendirilmektedir. Başlangıçta yalnızca belirli kristallerde gözlemlenen bu özellik, zamanla bazı seramik ve polimer yapılara da kazandırılabilmiştir [2]. 1880'lerden beri bazı malzemelerin piezoelektrik özellikler sergileyebildiği bilinmektedir. Günümüze kadar yaygın olarak kullanım imkanı bulmuş olan başlıca piezoelektrik malzemelerin başında Pb(Zr,Ti)O_3 (PZT) ve kimyasal modifikasyonları gelmektedir [3]. Halen günümüzde en üstün piezoelektrik özellikleri sağlayan perovskit kristal yapılı PZT-esaslı malzemeler, bileşimdeki kurşunun (Pb) toksik olması nedeniyle üretimi ve kullanımına bazı yasal kısıtlamalar getirilmiştir [4]. Bu nedenle son yıllarda çevre dostu kurşunsuz piezoelektriklerin üretimi ve karakterizasyonu üzerine yoğun araştırmalar yapılarak PZT esaslı sistemlere eşdeğer önemli seramik kompozisyonlar geliştirilmiştir. Aslında PZT'den önce keşfedilmiş olan yine perovskit kristal yapılı $BaTiO_3$ (BT) ile birlikte olumlu sonuçlar veren iki diğer perovskit kristal yapılı kurşunsuz piezoelektrik seramik malzemeler (K,Na)NbO_3 (KNN) ve (Bi,Na)TiO_3 (BNT) sistemleridir [5]. Son yıllarda en iyi özellikleri sağlayan sistemler arasında BNT-BT ikili katı çözelti sistemleri önemli yer tutmaktadır [6]. Genellikle seramik kompozisyonlara izovalent, donör ya da akseptör işlevi olan bazı farklı dopant element ilaveleri yapılarak malzeme özelliklerinde önemli geliştirmeler sağlanmaktadır. Bu strateji doğrultusunda ülkemizin ulusal bir değeri olan borun (B^{+3}) katkılanmasıyla pek çok piezoelektrik seramikte özelliklerde ciddi iyileşmeler rapor edilmiştir [7]. Araştırma grubumuzda da çevre dostu ve kurşunsuz piezoelektrik özelliğe sahip 0,94($Bi_{0,5}Na_{0,5}$)TiO_3-0,06$BaTiO_3$ (BNT-6BT) tozların literatürde ilk kez B_2O_3 katkılı olarak katı hal yöntemiyle üretimi gerçekleştirilmiş ve piezoelektrik özelliklerde çok ciddi artışlar gözlemlenmiştir [8]. Ancak, seramik malzemelerde kırılganlık problemi pek çok uygulamalarda kullanımı sınırlayan bir sorundur. Öte yandan hafiflik, esneklik ve düşük sıcaklıklarda üretilebilirlik gibi pek çok avantaj sağlayabilen polimer malzemeler üzerinde ilk çalışmalar 1960'ların sonlarında gerçekleştirilmiş ve piezoelektrik özelliklerin yalnızca belirli polimerlere kazandırılabileceği anlaşılmıştır. Bu polimerler arasında en çok bilinen, –CH_2–CF_2– formülüne sahip polivinil florür (PVDF)'dür. PVDF'nin mikrometre boyutlarında filament olarak üretilmesiyle, piezoelektrik kaplamalar [9] ve kumaş üretiminin yolu açılmış ve mekanik enerjiyi elektrik enerjisine dönüştürebilen yüzeylerin, kumaş ve tekstil yapılarının üretimine başlanmıştır. 1969 yılında, piezoelektrik özelliği keşfedilen PVDF esaslı piezoelektrik polimerler ve potansiyel uygulama alanlarına ilişkin çalışmalar yoğun olarak sürdürülmektedir. Farklı kristal katkıları ile zenginleştirilen PVDF polimerlerin elektriksel özelliklerinde iyileştirme çalışmaları başlıca kritik öneme sahip konular arasında yer almakta olup bu anlamda ciddi gelişmeler literatürde rapor edilmiştir. [2]. PVDF esaslı polimerlerin hafiflik ve esneklik gibi avantajlarına rağmen görece düşük olan piezoelektrik özelliklerini geliştirme yöntemlerinden biri olan kompozit yapma yaklaşımı giderek yaygınlaşan pratik bir tekniktir. Bu anlamda üstün piezoelektrik özellikli seramik partiküllerin dolgu olarak PVDF polimer matrise katkılanması üzerine pek çok çalışma gerçekleştirilmektedir. Kompozit yapma işlemleri sırasında yaşanılabilecek dispersiyon ve topaklanma sorunlarının aşılması ve PVDF polimerde beklenen iyileşmelerin sağlanabilmesi için dolgu olarak kullanılabilecek nano boyutta piezoseramik toz üretimi kritik öneme sahiptir. Bu amaçla son yıllarda üstün piezoelektrik özellikleri literatürde rapor edilmiş olan polimer-seramik kompozit yapılar incelendiğinde bunlar arasında PZT gibi kurşun içerikli kompozisyonların [10] yanı sıra, BT [11], KNN [12] ve BNT [13] gibi çevre dostu ve kurşunsuz piezoelektrik özelliğe sahip seramik partiküllerin kullanıldığı görülmektedir. Ayrıca, hidrotermal yöntem ile üretilen BNT-6BT nanofiberlerin aynı yöntemle üretilen farklı kompozisyonlara kıyasla daha yüksek piezoelektrik özellik (26 pm V^{-1}) gösterdiği rapor edilmiştir [14]. Literatürde ilk kez üstün özellikleri rapor edilen katı hal yöntemiyle üretilmiş B_2O_3 (B^{+3}) katkılı 0,94($Bi_{0,5}Na_{0,5}TiO_3$-0,06$BaTiO_3$ (BNT-6BT) tozların bu çalışmada hidrotermal yöntem ile üretimi ve karakterizasyonu hedeflenmiştir. Böylece kompozit yapımına daha elverişli olması amaçlanmaktadır. Çalışmanın çıktıları ile literatürde çokça çalışılan çevre ve insan sağlığına zararlı Pb katkılı piezoelektrik malzemelerin yerini alabilecek özellik ve performansı sağlayan alternatif kurşunsuz, doğa ve çevre dostu piezoseramik kristalin tozlar üretilerek polimer malzemelere katkı olarak kullanıma uygun malzeme geliştirme sürecine katkı yapmak hedeflenmektedir. Çalışmanın sonraki adımı olarak üretilen piezoseramik tozların, katkı (dolgu) olarak PVDF polimerinde kullanılarak elektroeğirme ile fiber oluşumu gerçekleştirilmesi planlanmıştır. Araştırma kapsamında elde edilecek olumlu sonuçlar mikroelektronik endüstrisinin en yenilikçi ürünleri olan minyatür sistemlerin enerji gereksinimi için küçük ölçekli bir enerji kaynağı olarak piezoelektrik malzemelerin ve havacılıktan biyomedikal uygulamalara kadar

önemi artarak devam eden piezoelektrik polimerlerin üretiminde borun özellikleri geliştirici işlevselliğinin daha iyi anlaşılmasına katkı sağlama potansiyeline sahiptir.

2. Malzemeler ve Yöntemler (Materials and Methods)

BNT ile ilgili yapılan çalışmalarda mineralleştiricinin konsantrasyonu, BNT nanopartiküllerinin yapısının ve morfolojisinin kontrolünde baskın rol oynamıştır. BNT nanoliflerinin büyümesi için en uygun mineralleştirici konsantrasyonunun NaOH=12 M olduğu bulunmuştur [14]. Ayrıca, 48 saatlik hidrotermal süre ve 200°C sıcaklık, saf perovskit fazlı BNT nanoliflerinin üretimini gerçekleştirmek için optimize edilmiş koşullar olarak kabul edilmiştir [15]. Bu çalışmada da hidrotermal reaksiyon için sıcaklık 200°C ve süre 48 saat olarak belirlenmiştir ve $0,94(Bi_{0,5}Na_{0,5})TiO_3$-$0,06BaTiO_3$ tozların üretimi katkısız BNT-6BT ve %1 mol Bor (B^{+3}) katkısı ile BNT-6BT+ %1 mol B^{+3} olarak gerçekleştirilmiştir. Üretim aşamasında sodyum kaynağı olarak kullanılan NaOH konsantrasyonu 12 M olarak, diğer bileşenler için ise tuzlar, hidroksitler ve oksitler kullanılmıştır. Sonrasında üretilen tozlar ağırlıkça %10 oranında PVDF polimerine katkılandırılmıştır.

Hidrotermal yöntemde molce %1 B^{+3} katkılı BNT-6BT seramik tozlarının sentezinde başlangıç tozları olarak literatürde de uygun olduğu rapor edilen [16] $BiCl_3$ (%98, Abcr, Almanya), NaOH (%97 AFG Bioscience, ABD), BaOH (%95, Abcr, Almanya), TiO_2 (%99,7, TCI, Belçika) ve B_2O_3 (%99,98, Alfa Aesar, ABD) kullanılmıştır. Katkı oranının molce %1 olarak seçilmesinde, daha önce ticari B_2O_3 kullanılarak gerçekleştirilen bir çalışmada en üstün piezoelektrik özelliklerin %1 mol B^{+3} ilavesiyle elde edilmesi belirleyici olmuştur [8]. Yüksek saflıktaki başlangıç hammaddeleri stokiyometriye uygun olarak tartılıp, önceden hazırlanan 12 M NaOH çözeltisine ilave edilmiştir. Hazırlanan NaOH çözeltisine stokiyometrik olarak 0,1 M B_2O_3, 1 M $BiCl_3$, 0,1 M $Ba(OH)_2$ ve 0,2 M TiO_2 tozu ilave edilmiştir. Hidrotermal reaktör 100 ml olduğu için çözelti 12 M NaOH konsantrasyonu için 80 ml hazırlanmıştır ve Tablo 1'de toz üretim reçeteleri verilmiştir.

Çözelti 3 saat boyunca manyetik karıştırıcıda oda sıcaklığında karıştırıldıktan sonra hidrotermal reaktöre alınmıştır. Reaktör döner mekanizmaya sahip etüve bağlandıktan sonra 200°C'de 48 saat süreyle reaksiyonun gerçekleşmesi sağlanmıştır. Etüv oda sıcaklığına geldikten sonra çözelti kantitatif filtre kağıtlarıyla (mavi band-çok yavaş) filtrasyon işlemi gerçekleştirilmiştir. NaOH çözeltisinin tamamen uzaklaşmasını sağlamak amacıyla filtrelenen tozlar manyetik karıştırıcıda saf su ile üç sefer yıkanıp, her yıkamanın ardından tekrar filtre edilmiştir.

Sadece PVDF ile yapılan çalışmalarda konsantrasyonunun %15'in altına düşmesi; aynı şekilde 15 kV uygulanarak ve optimal koşullar kullanılarak kusurlu, yani boncuklu yapıya sahip nano lifler elde edildiği literatürde rapor edilmiştir. Eğirme voltajı 20 kV'a çıkartıldığında boncuklu yapıda azalma olduğu gözlemlenmiştir. Bu sonuçlardan da anlaşılacağı üzere düşük voltajın, uygun gerdirme kuvvetlerine izin vermediği görülmektedir [17]. Bu bulgular doğrultusunda elektroeğirme sürecinde 10, 15 ve 20 kV farklı eğirme voltajları ve akış hızı 0,5 ve 1 ml/sa olarak belirlenmiştir. Elektroeğirme işlemi öncesi hazırlanan çözeltilerde polimer konsantrasyonu ve katkı oranı sabit tutulmuş olup, 70/30 DMF/aseton solvent oranı kullanılmış ve başlangıç polimeri (PVDF) konsantrasyonu ağırlıkça %15 olarak belirlenmiştir.

Oda sıcaklığında kurutulan tozlara sonrasında X-ışını kırınımı (XRD) analizi (D8 Advance model, CuKα λ=1.5406 Å, Bruker, ABD) yapılarak istenilen kristal fazların oluşup oluşmadığı incelenmiştir. Hazırlanan NaOH çözeltisiyle elde edilen toz parçacıklarına ve elektroeğirme sonucu oluşan fiber yapılara mikroyapı görüntülemesi ve yarı kantitatif elementel analizleri Enerji Dağıtıcı X-Işını Spektroskopisi (EDX) ile birleştirilmiş Taramalı Elektron Mikroskobu (SEM-EDX; LEO 1430VP, Zeiss, Almanya) tekniği ile 10 veya 20 KX büyütmelerde gerçekleştirilmiştir. Sonrasında PVDF polimerinde piezoelektrik özellik gösteren β fazının yüzde miktarının hesaplanabilmesi için fourier dönüşümlü kızılötesi spektroskopisi (FT-IR; L1600401, Perkin Elmer, ABD) analizi yapılmış ve sonuçlar literatür ışığında değerlendirilmiştir.

3. Sonuçlar ve Tartışma (Results and Discussion)

Şekil 1'de, 12 M NaOH çözeltisiyle hazırlanan BNT-6BT ve BNT-6BT+ %1 mol B^{+3} piezoseramik tozlarının 2θ=20-70° aralığındaki XRD sonuçları verilmiştir. Katkısız ve B^{+3} katkılı tozlara ait XRD desenleri incelendiğinde, %1 mol oranında B^{+3} katkılı örneklerde

Tablo 1. Hidrotermal yöntem ve 12 M NaOH çözeltisi ile üretilen BNT-BT+ %1 mol B^{+3} toz reçetesi (Recipe of BNT-6BT+1 mol % B^{3+} powders synthesized via hydrothermal method with 12M NaOH solution)

Hammadde	Kompozisyon	Molarite	Molekül Ağırlığı (g/mol)	100 ml	80 ml Nihai Ağırlık (g)
$BiCl_3$	0,94	0,1	315,34	2,9642	2,37136
NaOH	0,94	12	39,997	47,9964	38,3971
TiO_2	1	0,2	79,866	1,5973	1,27784
$Ba(OH)_2$	0,06	0,1	171,344	0,1028	0,08224
B_2O_3	0,005	0,1	69,62	0,0035	0,00280

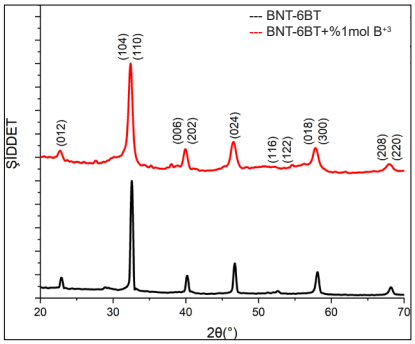

Şekil 1. Hidrotermal yöntem ile 12M NaOH çözeltisi ile üretilen BNT-6BT ve BNT-6BT+%1 mol B^{+3} tozlarının XRD spektrumları (XRD spectra of BNT-6BT and BNT-6BT+1 mol % B^{3+} powders synthesized via hydrothermal method with 12M NaOH solution)

düşük şiddetli farklı bazı pikler gözlenmekle birlikte tüm örneklerde majör piklerin perovskit kristal yapısı (PDF 01-074-9531) ile uyumlu olduğu görülmüştür. Sonuç olarak gerek katkısız gerekse B^{+3} katkılı örneklere ait XRD desenleri belirgin olarak tek perovskit BNT-BT faz yapısının oluştuğunu göstermektedir.

Belirgin olarak ikincil bir faz tespit edilmemiştir, bu da B^{+3}'un homojen bir katı çözelti oluşturmak üzere BNT-BT perovskit kristal kafesine yayıldığını gösterir. Kristal kafesi oluşturan Ba^{+2}, Na^{+}, Bi^{+3}, Ti^{+4} ve B^{+3} katyonlarının iyonik yarıçapları sırasıyla 0,160, 0,139, 0,128, 0,061 ve 0,020 nm'dir. Hume-Rothery kurallarına göre son derece küçük iyonik yarıçapı nedeniyle, B^{+3} iyonunun BNT-6BT perovskit kafesinde ara yerlere yerleşmesi beklenmektedir [8]. Bu durum literatür verileriyle de uyumludur [18].

Hidrotermal yöntem ile üretimleri gerçekleştirilen, piezoelektrik toz parçacıklarına ve elektroeğirme sonucu oluşan fiber yapıların karakterizasyonu için gerçekleştirilen SEM-EDX analizlerinden sağlanan morfoloji ve yarı kantitatif elementel bileşimlere ilişkin veriler değerlendirilmiştir. Şekil 2'de, 12 M NaOH çözeltisiyle üretilmiş BNT-6BT+%1 mol B^{+3} tozunun SEM görüntüleri; Şekil 3'te ise aynı toza ait EDX analiz sonuçları yer almaktadır.

Şekil 4'te, 12 M NaOH çözeltisiyle üretilmiş BNT-6BT tozlarının sırasıyla SEM görüntüleri ve EDX analiz sonuçları verilmiştir.

Şekil 2 ve 4'te verilen SEM görüntüleri incelendiğinde gözlemlenen fiber, plakacık ve kübik yapı oluşumlarının literatür ile uyumlu olduğu görülmektedir [15]. Tozlarda meydana gelen aglomerasyon normal kabul edilir ve katkı olarak kullanıldığında çözelti içerisinde dağıldığı, bu aglomerasyonun ortadan kalktığı görülmüştür. Şekil 3 ve 4'te verilen EDX analiz sonuçlarında başlangıç hammaddeleri olarak kullanılan tozların elementel olarak varlığı tespit edilmiştir.

PVDF ile hazırlanan ve elektroeğirme yöntemi kullanılarak bakır (Cu) hedef üzerine toplanan

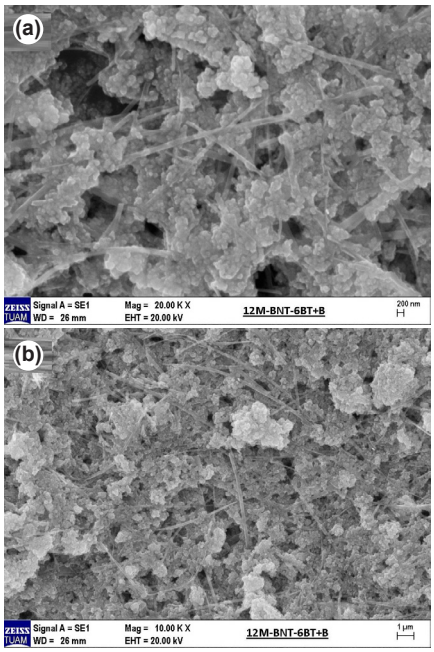

Şekil 2. 20.000X (a) ve 10.000X (b) 12M NaOH çözeltisi ile üretilen BNT-6BT+ %1 mol B^{+3} tozunun SEM görüntüleri (Ölçek çubukları a) 200 nm, b) 1 µm). (20,000X (a) and 10,000X (b) SEM images of BNT-6BT+1 mol % B^{3+} powders synthesized via hydrothermal method with 12M NaOH solution (Scale bars a) 200 nm, b) 1 µm)

nanolifler, altın (Au) ile kaplanmıştır ve SEM-EDX analiz sonuçları Şekil 4, 5, 6 ve 7'de verilmektedir. Bu sonuçlara bakıldığında oluşan boncuklu yapının var olabileceği anlaşılmaktadır [19]. Ayrıca oluşan liflerin kalınlığı üretilen örneklerle uyumludur. Bu veriler

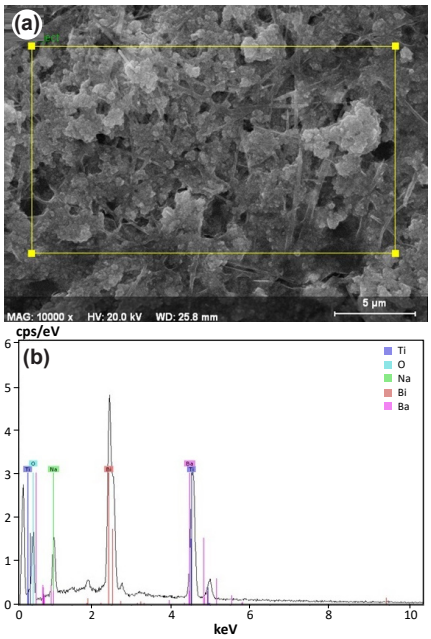

Şekil 3. 12M NaOH çözeltisi ile üretilen BNT-6BT+ %1 mol B^{+3} tozunun a) 10.000X SEM görüntüsü (Ölçek çubuğu: 5 µm) ve b) EDX spektrumu. (a) 10.000X SEM image (Scale bar: 5 µm) and b) EDX spectrum of BNT-6BT+1 mol % B^{3+} powders synthesized via hydrothermal method with 12M NaOH solution)

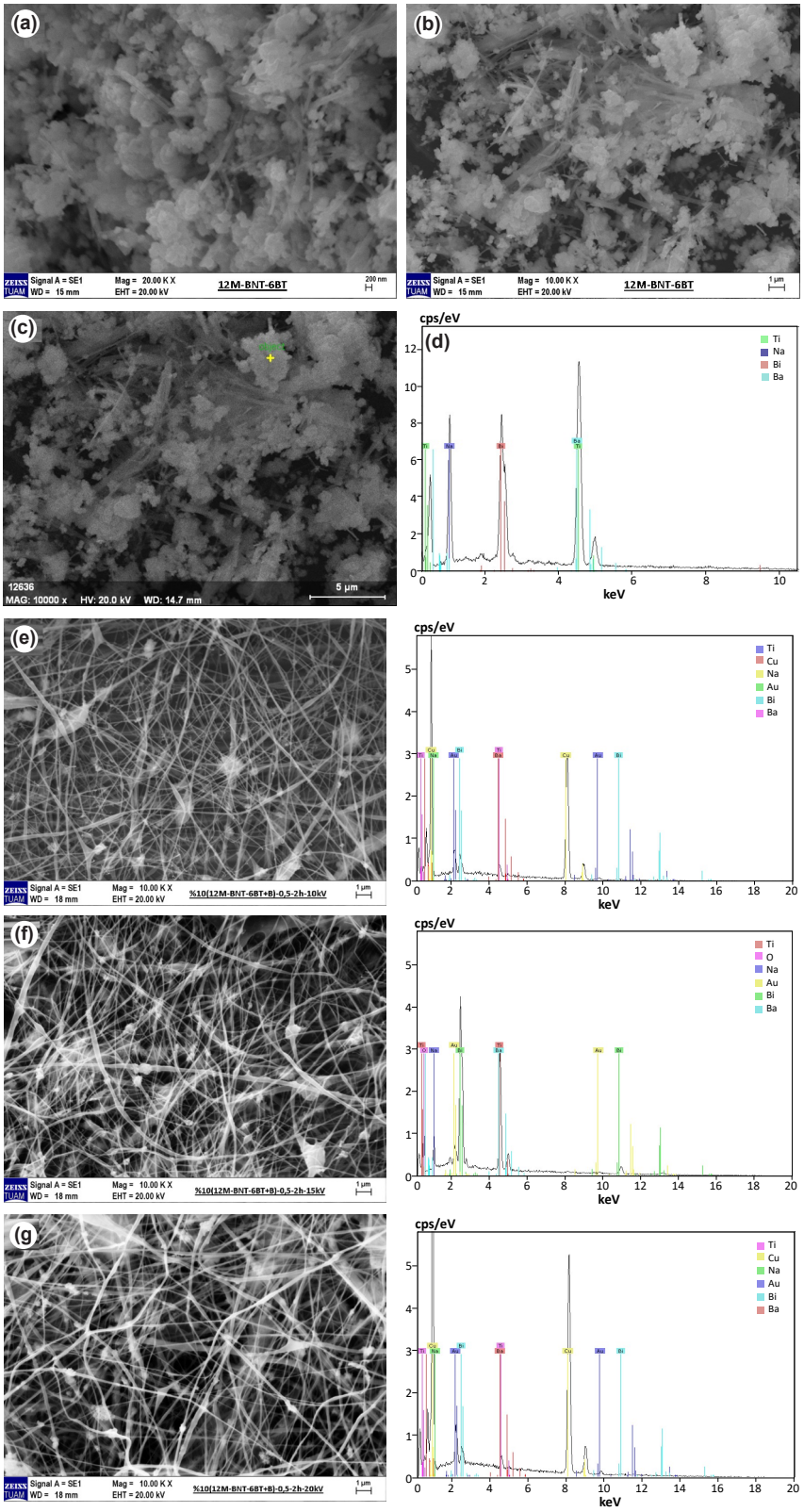

Şekil 4. 12M NaOH çözeltisi ile üretilen BNT-6BT tozunun a) 20.000X (Ölçek çubuğu: 5 µm) ve b) 10.000X (Ölçek çubuğu: 10 µm) SEM spektrumu. 12M NaOH çözeltisi ile üretilen BNT-6BT tozunun c) 10.000X SEM görüntüsü (Ölçek çubuğu: 5 µm) ve d) EDX spektrumu. 12M NaOH çözeltisi ile üretilen BNT-6BT+ %1 mol B^{+3} tozunun, 70/30 DMF/aseton-%15 PVDF çözeltisine %10 katkıyla e)10 kV f)15 kV g)20 kV ile 0,5 ml/sa akış hızında üretilen SEM görüntüleri ve EDX spektrumları (Ölçek çubuğu: 1µm). (a) 20.000X (Scale bar: 5 µm) and b) 10.000X (Scale bar: 10 µm) SEM spectrum of BNT-6BT powders synthesized via hydrothermal method with 12M NaOH solution. c) 10.000X SEM image (Scale bar: 5 µm) and d) EDX spectrum of BNT-6BT+1 mol % B^{3+} powders synthesized via hydrothermal method with 12M NaOH solution. SEM images and EDX spectra of 10% BNT-6BT+1 mol % B^{3+} powders fabricated with 12M NaOH solution, with 10% addition to 70/30 DMF/acetone-15% PVDF solution, produced with e)10 kV f)15 kV g)20 kV at a flow rate of 0.5 ml/h SEM images and EDX spectra (Scale bar: 1µm)

ışığında katkılanan BNT-BT ve BNT-BT+%1 mol B^{+3} piezoelektrik seramik tozunun, oluşan fiber kalınlığında olumsuz bir etkisinin olmadığı anlaşılmaktadır.

Şekil 4 ve 5 incelendiğinde 0,5 ml akış hızının 0,1 ml akış hızına göre, bu kompozisyon için nispeten daha ince fiber oluşumuna katkıda bulunduğu gözlemlendi. Ayrıca voltajın artmasıyla birlikte fiber ortalama çapının arttığı görüldü. Benzer durum Şekil 6 ve 7 incelendiğinde de geçerlidir. FT-IR analizi sonucunda β fazındaki artış gözlemlenmesi, piezoelektrik özelliklerin arttığı yönünde yorumlanmaktadır [17]. Piezoelektrik β fazının tayini bu açıdan önemlidir. PVDF polimer malzemelerde piezoelektrik özellik gösteren faz β fazıdır. PVDF; yapısı ile de doğal olarak ilişkili olan piezo, piroelektrik özelliklerinden dolayı yaygın şekilde incelenmiş, yarı kristalin bir polimerdir. İçlerinde α ve β fazlarının en yaygın fazlar olduğu 5 farklı kristal yapı (α, β, γ, δ ve ε) rapor edilmiştir. PVDF birincil olarak α fazından oluşmaktadır ve bu faz termal olarak kararlı olup, moleküler dipollerin antiparalel olduğu TGTG' (T-trans, G-gauche+, G'-gauche) dihedral yapı gösterir, bu da non-polar kristal yapı ile sonuçlanır. β fazı, polar C-F ve C-H bağlarının karbon omurgasına dikey bir dipol momentine sahip olduğu TTTT yapısı gösterir. Ek olarak, tüm zincirler dipollerle paralel doğrultuda yönlenmektedir, bu nedenle β fazı diğer fazlar arasında en yüksek kendiliğinden polarizasyona sahip olan fazdır. Ortam sıcaklığı ve basıncı altında kinetik olarak kararlı olan β fazı, üstün piezo ve piroelektrik özellikler gösteren ve dolayısıyla piezoelektrik kumaşların tasarımı için en ilgi çekici fazdır [20]. Bu nedenle numunelere FT-IR analizi yapılmış ve sonuçlar Şekil 7'de verilmiştir. PVDF'nin üç ana α, β ve γ polimorfu için FT-IR absorpsiyon zirveleri üç ana kategoriye ayrılabilir. Bunlar; her üç fazda da ortaya çıkan ortak pikler, üç aşamadan yalnızca birinde görünen özel zirveler ve iki farklı fazdan gelebilecek çift zirveler. Genel olarak, spektrum 881, 1071, 1176 ve 1401 cm^{-1} civarında yüksek yoğunluk daha önce bazı makalelerde kristal fazları karakterize etmek için kullanılmıştır. Bununla birlikte, 876-885, 1067-1075, 1171-1182 ve 1398-1404 cm^{-1} aralığındaki pikler, α^{-}, β^{-} ve γ^{-} fazlarının örneklerinde veya diğer karışık sistemlerde benzer özelliklere sahiptir. Başka bir deyişle, bunlar her üç fazda da ortaya çıkan ortak

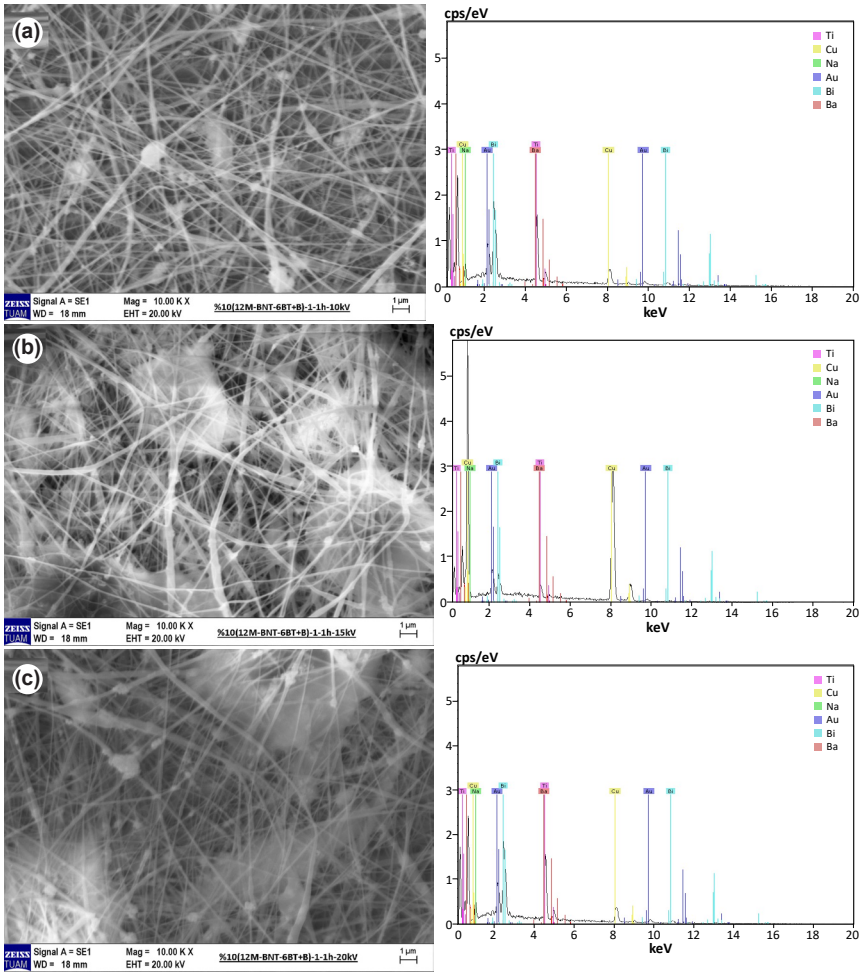

Şekil 5. 12M NaOH çözeltisi ile üretilen BNT-6BT+ %1 mol B^{+3} tozunun, 70/30 DMF/aseton-%15 PVDF çözeltisine %10 katkıyla a)10 kV b)15 kV c)20 kV ile 1 ml/sa akış hızında üretilen SEM görüntüleri ve EDX spektrumları (Ölçek çubuğu: 1μm). (SEM images and EDX spectra of 10% BNT-6BT+1 mol % B^{3+} powders fabricated with 12M NaOH solution, with 10% addition to 70/30 DMF/acetone-15% PVDF solution, produced with a)10 kV b)15 kV c)20 kV at a flow rate of 1 ml/h SEM images and EDX spectra (Scale bar: 1μm)

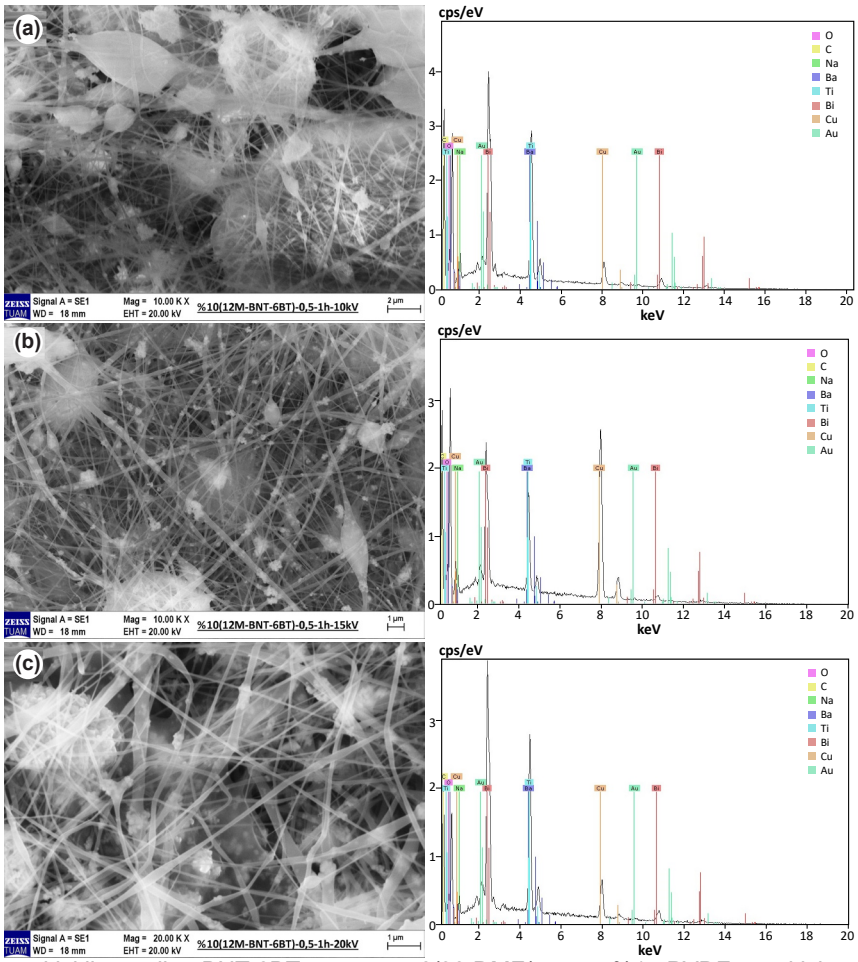

Şekil 6. 12M NaOH çözeltisi ile üretilen BNT-6BT tozunun, 70/30 DMF/aseton-%15 PVDF çözeltisine %10 katkıyla a)10 kV b)15 kV c)20 kV ile 0,5 ml/sa akış hızında üretilen SEM görüntüleri ve EDX spektrumları (Ölçek çubuğu: a)2μm, b, c) 1μm). (SEM images and EDX spectra of 10% BNT-6BT powders fabricated with 12M NaOH solution, with 10% addition to 70/30 DMF/acetone-15% PVDF solution, produced with a)10 kV b)15 kV c)20 kV at a flow rate of 0.5 ml/h SEM images and EDX spectra (Scale bar: a) 2μm, b, c) 1μm)

zirvelerdir. Özel tepe noktaları, karşılık gelen kristal fazları tanımlamak için kullanılabilirken, ikili tepe noktaları, küçük dalga sayısı kaymaları (tipik olarak 2 cm^{-1} içinde) veya deneysel koşullara bağlı olarak gerçekten farklı fazlar için deneysel belirsizliğin sonuçları olabilir. Spesifik olarak, α fazı için özel tepe noktaları (α fazının karakteristik bantları) 410, 489, 532, 614, 763, 795, 854, 975, 1149, 1209, 1383 ve 1423 cm^{-1} civarındadır; β fazı için özel tepe noktaları 445, 473 ve 1275 cm^{-1} civarındadır ve γ fazı için özel tepe noktaları 431, 482, 811 ve 1234 cm^{-1} civarındadır. Buna karşılık, zirveler 837-841 ve 508-512 cm^{-1} aralığı, birçok farklı numunede görünebilmesine rağmen, β ve γ fazı için absorbans, α fazınınkinden çok daha güçlüdür. Bu nedenle bu iki tepe noktası (840* ve 510* cm^{-1}) elektroaktif β ve/veya γ fazlarını karakterize etmek için kullanılabilir. β ve γ fazları 1428-1432 cm^{-1} aralığında çok yakın pikler gösterse de, çeşitli sonuçlar sırasıyla 1431 ve 1429 cm^{-1}'deki piklerin β ve γ fazlarının karakteristik bantları olarak kullanılabileceğini desteklemektedir. Daha önce bazı yazarlar tarafından β fazına atanan 600 cm^{-1} bandı, PVDF' i karakterize etmek için kullanılmamalıdır, çünkü bu bant, 613 cm^{-1}'deki diğer yoğun tepe noktası nedeniyle, α fazı olanlar da dâhil olmak üzere birçok numunede yaygın olarak görülür. Sadece yüksek sıcaklıkta kristalleşme γ-fazında, 776 ve 833 cm^{-1} bantlarının diğer γ-fazı hâkimiyet örneklerinde oldukça nadiren gözlendiği belirtilmektedir. Üç fazın miktarları herhangi bir yüzdede olabileceğinden, bu fazları izlemek için evrensel ama basit bir prosedür oluşturmak bu nedenle çok önemlidir. 763 ve/veya 614, 1275 ve 1234 cm^{-1}'deki bantların sırasıyla α, β ve γ fazlarını ayırt etmek ve tanımlamak için tutarlı bir şekilde kullanılabileceği bulunmuştur [21].

840* cm^{-1} bandı, diğer bant bilgilerine dayalı olarak β, γ veya her iki faza atanabildiğinden, elektroaktif β ve γ fazlarının (F_{EA}) herhangi bir numunedeki kristal bileşenler cinsinden fraksiyonu, örneğin sadece iki faz (α + β, α + γ veya β + γ) veya üç faz (α + β + γ) içeren bir numune, Eş. 1 ile ölçülebilir:

$$F_{EA} = \frac{I_{EA}}{\left(\frac{K_{840^*}}{K_{763}}\right) I_{763} + I_{EA}} X100 \quad (1)$$

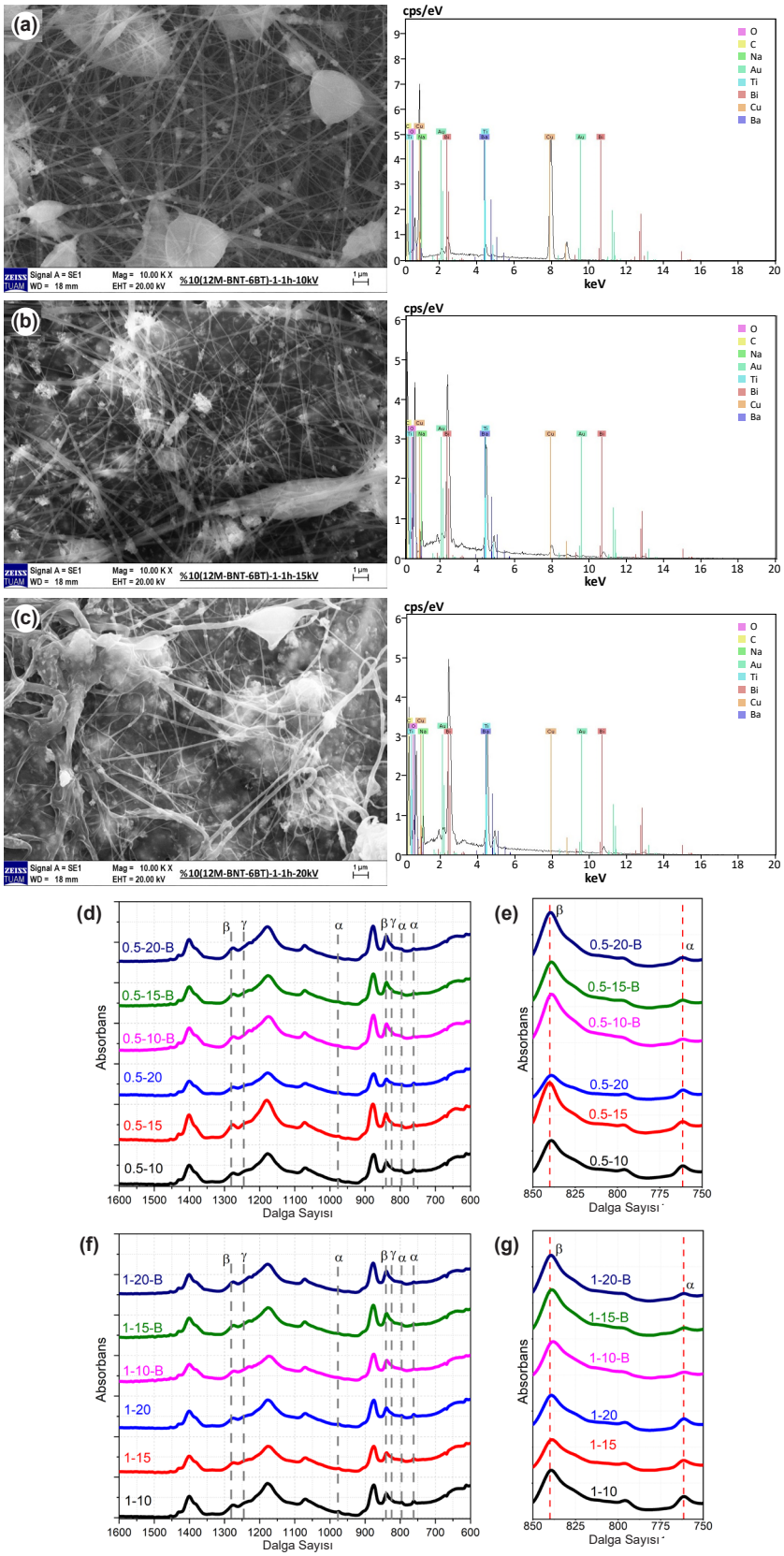

Şekil 7. 12M NaOH çözeltisi ile üretilen BNT-6BT tozunun, 70/30 DMF/aseton-%15 PVDF çözeltisine %10 katkıyla a)10 kV b)15 kV c)20 kV ile 1 ml/sa akış hızında üretilen SEM görüntüleri ve EDX spektrumları (Ölçek çubuğu: 1µm). 12M NaOH çözeltisi ile sentezlenen BNT-6BT+ %1 mol B^{+3} ve BNT-6BT tozu kullanılarak ve 10, 15 ve 20 kV eğirme voltajı uygulanarak d) ve e) 0,5, f) ve g)1 ml akış hızında çekilen fiber yapının FT-IR analiz sonuçları (SEM images and EDX spectra of 10% BNT-6BT powders fabricated with 12M NaOH solution, with 10% addition to 70/30 DMF/acetone-15% PVDF solution, produced with a)10 kV b)15 kV c)20 kV at a flow rate of 1 ml/h SEM images and EDX spectra (Scale bar: 1µm). FT-IR results of the fiber structure produced with d) and e)0.5 and f) and g)1 ml of flow rates applying 10, 15 and 20 kV of spinning voltages and using BNT-6BT+1 mol % B^{3+} and BNT-6BT powders synthesized with 12M NaOH solution)

Tablo 2. 12M NaOH çözeltisi ile sentezlenen BNT-6BT+ %1 mol B^{+3} ve BNT-6BT tozu kullanılarak ve 10, 15 ve 20 kV eğirme voltajı uygulanarak 0,5 ve 1 ml akış hızında üretilen fiber yapının FT-IR analiz sonuçları (FT-IR results of the fiber structure produced with a)0.5 and b)1 ml of flow rates applying 10, 15 and 20 kV of spinning voltages and using BNT-6BT+1 mol % B^{3+} and BNT-6BT powders synthesized with 12M NaOH solution)

	0,5ml-2h			1ml-1h		
	10kV	**15kV**	**20kV**	**10kV**	**15kV**	**20kV**
Katkısız	53,7549	57,2876	51,3687	53,7612	52,9793	54,2348
B^{+3} Katkılı	59,3990	58,3594	60,5651	55,5921	57,5586	59,5497
Değişim (%)	10,50	1,87	17,90	3,41	8,64	9,80

Burada, I_{EA} ve I_{763} sırasıyla 840* ve 763 cm^{-1}'deki absorpsiyon değerleridir; K_{840*} ve K_{763}, değerleri sırasıyla 7,7x10^4 ve 6,1x10^4 cm^2 mol^{-1} olan ilgili dalga sayılarındaki absorpsiyon katsayılarıdır [21].

β Fazının miktarını belirlerken fazlara ait karakteristik pik şiddetleri yukarıdaki Eş. 2 yardımıyla hesaplanmış sonuçlar Tablo 2'de paylaşılmıştır.

$$F_\beta = \frac{A_\beta}{(1{,}26)A_\alpha + A_\beta} X100 \quad (2)$$

4. Sonuçlar (Conclusions)

Bu çalışmada, B_2O_3 kaynağı kullanılarak üretilen %1 mol B^{+3} katkılı BNT-6BT piezoseramik tozların 12M NaOH çözeltisi ile gerçekleştirilen toz üretim işleminin, PVDF piezoelektrik polimerine katkı olarak kullanılabilirliği incelenmiştir. Üretilen tüm piezoseramik tozların perovskit kristal yapı ile uyumlu olduğu XRD desenleri ile doğrulanmıştır. Hidrotermal yöntemin en önemli avantajı morfolojinin kontrol edilebilmesi ve sentezlemenin daha düşük sıcaklıkta gerçekleşmesiyle birlikte enerji sarfiyatının düşmesidir. Bu sonuçlar, ülkemiz zenginliklerinden farklı bor madenlerinin polimer-seramik kompozit yapıdaki piezoelektrik malzemelerde özellikleri iyileştirmek amacıyla kullanılabilecek potansiyel bir katkı olarak değerlendirilebilmesi konusunda ışık tutmaktadır. XRD analizleri sonucunda; hidrotermal yöntem ve 12M NaOH çözeltisi ile üretimi gerçekleştirilmiş olan BNT-6BT ve BNT-6BT+ %1 mol B^{+3} piezoelektrik tozlarından alınan X-Işınları Kırınımı (XRD) analizi sonucunda istenen perovskit fazının oluştuğunu ortaya koymaktadır. SEM analizleri sonucunda; eğirme voltajının fiber kalınlığı değişiminde büyük değişimlere neden olmadığı, Eğirme voltajının ferroelektrik özelliklere katkıda bulunabileceği, EDX analizlerinde katkı olarak kullanılan tozun fiber yapısına dahil olduğu anlaşılmıştır. Literatürde verilen PVDF ile üretilmiş fiber yapısıyla uyumlu olduğu görülmektedir. FT-IR analizleri sonucunda; B^{+3} katkısıyla üretilen BNT-6BT PVDF'e katkı olarak kullanıldığında örneklerin tamamında β fazında %1,87 ile %17,90 arasında değişen oranlarda artışa neden olmuştur.

5. Teşekkürler (Acknowledgements)

Bu çalışma, Afyon Kocatepe Üniversitesi, Bilimsel Araştırma Projeleri Koordinasyon Birimi tarafından 21.FEN.BİL.41 numaralı proje ile desteklenmektedir.

6. Yazar Katkısı Beyanı (Author Contribution Statement)

Serhat Tıkız: Deneysel çalışmalar, metodoloji, analizler, kaynaklar, makale yazımı.

Metin Özgül: Kavramsal planlama, metodoloji, analiz sonuçlarının irdelenmesi, makale yazımı ve inceleme, danışmanlık.

Kaynaklar (References)

[1] Dittmer, R. (2013). *Lead-free piezoceramics: Ergodic and nonergodic relaxor ferro-electrics based on bismuth sodium titanate*. [Doctoral dissertation, Wilmington Darmstadt Technical University]. https://core.ac.uk/download/pdf/17179686.pdf

[2] Genenko, Y. A., Glaum, J., Hoffmann, M. J., & Albe, K. (2015). Mechanisms of aging and fatigue in ferroelectrics. *Materials Science and Engineering B: Solid-State Materials for Advanced Technology*, *192*(C), 52-82. https://doi.org/10.1016/j.mseb.2014.10.003

[3] Panda, P. K., & Sahoo, B. (2015). PZT to Lead free piezo ceramics: A review. *Ferroelectrics*, *474*(1), 128-143. https://doi.org/10.1080/00150193.2015.997146

[4] Li, Y., Moon, K., & Wong, C. P. (2005). Electronics without lead. *Science*, *308*(5727), 1419-1420. https://doi.org/10.1126/science.1110168

[5] Nguyen, T. N., Thong, H. C., Zhu, Z. X., Nie, J. K., Liu, Y. X., Xu, Z., … & Wang, K. (2021). Hardening effect in lead-free piezoelectric ceramics. *Journal of Materials Research*, *36*(5), 996-1014. https://doi.org/10.1557/s43578-020-00016-1

[6] Zidani, J., Alaoui, I. H., Zannen, M., Birks, E., Chchiyai, Z., Majdoub, M., … & Lahmar, A. (2024). On the lanthanide effect on functional properties of 0.94Na0.5Bi0.5TiO3-0.06BaTiO3 ceramic. *Materials*, *17*(8). https://doi.org/10.3390/ma17081783

[7] Salimkhani, H., Fulanović, L., & Frömling, T. (2024). Sinterability of sodium bismuth titanate-based electroceramics at low temperatures. *Journal of the European Ceramic Society*, *44*(3), 1570-1580. https://doi.org/10.1016/j.jeurceramsoc.2023.10.056

[8] Ozgul, M., & Kucuk, A. (2016). B2O3 doping in 0.94(Bi0.5Na0.5)TiO3-0.06BaTiO3 lead-free piezoelectric ceramics. *Ceramics International*, *42*(16), 19119-19123. https://doi.org/10.1016/j.ceramint.2016.09.073

[9] Fang, X. Q., Huang, M. J., Liu, J. X., & Feng, W. J. (2014). Dynamic effective property of piezoelectric composites with coated piezoelectric nano-fibers. *Composites Science and Technology*, *98*, 79-85. https://doi.org/10.1016/j.compscitech.2014.04.017

[10] Jain, A., Prashanth, K. J., Sharma, A. K., Jain, A., & Rashmi, P. N. (2015). Dielectric and piezoelectric properties of PVDF/PZT composites: A review. *Polymer Engineering and Science*, *55*(7), 1589-1616. https://doi.org/10.1002/pen.24088

[11] Guo, S., Duan, X., Xie, M., Aw, K. C., & Xue, Q. (2020). Composites, fabrication and application of polyvinylidene fluoride for flexible electromechanical devices: A review. *Micromachines*, *11*(12), 1-29. https://doi.org/10.3390/mi11121076

[12] Tripathy, A., Maria Joseph Raj, N. P., Kim, S. J., & Ramadoss, A. (2023). Elucidating the piezoelectric, ferroelectric, and dielectric performance of lead-free KNN/PVDF and ıts copolymer-based flexible composite films. *ACS Applied Electronic Materials, 5*(10), 5422-5431. https://doi.org/10.1021/acsaelm.3c00306

[13] Kurakula, A., Graham, S. A., Manchi, P., Paranjape, M. V., & Yu, J. S. (2024). Enhanced energy harvesting ability of bismuth sodium titanate/polyvinylidene fluoride composite film-based piezoelectric nanogenerators for mechanical energy scavenging and safety-walker applications. *Materials Today Sustainability*, 25. https://doi.org/10.1016/j.mtsust.2023.100616

[14] Ghasemian, M. B., Rawal, A., Wang, F., Chu, D., & Wang, D. (2017). Lattice evolution and enhanced piezoelectric properties of hydrothermally synthesised 0.94(Bi0.5Na0.5)TiO3-0.06BaTiO3 nanofibers. J*ournal of Materials Chemistry C*, *5*(42), 10976-10984. https://doi.org/10.1039/c7tc03812g

[15] Lu, R., Yuan, J., Shi, H., Li, B., Wang, W., Wang, D., & Cao, M. (2013). Morphology-controlled synthesis and growth mechanism of lead-free bismuth sodium titanate nanostructures via the hydrothermal route. *CrystEngComm*, *15*(19), 3984-3991. https://doi.org/10.1039/c3ce40139a

[16] Ghasemian, M. B., Lin, Q., Adabifiroozjaei, E., Wang, F., Chu, D., & Wang, D. (2017). Morphology control and large piezoresponse of hydrothermally synthesized lead-free piezoelectric (Bi0.5Na0.5)TiO3 nanofibres. *RSC Advances*, *7*(25), 15020-15026. https://doi.org/10.1039/c7ra01293d

[17] Cozza, E. S., Monticelli, O., Marsano, E., & Cebe, P. (2013). On the electrospinning of PVDF: Influence of the experimental conditions on the nanofiber properties. *Polymer International*, *62*(1), 41-48. https://doi.org/10.1002/pi.4314

[18] Qi, J. Q., Chen, W. P., Wang, Y., Chan, H. L. W., & Li, L. T. (2004). Dielectric properties of barium titanate ceramics doped by B2O3 vapor. *Journal of Applied Physics*, *96*(11), 6937-6939. https://doi.org/10.1063/1.1814167

[19] Haghi, A. K., & Akbari, M. (2007). Trends in electrospinning of natural nanofibers. *Physica Status Solidi (A) Applications and Materials Science*, *204*(6), 1830-1834. https://doi.org/10.1002/pssa.200675301

[20] Soin, N., Shah, T. H., Anand, S. C., Geng, J., Pornwannachai, W., Mandal, P., … & Siores, E. (2014). Novel “3-D spacer” all fibre piezoelectric textiles for energy harvesting applications. *Energy and Environmental Science*, *7*(5), 1670-1679. https://doi.org/10.1039/c3ee43987a

[21] Cai, X., Lei, T., Sun, D., & Lin, L. (2017). A critical analysis of the α, β and γ phases in poly(vinylidene fluoride) using FTIR. *RSC Advances*, *7*(25), 15382-15389. https://doi.org/10.1039/c7ra01267e

TENMAK BOREN BOR ARAŞTIRMA ENSTİTÜSÜ

BOR DERGİSİ
JOURNAL OF BORON
https://dergipark.org.tr/boron

Valorization of boron derivatives in polyurethane-based foams for reduced ignitability and thermal conductivity

Gökhan Gürlek [1,*], **Lütfiye Altay** [1]

[1]*Ege University, Faculty of Engineering, Department of Mechanical Engineering, İzmir, 35100, Türkiye*

ARTICLE INFO

Article history:
Received September 16, 2024
Accepted October 30, 2024
Available online December 31, 2024

Research Article

DOI: 10.30728/boron.1551164

Keywords:
Boron derivatives
Ignitability
Polyurethane
Thermal conductivity

ABSTRACT

Polyurethane (PU) based materials have wide application areas, especially in the thermal insulation, construction, and automotive sectors, due to their properties such as thermal and electrical insulation, lightness, and high compressive strength. In addition, studies on converting boron and its derivatives into value-added products have gained importance. In this study, the mechanical, physical, thermal, and ignitability properties of the composite materials obtained by adding boron derivatives of different weight fractions into PU were examined. Boron derivatives such as ground ulexite (U), borax pentahydrate, borax decahydrate, and ground colemanite (Col) were added to PU at 1, 3 and 5% by weight. It was shown that the density, thermal conductivity and compression modulus values increase when boron derivatives are used in PU-based composites. At the same time, the addition of ground U or Col to the PU foam reduced the water absorption value and made a positive contribution to the water absorption capacity. The PU material with 5 wt % Col added produced the greatest results, whereas 3.14% was discovered to be the lowest water absorption capability. The addition of boron derivatives increased the ignitability properties of PU foam composites. In particular, ground U or borax pentahydrate fillers showed substantial improvement in ignitability tests of PU foam composites. U (1%) demonstrated exceptional performance, reducing the PU's self-extinguishing time from 2.96 to 0 s.

1. Introduction

Sustainability has become increasingly important in the construction industry, especially because of its enormous ecological impact on all aspects of life and science. Reducing heat losses in buildings and thus increasing energy efficiency is crucial for sustainability [1]. One of the most important issues to consider in the design and construction of energy-efficient buildings is the selection of insulation materials [2]. These insulation materials include stone wool, glass wool, cellulose, sheep wool, polyurethane (PU) foam, expanded polystyrene, and extruded polystyrene [3]. PU foam is known for its excellent thermal insulation properties due to its low thermal conductivity (0.020-0.027 W/mK) compared to other materials, and accounts for approximately 80-90% of the insulation materials used in applications [3,4].

PU foams have been widely used in thermal insulation products such as refrigerators, freezers, and water heaters, as well as in panels designed for heat, sound and vibration insulation in buildings. They are also used in automobile and aircraft seating, interior panels for aircraft, sandwich structures in high-performance sports cars, biofilters in water treatment and waste air, microporous absorption materials, biocatalyst (enzyme) transporters in biotechnologies and lightweight packaging materials with high surface area [5-8]. Due to their wide range of applications, research into developing PU-based foams with properties tailored for specific industries, thermal insulation and the automotive industry, has accelerated in recent years. A study investigated the effects of different sizes expended graphite (EG) on the flame-retardant properties of rigid PU foam (RPUF) with a high density of 0.45 g/cm^3 [9]. They concluded that larger EG particles significantly improved the flame retardant (FR) properties of RPUF composites, while smaller EG particles resulted in poorer flame retardancy in the composites [9]. The effects of EG/bis(4-aminoanilinium) phenyl phosphonate (FR1) and pure EG FR additives on the cellular structure, thermal characteristics, flame retardancy, and compression strength of RPUF were also examined. When the ratio of EG to FR1 is 12 to 1, they obtained the best flame-retardant results [10]. Another study aimed to increase the fire resistance of rigid PU foams by adding 5, 10 and 15 wt. % nano clay and intumescent FR [11]. The experimental findings demonstrated that, despite a modest increase in thermal conductivity, the addition of nano clay or intumescent FR improved the foams' thermal conductivities, thermal stability, and fire resistance [11]. When the research was examined, it was seen that it focuses on issues such

*Corresponding author: gokhan.gurlek@ege.edu.tr

as thermal insulation, combustion resistance, thermal degradation, durability, sound absorption, and density. A common theme in these studies was the ignitability of PU foam materials, reflecting an ongoing effort to improve fire safety properties in various applications.

PU-based foam products are highly combustible when exposed to extreme heat or oxygen. These materials have caused worldwide concern due to their high ignitability and improving their fire safety is of extreme importance [12]. PU-based foam materials emit large amounts of smoke and toxic gases during combustion [13]. These toxic effects can be reduced by the addition of FR additives. The main FRs used depending on the structure of PU-based foam materials include inorganic FRs, intumescent systems, FRs containing phosphorus, silicon and boron. These additives play a key role in reducing thermal degradation, the release of toxic smoke and the burning tendency of PU-based foam materials, making their use essential in ensuring fire safety [14]. There are several studies discussing the use and potential industrial applications of chlorinated FRs in PU foams. Chlorinated FRs are common in PU manufacturing due to their efficiency in inhibiting flame spread, but they pose environmental concerns and health risks, leading to increased research on alternatives.

Some studies note that mineral-based additives (such as clay and metal hydroxides), while inexpensive, tend to affect the processing of foam materials due to their particle size, have the potential to cause blockages in production lines, and be chemically inert to the PU matrix [15]. As seen from studies, small particles tend to agglomerate. These large agglomerates can cause blockages as they pass through pipes and prevent the fluid from being properly delivered. This can cause production downtime. An uneven distribution of material can negatively impact the quality of the final product, which can lead to rework requirements during the production process. Large particles can block flow or make it harder for the fluid to move. Large particles also settle to the bottom more quickly or cause blockages. This can increase processing time and reduce efficiency. Large particles are generally denser, which can lead to handling and storage difficulties. Despite such production disadvantages, it is possible to overcome these problems with optimum particle size and homogenization.

Taking these problems into consideration, studies have focused on the use of boron derivatives as flame retardant. Due to the good ignitability properties of boron derivatives, they can prevent further spread of combustion by forming an impermeable glass-like coating on the material surface during thermal degradation [16]. Studies have shown that boron derivatives are effective as FRs in polymer-based systems [17]. The most commercially significant boron minerals include tincal, boracite, colemanite (Col), ulexite (U), pandermite, szaybelite, kernit, and hydroboracite, although more than 230 boron minerals are known in nature. The primary boron minerals are Col (76%), tincal (22%), U (2%), which are converted into high-value products. Concentrated tincal, boric acid, borax decahydrate (BD), Etidot-67, borax pentahydrate (BP), anhydrous borax, zinc borate, sodium perborate, boron oxide, ground colemanite, calcined tincal, and ground U are the products that can be extracted from these ores [18]. While the boron reserve in Türkiye was around 600 million tons in 1978, according to the latest research, today Türkiye has around 3 billion tons of boron reserves. While Türkiye held a 16% share of the global boron market in the 1970s, it has recently become the world's largest borate producer, with a 47% market share [19]. Studies on the production of PU-based foam materials using boron derivatives are very limited in literature. A study explored its usability as FR by mixing N,N'-di(methyleneoxy-3-hydroxypropyl) urea and boric acid into the rigid PU-polyisocyanurate foam (PUR-PIR) [20] . As a result of the study, it was observed that with the addition of the boric acid, the brittleness of the PUR-PIR foam decreased and it showed good resistance to burning [20]. Another study incorporated boron oxide (B_2O_3) and its derivatives as fillers at 5-20% in weight fractions, which increased the rigid PU foam materials' resistance to thermal deterioration and combustion [21]. While the inclusion of boron oxide increased the thermal conductivity of the material, which could be seen as a drawback, the study found that as the B_2O_3 ratio increased, both the combustion resistance and the mass remaining after combustion significantly improved. [21]. A study examined studied the use of derivatives of hydroxyethyl urea that were boron-modified to create foamed PU materials, further exploring the FR properties of boron-based additives [22]. Following the study, it was observed that the boron-modified PU foams demonstrated good dimensional stability, compressive strength, and thermal insulation properties when compared to the non-modified PU foams obtained using hydroxyethyl urea derivatives [22]. The impact of untreated and silane-coated boron nitride nanofillers, as well as wrinkled and holey flash graphene, on the mechanical, physical, and thermal characteristics of flexible PU foams was examined [23]. Their findings indicated that both treated and untreated boron nitride nanoparticles were effective in significantly reducing the wet compression set of the foams, enhancing their mechanical resilience [23]. In another study, the effect of ammonium pentaborate added to PU foam material together with FRs on ignition properties was investigated. It was observed that the FR formed a thermal barrier by cross-linking with boron chemicals during combustion and increased combustion resistance [24]. In their study, Chmiel et al. synthesized oligoetherol PU foams from ethylene carbonate and boron derivative melamine diborate [25]. It was found that the products had high thermal resistance and could withstand temperatures around 175°C [25]. In another study, they included two boron-containing inorganic compounds, zinc borate and boron phosphate, into rigid PU foams

and examined the smoke suppression performance and FR effect of the system. It was revealed that both boron-containing inorganic compounds inhibited smoke/heat release [26]. TA study prepared sodium polyborate by dissolving boric acid and sodium tetraborate decahydrate in water and examined its flame retardancy properties [27]. The new material was produced by first wrapping polyvinyl alcohol on expandable graphite and then dipping it in boric acid aqueous solution. The improved flame retardancy was attributed to the suppression of the "popcorn" effect of expanded graphite by polyvinyl alcohol-boric acid [28]. Another study assessed studied the effects of triphenyl phosphate, aluminum trihydrate and zinc borate on thermal insulation, mechanical and FR properties of rigid PU foam composites [29].

Although many different additives and boron derivatives were investigated in rigid PU foam materials preferred as insulation materials, there is no study in which ground U, BP, BD, and ground Col are considered together and compared. In this study, the investigation of the effects of different boron derivatives such as ground U, BP, BD and ground Col with different water contents on the thermal conductivity, compressive strength, ignitability, density and water absorption capacity of the insulation material will make an original contribution to the literature.

In this study, boron derivatives were utilized as FRs in the development of a new PU-based foam material. PU-based composite material was produced by adding, 1-5 wt% of ground U, BP, BD, and ground Col as boron derivatives to enhance its thermal, mechanical, and physical properties. The thermal conductivity, compressive strength, ignitability, density, and water absorption capacity of the composites were investigated by various characterization techniques.

2. Materials and Methods

2.1. Materials

In this study, a mixture of 100 g/140 g polyol/isocyanate (Yücel Composite, Türkiye) was used to produce PU foam. Ground U (particle size, 75μm), BP (75μm), BD (63μm), and ground Col (45μm) were used as fillers in the composites at 1, 3, and 5 wt% in composites (Eti Maden, Türkiye). Boron minerals of Na origin are called ‘borax’, those of Ca origin are called ‘colemanite’ and those of Na-Ca origin are called ‘U’. As the amount of water in borax decreases, it transforms from decahydrate to pentahydrate.

2.2. Preparation of Composite Foams Consisting of Polyurethane and Boron Derivatives

Polyol and boron derivatives were mixed using a mechanical mixer at 800 rpm for 30 min. Isocyanate was then added to the homogeneous mixture and stirred for an additional 10 s before being poured into a 300 mm x 300 mm x 30 mm mold. The compositions of the test samples are given in Table 1.

Table 1. Mixing ratios for PU and boron derivatives

Sample	PU%	BD%	BP%	U%	Col%
PU	100	-	-	-	-
PU+BD1	99	1	-	-	-
PU+BD3	97	3	-	-	-
PU+BD5	95	5	-	-	-
PU+BP1	99	-	1	-	-
PU+BP3	97	-	3	-	-
PU+BP5	95	-	5	-	-
PU+U1	99	-	-	1	-
PU+U3	97	-	-	3	-
PU+U5	95	-	-	5	-
PU+Col1	99	-	-	-	1
PU+Col3	97	-	-	-	3
PU+Col5	95	-	-	-	5

Teflon cloth was used to coat the mold prior to the molding process to keep the material from sticking. The mold's cover was sealed and tightened after the material was poured into it. Following a curing period of 24 h at room temperature (22±3°C), the mold was opened, and the PU composite foam material with the desired mixture properties was removed from the mold as seen in Figure 1.

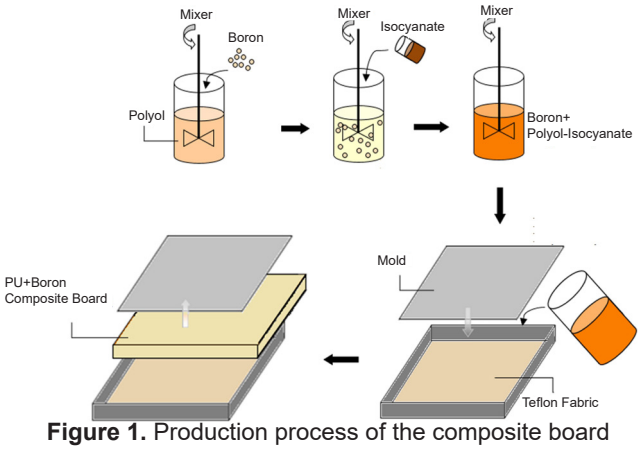

Figure 1. Production process of the composite board

2.3. Characterization

2.3.1. Density measurement

Using a densimeter (Mirage, Densimeter MD-200S, Japan) the specimens' densities were measured in accordance with ASTM D792.

2.3.2. SEM analysis

Scanning electron microscopy (SEM, Thermo Scientific, Apreo S, USA) was used to visualize the morphology of the neat PU and boron derivatives composites. Using a coating device (Leica, EM ACE600, Germany), samples were coated with Au/Pd prior to analysis.

2.3.3. Thermal conductivity

A heat flow meter (TA Insturments, FOX 314 Heat Flow Meter, USA) was used to measure, the thermal conductivity value of 300 mm x 300 mm x 10 mm PU samples and its composites in accordance with ISO 12667 standards.

2.3.4. Ignitability tests

The ignitability of test specimens was investigated in accordance with ISO 11925-2 standard. The midpoint of the specimens' lower edge was exposed to flame for 15 s during the ignitability test. Next, the amount of time it took for the flame to extend 150 mm above the application point was noted, and the amount of particles that caught fire during the 20 s was calculated in Figure 2.

Figure 2. Ignitability test

2.3.5. Compression test

Compression tests were carried out using an autograph (Shimadzu, Autograph AG-IS Series, Japan) universal testing apparatus in compliance with ISO 29469 standards. On the specimens with dimensions of 50 mm x 50 mm x 20 mm, a load was applied at a rate of 2 mm/min during the test. The elasticity modulus was calculated using the linear regression method.

2.3.6. Water absorption capacity measurement

Short-term water absorption capacity tests of the prepared composite samples were carried out according to ISO 29767. The samples were subjected to short-term water absorption tests at 23±5°C ambient temperature and 50±5% relative humidity conditions. Tests were conducted for 24 h under the specified conditions. Water absorption was calculated using Equ 1 [30] where w_0 refers to dry sample weight before immersion and w_1 stands for the weight of sample after immersion in water.

$$\text{Water absorption \% } (WA) = \frac{w_1 - w_0}{w_0} x100 \quad (1)$$

3. Results and Discussion

3.1. Density

Table 2 illustrates that the density values for the composites were greater than those of the pure PU. As expected, the density of the composites increased as the filler's weight percentage increased. It has been known that the density of PUs depends largely upon the density of the fillers [31]. Since the densities of U (2.13 g/cm^3), Col (2.42 g/cm^3), BD (1.73 g/cm^3), and BP (1.815 g/cm^3) are higher than that of PU, PU composite materials showed increased density values [32-34]. The highest density was found for PU composite material containing 5 wt% ground U and 5 wt% ground Col.

Table 2. Density values and ignitability test results of PU and its composites

Sample	Density (g/cm^3)	Ignitability Test
PU	0.052±0.00570	could not pass
PU+BD1	0.054±0.00245	could not pass
PU+BD3	0.057±0.00326	pass
PU+BD5	0.061±0.00245	pass
PU+BP1	0.055±0.00400	pass
PU+BP3	0.058±0.00735	pass
PU+BP5	0.061±0.00980	pass
PU+U1	0.053±0.00326	pass
PU+U3	0.056±0.00980	pass
PU+U5	0.062±0.00816	pass
PU+Col1	0.055±0.00490	pass
PU+Col3	0.059±0.00245	pass
PU+Col5	0.062±0.00490	could not pass

3.2. Morphology

Figure 3 shows the effects of different amounts of U contents, which give the worst results in terms of thermal conductivity values, on the morphological structure of PU foam. Most of the cell types of pure PU were hexagonal, the cell morphology was relatively complete, and the cell size distribution was relatively uniform. It was seen that the foam is a closed-cell

type. Here, the smooth texture of the foam material was disrupted when U is added. It was thought that increasing U amounts (especially 5%) caused the cells to shrink, due to the fact that the added U prevented the foam from expanding during curing and the increase in viscosity of the material [26]. However, the additives encourage more cell formation [35]. According to SEM images, adding 5% U in particular caused the cell walls to distort and reduced the homogeneity of the cell structure, which increased thermal conductivity and decreases compressive strength.

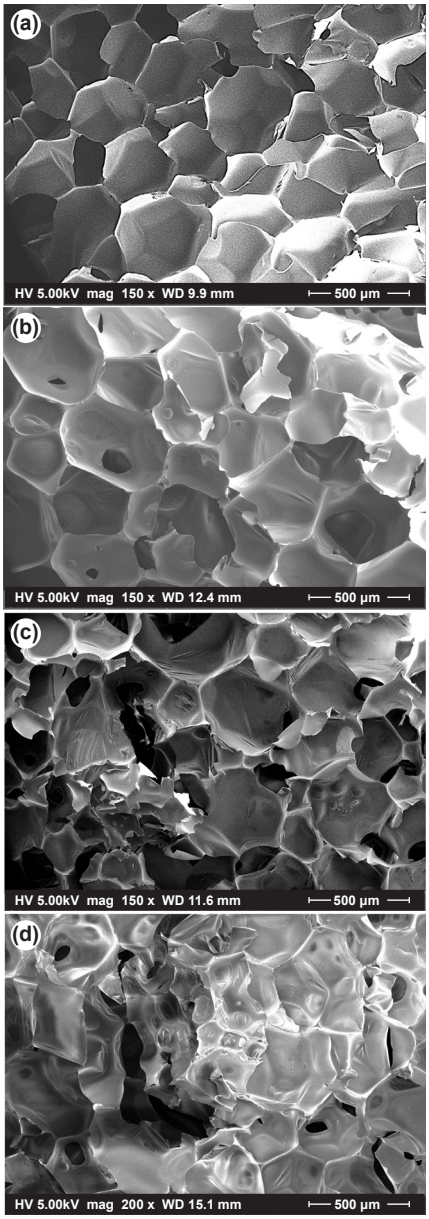

Figure 3. SEM images of a) neat PU, b) PU+U1, c) PU+U3, d) PU+U5

The SEM images of the morphology of the PU network after boron loading did not show much difference due to the low-weight fractions of the minerals and possible inhomogeneous distribution. Therefore, for visibility, SEM images of PU foams containing 5% boron derivative are given in Figure 4. No signs of aggregation were observed in the added boron particles. Relatively large particle sizes were found in the images with the same magnification value (×500) (Figure 4b, c). On the other hand, it was seen that the additive sizes in the images were smaller than the maximum grain sizes specified by the manufacturer.

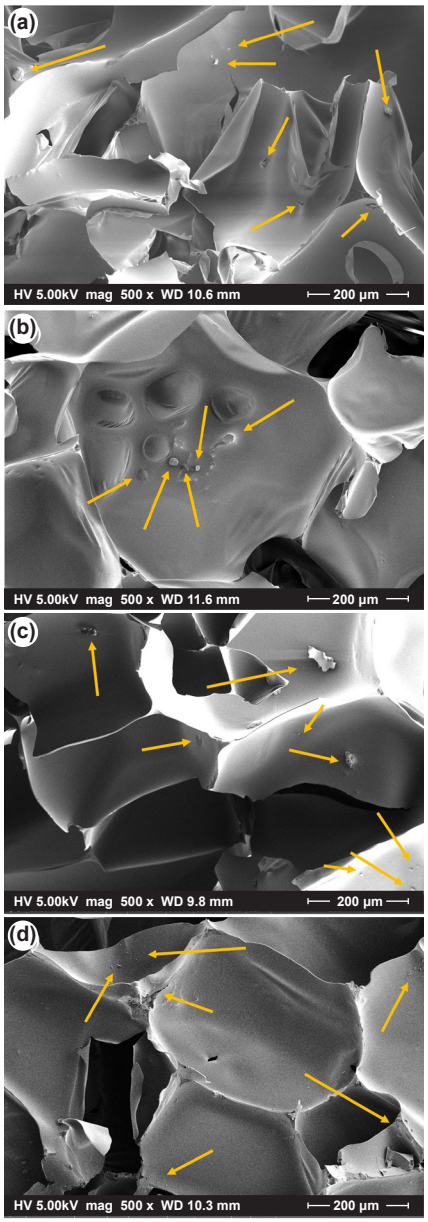

Figure 4. SEM images of a) PU+BD5, b) PU+BP5, c) PU+U5, d) PU+Col5

3.3. Thermal Conductivity

Figure 5 displays the thermal conductivity values of PU and its composites. Each sample was measured three times, and the average of the results was used. The results showed that PU had a thermal conductivity of 0.0289 W/mK. It was observed that the addition of boron derivatives to the material reduced the thermal conductivity. Typically, PU foam materials have thermal conductivity values between 0.02 and 0.03 W/mK [36]. Thermal conductivity values of U, Col, BP, and BD are given as 0.482 W/mK, 0.526 W/mK, 0.647 W/mK, and 0.740 W/mK, respectively [33,34,37].

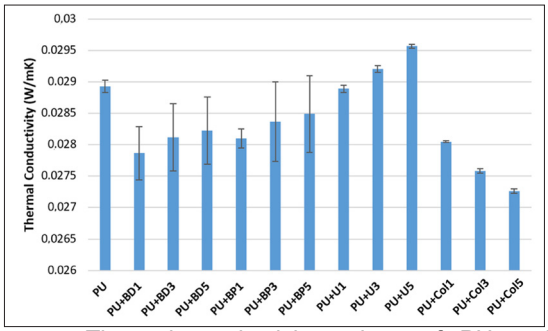

Figure 5. Thermal conductivity values of PU and its composites

It was observed that the addition of BD, BP, and Col contributes to the thermal insulation property of the material by decreasing the thermal conductivity value of the PU. The addition of BD and BP boron derivatives at low rates significantly reduced the thermal conductivity and made a greater contribution to the material. On the other hand, as the amount of Col increased in the composite foam, a significant decrease was observed in the thermal conductivity of the material. Interestingly, the only observed negative effect was associated with the composite foam containing ground U, which demonstrated reduced insulation properties compared to pure PU. The interface between polymer and filler plays an important role in determining the thermal conductivity of a composite material. Dislocations, point defects, and interface incompatibility with polymers and crystalline fillers such as boron derivatives cause a decrease in thermal conductivity [38]. In addition, the large particle size of ground U may have facilitated the filling of air gaps within the PU foam, further increasing thermal conductivity.

3.4. Ignitability

The ignitability test results are given in Table 2 and Figure 6. Figure 6a illustrates that the PU sample failed the test due to rapid flame spread and quick time to reach the 150 mm line. However, when boron derivatives were added to the PU, materials showed improved ignitability results as is seen in Figure 6. Notably, the slowest flame propagation was observed with a 5 wt% loading of U, as seen in Figure 6b.

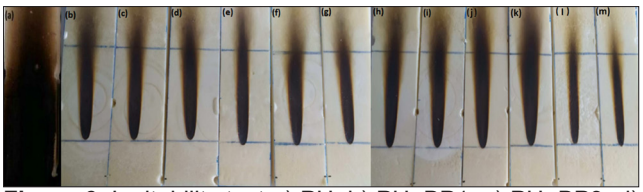

Figure 6. Ignitability test a) PU, b) PU+BP1, c) PU+BP3, d) PU+BP5, e) PU+BD1, f) PU+BD3, g) PU+BD5, h) PU+Col1, i) PU+Col3, j) PU+Col5, k) PU+U1, l) PU+U3, m) PU+U5

Figure 7 shows the self-extinguishing times of the foam materials after being exposed to flames for 15 s. The pure PU foam material extinguished itself in about 3 s. The foam material with the addition of 1% U was extinguished immediately upon removal of the flame. Although some increases in extinguishing time were observed with higher amounts of U, it still yielded better results compared to pure PU. The addition of BP significantly reduced the self-extinguishing time, with shorter extinguishing times noted across all weight fractions compared to pure PU foam. Considering the Col-filled PU composites, it affected the self-extinguishing results worse than the other fillers. It was observed that foam materials with 5% Col and 1% BD were added quenched longer than pure PU foam material. Boron compounds were reported to improve the FR properties of polymeric composites [39]. It was concluded that due to the flame-retardant properties of boron compounds, BD and boric acid fillers, reduced the ignitability of the composites obtained [40]. It has also reached the category of self-extinguishing materials at higher boric acid filler composites [40]. It was concluded in a study that boron-filled PU composites had reduced ignitability compared to PUs [41]. Current results revealed that the ignitability of the PU foam material increased with the addition of U and BP. On the other hand, Col and BD were found to be effective on ignitability at certain rates. Higher thermal conductivity allows heat to spread rapidly throughout the material, reducing the likelihood of heat accumulation at specific points. This can mean that heat from any ignition source is rapidly dissipated within the material, preventing the material from reaching the critical temperature required to sustain combustion. As a result, the material can self-extinguish more effectively when the heat source is removed. This is clearly seen in the example of U. In the self-extinguishing test, PU materials modified with BD performed worse than those modified with BP. However, as the amount of water in the additive increases, it is expected that the material will burn more difficultly and extinguish faster, but this is only up to a certain point. When there is more than a certain amount of water in the material and this water evaporates when the material is heated, the vapor comes out of the material in the vapor phase. Meanwhile, the increasing vapor pressure in the material causes the material to physically crack or deform [42]. The structure with surface fractures will be more exposed to flames, which reduces its resistance to burning.

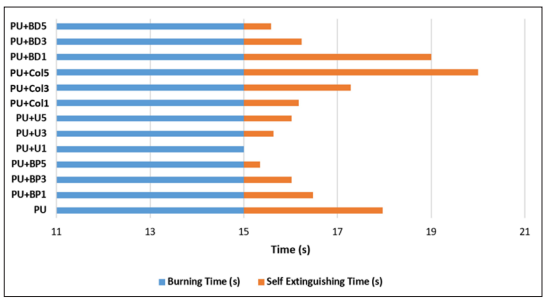

Figure 7. Self-extinguishing times of PU and its composites

3.5. Compression Tests

The compression strength and modulus of the PU composites were measured to gain additional insight into their mechanical properties. Each sample was

measured three times, and the average of the results was recorded. The compression properties of materials are given in Figure 8.

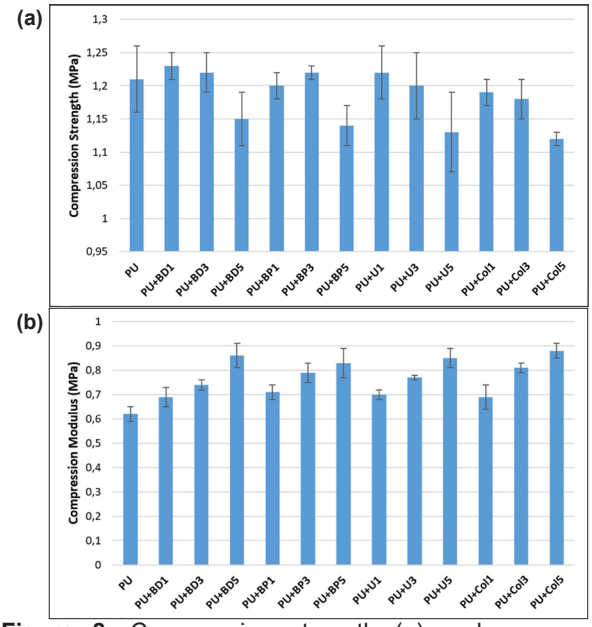

Figure 8. Compression strength (a) and compression modulus (b) of PU and its composites

When the compressive strengths are examined, it is seen that there is no significant change in strength with the addition of 1% and 3% of BD, BP, U, and Col fillers. However, when fillers are added at 5% their compressive strength decreases. Bishay et al. concluded that at higher filler contents, the compressive strength of the composites may decrease due to the inhibition of interaction between fillers and polymer matrix [43]. Similarly, it can be said that the decrease in compressive strength is due to the inhibition of the movement of the polymer chains due to the inhomogeneous distribution of boron fillers and may also be due to the deformation of the cell walls, especially at high additive levels such as 5%. The knowledge that the improvement of the mechanical properties of the composite material depends largely on the homogeneous distribution of the fillers is also supported by the literature [39]. Simultaneously, the formulae of BP and BD compounds (BP: $Na_2B4O_7.5H_2O$, BD: $Na_2B_4O_7.10H_2O$) contain water molecules. This can result in micro-voids at the interface between the polymer and fillers, which lower the mechanical properties of the material [44]. The decrease in compressive strength indicates the poor distribution of boron derivative fillers in the PU, the presence of defects such as voids, and interfacial incompatibility [45].

It is well known that cellular structure and density typically affect a material's mechanical properties [46]. When the compressive modulus values are examined, it is seen that the modulus increase with the increase in the ratio of fillers. This is because fillers give the composite its strength and modulus, whereas polymers are far weaker than fillers [47].

3.6. Water Absorption Capacity

The water absorption values of PU composite materials are shown in Figure 9.

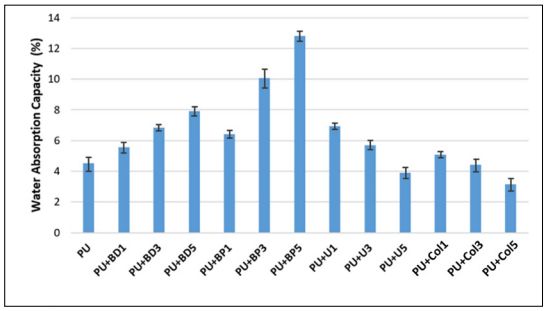

Figure 9. The water absorption capacity of PU and its composites

The water absorption capacity of the PU was found to be 4.51%. Among all the composite foam materials examined, the highest water absorption capacity was obtained in the 5 wt % BP filled PU composite with a value of 12.81%. Conversely, the lowest water absorption capacity was recorded for the 5% Col-filled PU composite, at 3.14. As the weight fraction of BP and BD increased, the water absorption capacity of the PU also increased. It is seen that boron derivatives containing borax contribute negatively to the water absorption property of the material. It is seen that the addition of U and Col at high fractions (5%) reduces the water absorption capacity of the material. The water absorption capacities increased slightly with the addition of boron derivatives at low fractions (1-3%). Specifically, the water absorption capacity decreased to 3.91% with the addition of 5% U to the PU, while it decreased to 3.14% when 5% Col was added to the PU. The difference in water absorption capacity is related to the chemical structures and crystal water content of these substances. BP and BD contain crystal structures that contain a certain amount of water molecules. The water-binding capacity of BP and BD forms is due to the ability of crystal structures to physically hold water. Water is found as a part of this crystal structure and therefore has a high water absorption capacity. U and Col, on the other hand, are structures that contain less water and have a lower capacity to hold water. In addition, the fact that the voids in the crystal structures of these compounds are in a structure that makes it difficult for water molecules to be held may also affect this situation.

4. Conclusions

In this study, effects of addition of boron derivatives on ignitability, thermal, mechanical and water absorption properties of PU composites were investigated. It was concluded that the density of the composites increased via the incorporation of boron derivatives into PU. According to the ignitability test, the U and BP fillers improved the ignitability properties PU foam material as it shortened the self-extinguishing time. Especially U (1%) provided outstanding performance and

decreased the self-extinguishing time of PU from 2.96 to 0 s. The addition of BD and BP boron derivatives at low fractions made a great contribution to the material by significantly reducing the thermal conductivity value of the PU foam material. With the addition of ground Col, the lowest thermal conductivity values were obtained, and the PU thermal conductivity value, which was 0.028 W/mK, decreased to 0.0272 W/mK. It was seen that the compressive modulus values increase with the addition of boron-derived fillers, but there was no significant change in compressive strength values when 1wt % and 3wt % BD, BP, U and Col are added. When the water absorption capacities were examined for all composite foam materials, it was observed that the addition of 5wt % U or 5wt % Col contributed positively to the PU foam material, but the addition of borax-containing boron derivatives (BP and BD) negatively contributed to the water absorption of the material. The best result was obtained with 5wt % Col was added to the PU material, and the lowest water absorption capacity was found to be 3.14%. This study has shown that material properties can be improved by adding different boron derivatives for different utilization purposes of PU foam materials. PU foams with lower thermal conductivity and better flammability properties have great potential for use in exterior construction applications and various industries where flammability is a major concern.

5. Acknowledgements

The authors are grateful for the funding from Ege University, Office of Scientific Research Projects (Project no: 21768). We would like to thank Prof. Dr. Mehmet Sarıkanat for his support. We would like to thank Eti Maden for their support in the supply of boron derivatives.

References

[1]. Andersons, J., Kirpluks. M., Cabulis. P., Kalnins. K., & Cabulis. U. (2020). Bio-based rigid high-density polyurethane foams as a structural thermal break material. *Construction and Building Materials*, *260*, 120471. https://doi.org/10.1016/j.conbuildmat.2020.120471

[2] Papadopoulos, A. M. (2005). State of the art in thermal insulation materials and aims for future developments. *Energy and Buildings*, *37*(1), 77-86. https://doi.org/10.1016/j.enbuild.2004.05.006

[3] Aditya, L., Mahlia, T. M. I., Rismanchi, B., Ng, H. M., Hasan, M. H., Metselaar, H. S. C., … & Aditiya, H. B. (2017). A review on insulation materials for energy conservation in buildings. *Renewable and Sustainable Energy Reviews*, *73*, 1352-1365. https://doi.org/10.1016/j.rser.2017.02.034

[4] Kim, J. M., Kim, J. H., Ahn, J. H., Kim, J. D., Park, S., Park, K. H., & Lee, J. M. (2018). Synthesis of nanoparticle-enhanced polyurethane foams and evaluation of mechanical characteristics. *Composites Part B: Engineering*, *136*, 28-38. https://doi.org/10.1016/j.compositesb.2017.10.025

[5] Gama, N. V., Soares, B., Freire, C. S. R., Silva, R., Neto, C. P., Barros-Timmons, A., & Ferreira, A. (2015). Bio-based polyurethane foams toward applications beyond thermal insulation. *Materials & Design*, *76*, 77-85. https://doi.org/10.1016/j.matdes.2015.03.032

[6] Suleman, S., Khan, S. M., Gull, N., Aleem, W., Shafiq, M., & Jamil, T. (2014). A comprehensive short review on polyurethane foam, *International Journal of Innovation and Scientific Research*, *12*(1), 165-169. Retrieved from https://ijisr.issr-journals.org/abstract.php?article=IJISR-14-294-05

[7] Skleničková, K., Abbrent, S., Halecký, M., Kočí, V., & Beneš, H. (2022). Biodegradability and ecotoxicity of polyurethane foams: A review. *Critical Reviews in Environmental Science and Technology*, *52*(2), 157-202. https://doi.org/10.1080/10643389.2020.1818496

[8] Das, A., & Mahanwar, P. (2020). A brief discussion on advances in polyurethane applications. *Advanced Industrial and Engineering Polymer Research*, *3*(3), 93-101. https://doi.org/10.1016/j.aiepr.2020.07.002

[9] Shi, L., Li, Z. M., Xie, B. H., Wang, J. H., Tian, C. R., & Yang, M. B. (2006). Flame retardancy of different-sized expandable graphite particles for high-density rigid polyurethane foams. *Polymer International*, *55*(8), 862-871. https://doi.org/10.1002/pi.2021

[10] Acuña, P., Lin, X., Calvo, M. S., Shao, Z., Pérez, N., Villafañe, F., ... & Wang, D. Y. (2020). Synergistic effect of expandable graphite and phenyl phosphonic-aniline salt on flame retardancy of rigid polyurethane foam. *Polymer Degradation and Stability*, *179*, 109274. https://doi.org/10.1016/j.polymdegradstab.2020.109274

[11] Aydoğan, B., & Usta, N. (2019). Fire behavior assessment of rigid polyurethane foams containing nano clay and intumescent flame retardant based on cone calorimeter tests. *Journal of Chemical Technology and Metallurgy*, *54*(1), 55-63.

[12] Cao, Z. J., Liao, W., Wang, S. X., Zhao, H. B., & Wang, Y.Z. (2019). Polyurethane foams with functionalized graphene towards high fire-resistance, low smoke release, superior thermal insulation. *Chemical Engineering Journal*, 361, 1245-1254. https://doi.org/10.1016/j.cej.2018.12.176

[13] Liu, X., Hao, J., & Gaan, S. (2016). Recent studies on the decomposition and strategies of smoke and toxicity suppression for polyurethane based materials. *RSC Advances*, *6*(78), 74742-74756. https://doi.org/10.1039/C6RA14345H

[14] Kairytė, A., Kirpluks, M., Ivdre, A., Cabulis, U., Vaitkus, S., & Pundienė, I. (2018). Cleaner production of polyurethane foam: Replacement of conventional raw materials, assessment of fire resistance and environmental impact. *Journal of Cleaner Production*, *183*, 760-771. https://doi.org/10.1016/j.jclepro.2018.02.164

[15] Choi, J. H., Chae, S. U., Hwang, E. H., & Choi, D. M. (2022). Fire propagation characteristics and fire risks of polyurethanes: Effects of material type (foam & board) and added flame retardant. *Fire*, *5*(4), 105. https://doi.org/10.3390/fire5040105

[16] Açikel, S. M. (2018). Development of commercial flame retardant in upholstery leathers by boron derivatives.

Textile and Apparel, *28*(4), 319-323. https://doi.org/10.32710/tekstilvekonfeksiyon.493101

[17] Gurlek, G., Altay, L., & Sarikanat, M. (2019). Thermal conductivity and flammability of ulexite filled rigid polyurethane materials. *Acta Physica Polonica A*, *135*(4), 825-828. https://doi.org/10.12693/APhysPolA.135.825

[18] Karslıoğlu, A., Onur, M. İ., & Balaban, E. (2022). Investigation of boron waste usage in civil engineering applications. *Niğde Ömer Halisdemir University Journal of Engineering Sciences*, *11*(3), 727-735. https://doi.org/10.28948/ngmuh.1084831

[19] Sokmen, N., & Buyukakinci, B. Y. (2018). The usage of boron/ boron compounds in the textile industry and its situation in Turkey. *CBU International Conference on Innovations in Science and Education*, *6*, 1158-1165. https://doi.org/10.12955/cbup.v6.1309

[20] Paciorek-Sadowska, J. (2012). Modification of purpır foams by boroorganic compound prepared on the basis of di(hydroxymethyl)urea. *Journal of Porous Materials*, *19*(2), 161-171. https://doi.org/10.1007/s10934-011-9456-y

[21] Yeler, O., Köseoğlu, M. F., Usta, N., & Demiryuğuran, F. (2015). Rijit poliüretan köpük malzemelere bor oksit ilavesinin ısıl bozunma ve yanma özelliklerine etkilerinin incelenmesi. *İleri Teknoloji Bilimleri Dergisi*, *99*, 34-39. Retrieved from https://dergipark.org.tr/en/pub/duzceitbd/issue/37903/365714

[22] Zarzyka, I. (2016). Preparation and characterization of rigid polyurethane foams with carbamide and borate groups: rigid polyurethane foams with carbamide and borate groups. *Polymer International*, *65*(12), 1430-1440. https://doi.org/10.1002/pi.5198

[23] Li, O., Tamrakar, S., Iyigundogdu, Z., Mielewski, D., Wyss, K., Tour, J. M., & Kiziltas, A. (2023). Flexible polyurethane foams reinforced with graphene and boron nitride nanofillers. *Polymer Composites*, *44*(3), 1494-1511. https://doi.org/10.1002/pc.27183

[24] Montemayor, M. D., Vest, N. A., Palen, B., Smith, D. L., & Grunlan, J. C. (2024). Boron-containing polyelectrolyte complex for self-extinguishing polyurethane foam. *ACS Applied Polymer Materials*, *6*(9), 5226-5234. https://doi.org/10.1021/acsapm.4c00400

[25] Chmiel, E., Oliwa, R., & Lubczak, J. (2019). Boron-containing non-flammable polyurethane foams. *Polymer-Plastics Technology and Materials*, *58*(4), 394-404. https://doi.org/10.1080/03602559.2018.1471717

[26] Xu, B., Zhao, S., Shan, H., Qian, L., Wang, J., & Xin, F. (2022). Effect of two boron compounds on smoke-suppression and flame-retardant properties for rigid polyurethane foams. *Polymer International*, 71(10), 1210-1219. https://doi.org/10.1002/pi.6403

[27] Tsuyumoto, I., Onoda, Y., Hashizume, F., & Kinpara, E. (2011). Flame-retardant rigid polyurethane foams prepared with amorphous sodium polyborate. *Journal of Applied Polymer Science*, *122*(3), 1707-1711. https://doi.org/10.1002/app.34025

[28] Dongmei, X., Xiu, L., Jie, F., & Jianwei, H. (2015). Preparation of boron-coated expandable graphite and its application in flame retardant rigid polyurethane foam. *Chemical Research in Chinese Universities*, *31*(2), 315-320. https://doi.org/10.1007/s40242-015-4101-y

[29] Akdogan, E., Erdem, M., Ureyen, M. E., & Kaya, M. (2020). Rigid polyurethane foams with halogen-free flame retardants: Thermal insulation, mechanical, and flame-retardant properties. *Journal of Applied Polymer Science*, *137*(1), 47611. https://doi.org/10.1002/app.47611

[30] Radzi, A. M., Sapuan, S. M., Jawaid, M., & Mansor, M. R. (2019). Water absorption, thickness swelling, and thermal properties of roselle/sugar palm fibre reinforced thermoplastic polyurethane hybrid composites. *Journal of Materials Research and Technology*, *8*(5), 3988-3994. https://doi.org/10.1016/j.jmrt.2019.07.007

[31] Taherishargh, M., Belova, I. V., Murch, G. E., & Fiedler, T. (2014). Low-density expanded perlite-aluminium syntactic foam. *Materials Science and Engineering: A*, *604*, 127-134. https://doi.org/10.1016/j.msea.2014.03.003

[32] Uçar, N., Çalık, A., Emre, M., & Akkurt, I. (2021). Physical radiation shielding properties of concrete contains colemanite and ulexite. *Indoor and Built Environment*, *30*(10), 1827-1834. https://doi.org/10.1177/1420326X20967974

[33] Product Technical Data Sheet-Borax Decahydrate. (2023). [Online] Available: https://www.etimaden.gov.tr/storage/uploads/2018/01/10-2017-Borax_Deca_Powder.pdf

[34] Product Technical Data Sheet- Borax Pentahydrate. (2023). [Online] Available: https://www.etimaden.gov.tr/storage/pages/March2023/TR-Etifert-B15.pdf

[35] Soyer, Ş., Gürlek, G., & Kılıç, E. (2023). Valorization of leather industry waste in polyurethane composites for reduced flammability. *Journal of Material Cycles and Waste Management*, *25*(1), 314-323. https://doi.org/10.1007/s10163-022-01533-3

[36] Zhang, H., Fang, W.Z., Li, Y. M., & Tao, W.Q. (2017). Experimental study of the thermal conductivity of polyurethane foams. *Applied Thermal Engineering*, *115*, 528-538. https://doi.org/10.1016/j.applthermaleng.2016.12.057

[37] Irgat, M. S., & Yukselen-Aksoy, Y. (2019). Thermal conductivity behavior of boron added sand-bentonite mixtures. *Proceedings of the XVII ECSMGE-2019, (Geotechnical Engineering, Foundation of the Future), Iceland*, 4388-4393. https://doi.org/10.32075/17ECSMGE-2019-0911

[38] Guerra, V., Wan, C., & McNally, T. (2019). Thermal conductivity of 2d nano-structured boron nitride (bn) and ıts composites with polymers. *Progress in Materials Science*, *100*, 170-186. https://doi.org/10.1016/j.pmatsci.2018.10.002

[39] Orhan, R., Aydoğmuş, E., Topuz, S., & Arslanoğlu, H. (2021). Investigation of thermo-mechanical characteristics of borax reinforced polyester composites. *Journal of Building Engineering*, 42, 103051. https://doi.org/10.1016/j.jobe.2021.103051

[40] Abdulrahman, S. T., Ahmad, Z., Thomas, S., Maria, H. J., & Rahman, A. A. (2020). Viscoelastic and thermal

properties of natural rubber low-density polyethylene composites with boric acid and borax. *Journal of Applied Polymer Science*, *137*(44), 49372. https://doi.org/10.1002/app.49372

[41] Łukasiewicz, B., & Lubczak, J. (2014). Polyurethane foams with purine ring and boron. *Journal of Cellular Plastics*, *50*(4), 337-359. https://doi.org/10.1177/0021955X14525958

[42] Kawagoe, M., Doi, Y., Fuwa, N., Yasuda, T., & Takata, K. (2001). Effects of absorbed water on the interfacial fracture between two layers of unsaturated polyester and glass. *Journal of Materials Science*, *36*, 5161-5167. https://doi.org/10.1023/A:1012437626988

[43] Bishay, I. K., Abd-El-Messieh, S. L., & Mansour, S. H. (2011). Electrical, mechanical and thermal properties of polyvinyl chloride composites filled with aluminum powder. *Materials & Design*, *32*(1), 62-68. https://doi.org/10.1016/j.matdes.2010.06.035

[44] Kuru, D., Akpinar Borazan, A., & Guru, M. (2018). Effect of chicken feather and boron compounds as filler on mechanical and flame retardancy properties of polymer composite materials. *Waste Management & Research*, *36*(11), 1029-1036. https://doi.org/10.1177/0734242X18804041

[45] Seki, Y., Sever, K., Sarikanat, M., Sakarya, A., & Elik, E. (2013). Effect of huntite mineral on mechanical, thermal and morphological properties of polyester matrix. *Composites Part B: Engineering*, *45*(1), 1534-1540. https://doi.org/10.1016/j.compositesb.2012.09.083

[46] Yurtseven, R. (2019). Effects of ammonium polyphosphate/melamine additions on mechanical, thermal and burning properties of rigid polyurethane foams. *Acta Physica Polonica A*, *135*(4), 775-777. https://doi.org/10.12693/APhysPolA.135.775

[47] Bajwa, S. G., Bajwa, D. S., Holt, G., Coffelt, T., & Nakayama, F. (2011). Properties of thermoplastic composites with cotton and guayule biomass residues as fiber fillers. Industrial *Crops and Products*, *33*(3), 747-755. https://doi.org/10.1016/j.indcrop.2011.01.017

TENMAK BOREN BOR ARAŞTIRMA ENSTİTÜSÜ

BOR DERGİSİ
JOURNAL OF BORON
https://dergipark.org.tr/boron

Evaluation of 2-formylphenylboronic and 3-chlorophenylboronic acid derivatives for *in vitro* cytotoxicity and cell migration

Bükay Yenice Gürsu [1], **Betül Yılmaz Öztürk** [1,*], **İlknur Dağ** [1,2]

[1]*Central Research Laboratory Application and Research Center, Eskisehir Osmangazi University, Eskisehir, 26040, Türkiye*
[2]*Vocational Health Services High School, Eskisehir Osmangazi University, Eskisehir, 26040, Türkiye*

ARTICLE INFO

Article history:
Received May 31, 2024
Accepted November 13, 2024
Available online December 31, 2024

Research Article

DOI: 10.30728/boron.1493431

Keywords:
2-formylphenylboronic acid
3-chlorophenylboronic acid
In vitro cytotoxicity
Wound healing

ABSTRACT

Wound treatment and skin regeneration are complex processes, and non-healing wounds pose a major socioeconomic burden in terms of health. Effective and alternative approaches are needed for successful wound management. Although boronic acid derivatives have been reported to have positive and strong effects on wound healing, phenyl-substituted boronic acid derivatives can be used as more regenerative and effective compounds in healing. In this study, the *in vitro* cytotoxic effects of 2-formylphenylboronic acid and 3-chlorophenylboronic acid on L929 fibroblast cell lines were investigated using WST-8 analysis, and their wound healing effects were investigated by cell migration test. Our data reveal concentration-dependent effects of both boronic acid derivatives. For 2-formylphenylboronic acid, dosage applications between 3.90-31.25 µg/ml showed a viability of 84% and above, and at higher concentrations, the viability was found to be 5-10%. For 3-chlorophenylboronic acid, a viability rate of 64-109% is observed as a result of dosage applications between 3.90-250 µg/ml, while the percentage of viability decreases to 17% at a concentration of 500 µg/ml. Cell migration test data show that the effects of phenylboronic acid (PBA) derivatives in terms of cell migration increase as time increases, and the effect of 2-formylphenylboronic acid at the 24th hour is quite effective in terms of cell migration. Since the wound healing effect of PBA derivatives is concentration dependent, it should be taken into consideration that the use of high concentrations may be toxic.

1. Introduction

Wounds that disrupt the integrity of the skin and mucosa due to various factors can heal through a very complex process in the body. While factors such as age, nutrition, and smoking affect healing, infections caused by microorganisms in the wound area are also quite common. Nutrition of the scar tissue by ensuring perfusion and oxygen exchange in the wound area is a critical factor [1]. Therefore, wound management imposes a serious economic burden on healthcare systems and has dramatic effects on individuals with chronic, traumatic, or surgical wounds [2]. Various materials such as films, foams, hydrogels, and hydrocolloids are recommended for dressing purposes or as tissue adhesives in treatment, but problems such as poor biocompatibility or limited tissue adhesion have still not been fully overcome. New and effective alternatives that prevent wound healing are needed.

Boron is a trace element that is in group 3A of the periodic table and is considered a semi-metal and is found in nature as a compound with oxygen. While it is reported that boron is necessary in physiological events such as ensuring the rigidity of the cell wall in plants, pollination, growth, flowering, or seed formation, its roles in the human and animal bodies have not yet been fully clarified. Boron is found in a number of natural products isolated from bacteria and may show antibiotic activity. These natural products also support that boron can be tolerated in biological systems. Boron also attracts great attention in the field of health and has positive effects on cancer, bone health, wound healing, and the immune system. It is reported in the literature that boron plays a role in events such as ion transport, hormone production, calcium metabolism or bone development, and that it increases the healing rate in deep wounds and reduces the duration of stay in intensive care. It is also stated that boron derivatives increase keratinocyte migration and extracellular matrix turnover by increasing matrix metalloproteinase expression [3, 4]. Organic compounds containing boron moieties have a wide range of applications in synthetic organic chemistry. Boronic acid contains organic compounds containing a trivalent boron structure. One of them has an alkyl substitution and the other two have a hydroxyl group [5]. Boronic acids are not found in nature and are synthesized in the laboratory [6]. In addition to their high reactivity and stability, an important feature

*Corresponding author: byozturk@ogu.edu.tr

is that they have a very low toxicological profile [7]. They are also very popular because they are easy to synthesize and can be used in many chemical and biological reactions [8]. Boronic acids, with their 'saccharide binding' properties, attract great attention both in the research of biological systems and in the identification of metabolites in the pathology of diseases such as diabetes. Various studies state that they can bind to glycoproteins in the cell membrane, thus accelerating wound healing by proliferating cells such as lymphocytes. It is also known that boronic acid can bind to macromolecules containing cis-diol functional groups, thanks to its boronate ester rings. This situation causes boronic acid to covalently interact with components with cis-diol functionality, such as teichoic acid or lipopolysaccharide, found in the bacterial cell wall [9, 10]. Since phenyl-substituted boronic acid (PBA) derivatives exhibit interesting properties in terms of synthetic, application, and structural aspects, they are used in many areas such as sensors, receptors, polymers, drug active ingredients, cancer treatment, organic synthesis, and functionalized nanoparticles. There are many experimental and theoretical studies on the molecular structures and spectroscopic properties of PBA and its derivatives. Recent research reveals the important antibacterial and anticancer properties of PBA and its derivatives [5].

Formyl-substituted phenylboronic acids are noteworthy because they contain a reactive aldehyde group and can interact with the neighboring boronic unit in many ways thanks to the formyl group [11]. 2-formylphenylboronic acid shows many interesting properties in terms of synthetic, application, and structural aspects. Recent studies support the antimicrobial/antifungal activity of 2-formylphenylboronic acid and its anticancer or wound healing properties by adding it to the structure of various nanomaterials [12-14]. To our knowledge, there is no study yet on the biological effects of 3-chlorophenylboronic acid in the literature. In this study, the *in vitro* cytotoxicity of 2-formylphenylboronic acid and 3-chlorophenylboronic acid on L929 cell lines was evaluated and the effects of these components on cell migration were investigated in the light of the findings.

2. Materials and Methods

2.1. Cytotoxicity Test

The fibroblast L929 cell line of ATCC CCL-1 origin and passage number 16 was used in the study. Cells were grown in T25 flasks and EMEM medium containing 10% FBS (P30-1301, Pan Biotech, Germany) and checked twice a day. The cells were allowed to reach over 70 % confluency (Doubling time: 22-26 hours). After the samples were prepared at a concentration of 1 mg/mL, they were exposed to UV light for 30 minutes, dissolved in 100 µL DMSO and homogenized with the medium. Concentrations to be used later were diluted with complete medium. After adding 500 µL Trypsin-EDTA (15400054, Gibco, USA) to the cells that reached confluency, they were waited for 3-5 minutes at a 37°C and 5% CO_2 environment. The cells were examined under an inverted microscope (Zeiss Primovert, Germany), and when it was determined that they were dissociated, medium containing 10% FBS was added. It was centrifuged at 300xg for 5 minutes, the medium was discarded, and 1 mL EMEM medium was added onto the cells. Counting was done with trypan blue (1525061, Gibco, USA) on the Logos Luna II device (Logos Biosystems, South Korea), and 10% FBS medium was added to obtain 10^4 cells per well.

For the purpose of performing the cytotoxicity test, the medium in the culture plate was removed when 70% confluency was reached in each well. After the addition of fresh medium, samples were added to the cell dish. Three replicates were studied for each group. Eight different concentrations of both boronic acid derivatives were applied to the cells (500, 250, 125, 62.5, 31.25, 15.62, 7.81, 3.90 µg/mL). Cells were kept in the incubator for 22 hours after exposure. Apart from the test samples, the so-called negative well contained only medium and cells (growth control). The positive well contained 2 µL H_2O_2 (a drug control with known toxicity) in addition to the medium and cells. Finally, blank wells were prepared by adding only the medium. At the end of 22 hours, 10% of the well volume (equal to 20 µL WST-8 in the experiment) of WST-8 solution was added. The cell culture container was wrapped with aluminum foil and kept in the incubator for another 2 hours, and at the end of 2 hours, spectrophotometric readings were taken at wavelengths of 450 nm and 630 nm. The results were formulated, and the % viability was determined (Equation 1):

$$\% \text{ Viability } = \frac{(\text{Sample Well} - \text{Blank})}{(\text{Negative Control} - \text{Blank})} \times 100 \quad (1)$$

2.2. In vitro Cell Migration Tests

In order to determine the cell migration of boronic acid cells and therefore the possibility of wounding, a wound healing model should be prepared by testing cell components, looking at L929, which is a fibroblast cell. The samples were added to 48-well tissue culture dishes in EMEM medium supplemented with 10% FBS, 1% penicillin-streptomycin, and 4 mM L-glutamine at a volume of $2x10^4$ cells/ml and kept until the grown monolayer was covered. Then, the surface was scratched from one end to the other in a single move with a sterile pipette tip (200 µl), and the *in vitro* wound model was recorded. To remove the shield protection during the scratching process, the upper medium was removed and washed with PBS. After the cytotoxicity experiment, effective substances containing boronic acid derivatives were applied at recorded doses and incubated for 24 hours at 37°C in a 5% CO_2 incubator. The negative control group was also included in the study, the created wound model was viewed on an inverted microscope (Zeiss Primovert, Germany) and

placed at hour 0 with at least two images from the well. Likewise, the samples were digitally photographed at the 12th and 24th hours to integrate the necessary programming. The captured images were analyzed using the Image J image analysis program. The entire area and wound areas of this intended program were calculated. The wound closure rate was calculated with the following formula (Equation 2):

$$\text{Wound closure rate} = [\frac{\text{Area}_{t0} - \text{Area}_{t24}}{\text{Area}_{t0}}] \times 100 \quad (2)$$

Here, Area_{t0} refers to the measured area of the photo taken at the beginning, and Area_{t24} refers to the area of the photo taken at the 12th-24th hour.

2.3. Statistical Analyses

All experiments were independently repeated three times, and the data were recorded as the mean value with standard deviation. In order to determine the significant differences among ANOVA, Tukey honest significance test (HSD) test, and single direction variance analysis. The wound closure rate between treatment groups and control groups was analyzed using the SPSS26 package (USA). All data analyses were assessed based on 0.05 and 0.01 significance.

3. Results

According to 24-hour WST-8 cytotoxicity analysis data, it was determined that both phenylboronic acid derivatives used in the study were not toxic to the cells. Table 1 and Figure 1 express the percentage viability of 2-formylphenylboronic acid on L929 cells. When the percentage viability values observed in the cells according to the concentrations studied were examined, the percentage viability rates were quite low at the concentrations of 2-formylphenylboronic acid applied between 500 and 62.5 µg/mL and were approximately 5-10%, but a significant increase in viability began to be observed at the concentration applied at 31.25 µg/mL ($p < 0.05$). This rate was found to be approximately 90.9%. In line with the data obtained at lower doses, the highest survival percentage was obtained at a concentration of 7.81 µg/mL, approximately 115%, and this concentration was chosen to be used in the wound healing study ($p < 0.05$).

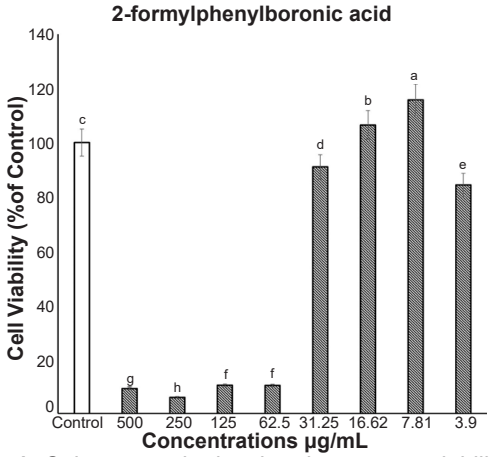

Figure 1. Column graph showing the percent viability rates as a result of applying 2-formylphenylboronic acid at concentration rates of 500-3.90 µg/mL on L929 fibroblast cells. Different lowercase letters indicate that the concentrations for each 2-formylphenylboronic acid were significantly different from each other according to Tukey's HSD test ($p < 0.05$)

Table 2 and Figure 2 express the percentage viability rates of 3-chlorophenylboronic acid on L929 cells. When the percentage viability values observed in the cells according to the concentrations studied

Table 1. Absorbance values (ABS), mean percent viability (MEAN), and percent standard deviation (STD) of viability values (24 hours) obtained as a result of applying 2-formylphenylboronic acid at concentration rates of 500-3.90 µg/mL on L929 fibroblast cells ($p < 0.05$)

Concentrations	ABS			MEAN	STD	Tukey's HSD test
500 µg/mL	0.372	0.394	0.405	9.219	1.482	g
250 µg/mL	0.360	0.366	0.354	5.942	0.529	h
125 µg/mL	0.384	0.420	0.400	10.407	1.591	f
62.5 µg/mL	0.390	0.404	0.408	10.335	0.834	f
31.25 µg/mL	1.232	1.110	1.100	90.997	6.483	d
15.62 µg/mL	1.311	1.321	1.240	106.482	3.895	b
7.81 µg/mL	1.438	1.401	1.292	115.808	6.695	a
3.90 µg/mL	1.107	1.059	1.092	84.372	2.166	e
POZ	0.531	0.507	0.528	23.443	1.153	
NEG	1.235	1.202	1.255	100	2.361	c
BLANK	0.309	0.294	0.312	0	0.851	

(*Different lowercase letters indicate that the concentrations for each 2-formylphenylboronic acid were significantly different from each other according to Tukey's HSD test.)

Table 2. Absorbance values (ABS), mean percent viability (MEAN), and percent standard deviation of viability values (24 hours) obtained as a result of applying 3-chlorophenylboronic acid at concentration rates of 500-3.90 µg/mL on L929 fibroblast cells ($p < 0.05$)

Concentrations	ABS			MEAN	STD	Tukey's HSD test
500 µg/mL	0.457	0.478	0.467	17.537	0.927	c
250 µg/mL	0.801	1.007	0.904	64.710	9.085	b, c
125 µg/mL	0.896	0.904	1.055	69.860	7.901	a, b, c
62.5 µg/mL	1.072	1.270	1.171	93.554	8.732	a, b, c
31.25 µg/mL	1.141	1.274	1.208	97.515	5.866	a, b
15.62 µg/mL	1.304	1.215	1.428	109.183	9.436	a
7.81 µg/mL	1.298	1.145	1.321	102.593	8.439	a
3.90 µg/mL	0.953	0.908	0.996	69.932	3.881	a, b, c
POZ	0.531	0.507	0.528	23.443	1.153	
NEG	1.235	1.202	1.255	100	2.361	a, b
BLANK	0.309	0.294	0.312	0	0.851	

(*Different lowercase letters indicate that the concentrations for each 2-formylphenylboronic acid were significantly different from each other according to Tukey's HSD test.)

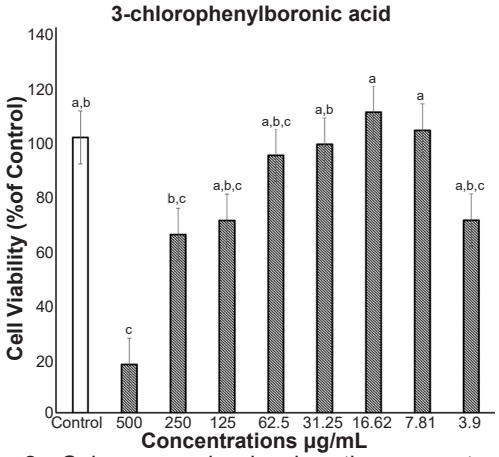

Figure 2. Column graph showing the percent viability rates as a result of applying 3-chlorophenylboronic acid at concentration rates of 500-3.90 µg/mL on L929 fibroblast cells. Different lowercase letters indicate that the concentrations for each 3-chlorophenylboronic acid were significantly different from each other according to Tukey's HSD test ($p < 0.05$)

were examined, when 3-chlorophenylboronic acid was applied at a concentration of 500 µg/mL, the percentage viability rate was quite low (17.5%), but a significant increase in viability was observed at the concentration applied at 250 µg/mL, and this rate was approximately 64% ($p < 0.05$). The concentration with a significant increase in viability was determined as 62.5 µg/mL (93%). The concentration that showed the highest cell viability at lower concentrations was 15.62 µg/mL (109%), and this concentration was chosen to be used in the wound healing study ($p < 0.05$).

In the cell stratch test, cell images obtained with an inverted microscope as a result of the 0th, 12th, and 24th hour applications of both boronic acid derivatives are presented in Figure 3, and the percent wound closure rates are presented in Figure 4. According to the data obtained, it was observed that there was a cell migration of 7.04 inches at the 0th hour, 6.81 inches at the 12th hour, and 6.55 inches at the 24th hour in the control

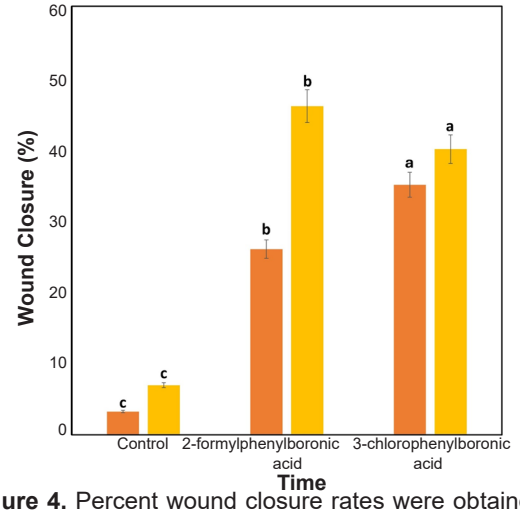

Figure 4. Percent wound closure rates were obtained as a result of 12, and 24 hour application of 2-formylphenylboronic acid (7.81 µg/mL) and 3-chlorophenylboronic acid (15.62 µg/mL) on L929 cell lines by cell stratch test. Different lowercase letters indicate that the concentrations for each 2-formylphenylboronic acid and 3-chlorophenylboronic acid were significantly different from each other according to Tukey's HSD test ($p < 0.05$)

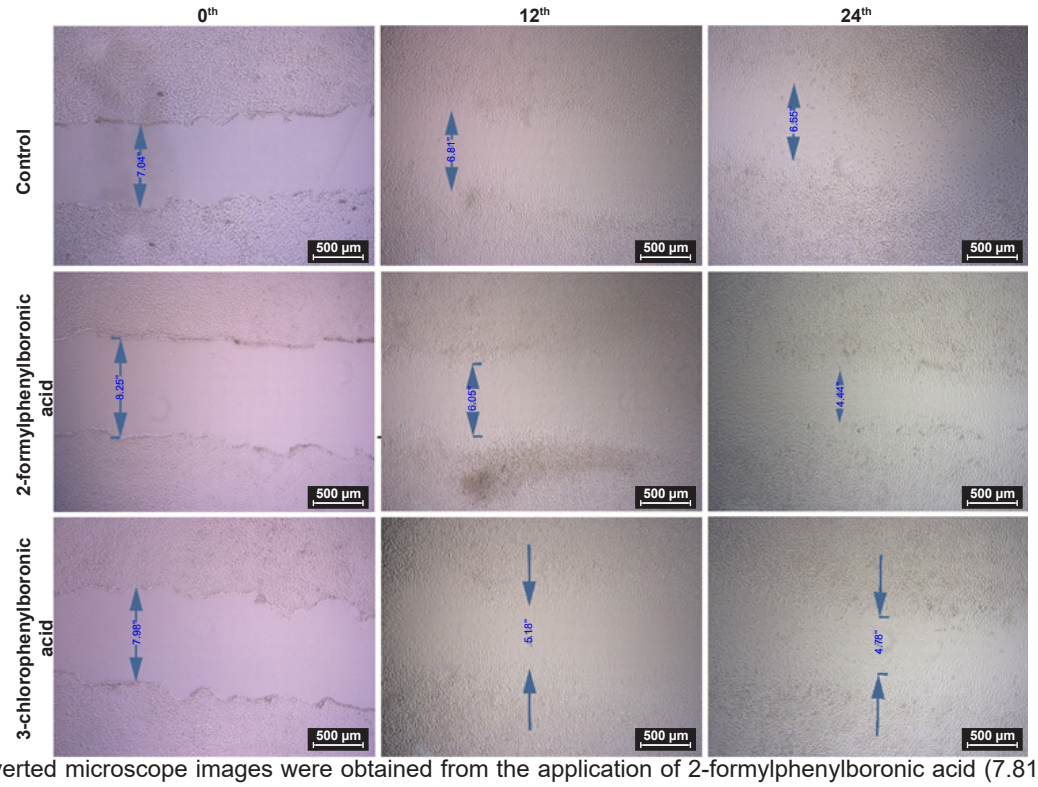

Figure 3. Inverted microscope images were obtained from the application of 2-formylphenylboronic acid (7.81 µg/mL) and 3-chlorophenylboronic acid (15.62 µg/mL) for 0, 12, and 24 hours using the cell stratch test on L929 fibroblast cell lines (Scale bar: 500 µm)

group. In the 2-formylphenylboronic acid-applied group, there was a cell migration of 8.25 inches at the 0th hour, 6.05 inches at the 12th hour, and 4.44 inches at the 24th hour, and this result was higher than the effect seen in the control. When evaluated statistically, there was a significant difference in wound healing between the control group and the group receiving 7.81 µg/mL 2-formylphenyl boronic acid in the 12 and 24 hour periods (P<0.01). In the 3-chlorophenylboronic acid-applied group, it was observed that there was a cell migration of 7.98 inches at the 0th hour, 5.18 inches at the 12th hour, and 4.76 inches at the 24th hour. This group also had a stronger effect compared to the control, but it was observed that there was a similar but slower effective cell migration to the 2-formylphenylboronic acid-applied group. When evaluated statistically, there was a significant difference in wound healing between the control group and the group receiving 15.62 µg/mL 3-chlorophenylboronic acid in the 12 and 24 hour periods (P<0.01).

In line with the data presented in Figure 4, a wound closure rate of 3.36% at the 12th hour and 6.96% at the 24th hour was achieved in the control group. In the 2-formylphenylboronic acid-applied group, there was a wound closure of 26% at the 12th hour and 46% at the 24th hour. As a result of the application of 3-chlorophenylboronic acid, a wound closure of 35% was detected at the 12th hour and 40% at the 24th hour. At the same time, with the multiple comparison test, there are significant differences between the groups, namely between the control and 2-formylphenylboronic acid, between 2-formylphenylboronic acid and 3-chlorophenylboronic acid, and between 3-chlorophenylboronic and the control group (P<0.01).

4. Discussion

Boron is absorbed into the human body in the form of boric acid and circulates. It has been reported in the literature that boric acid is protective against lung cancer, and some *in vitro* studies have reported that it reduces cell proliferation, migration, and invasion in tumors such as melanoma, prostate, breast cancer, colon cancer, and hepatocellular carcinoma [15-18]. In a previous study, the effects of boric acid on human non-small cell lung cancer cells (A549) were investigated through the TGF-β signaling pathway. The authors investigated cytotoxicity analysis with the MTT test, apoptosis test with Annexin V/PI and immunofluorescence analyses, and expression levels of TGF-β and SMAD2/3/4 genes with real-time polymerase chain reaction (RT-qPCR) and found that boric acid has both anti-proliferative and anti-proliferative properties. They also showed that it has anti-apoptotic activity [19].

Boronic acids, a group of boron compounds, are very popular with their properties, such as being stable, non-toxic, and easy to synthesize, and they can be used in many chemical and biological reactions [8]. They are of great importance due to their high reactivity and stability and are used in many areas such as sensors, receptors, polymers, drug active ingredients, cancer treatment, organic synthesis, and functionalized nanoparticles. Research on boronic acid today covers new compound classes and various application areas of these compounds. The tetrahedral boron atom geometry in boronic acid is very similar to the enzyme-catalyzed substrate tetrahedral transition state. This has enabled the biological activities of boron-containing compounds to be intensively examined [20]. Substituents in the phenylboronic acid structure greatly affect the molecular and chemical structure of the molecule, and therefore its properties [21]. It is reported in the literature that phenylboronic acid is much more potent than boric acid in targeting the metastatic and proliferative properties of cancer cells. Additionally, boronic acid and its esters are thought to have no intrinsic toxicity problems. However, it is still unknown how PBA inhibits cell growth *in vitro* and *in vivo* [22, 23]. Studies showing the potential effects of phenylboronic acid derivatives on wound healing are quite limited and detailed studies are needed. This study covers the evaluation of the *in vitro* cytotoxicity and effects of two different boronic acid derivatives (2-formylphenylboronic acid and 3-chlorophenylboronic acid) on cell migration.

Our cytotoxicity test data support that both phenylboronic acids used are not toxic to the L929 cell line, but high concentrations lead to a decrease in viability. In their study examining the cytotoxic activity of phenyl boroxine acid, Marasovic and colleagues used mouse mammary adenocarcinoma 4T1, mouse squamous cell carcinoma SCCVII, hamster lung fibroblast V79, and mouse dermal fibroblasts L929 cell lines. The cytotoxic effects on the tested tumor and non-tumor cell lines showed dose-dependent changes, among the concentrations studied (0.1, 1.0, and 10 mg/ml), a PBA dose of 10 mg/ml significantly reduced the survival of the cells compared to the control group [24]. In our study, much lower PBA concentrations were used (500-3.90 µg/ml), and the lowest viability observed concentration was determined as 500 µg/ml.

The majority of studies on the biological properties of phenylboronic acid in the literature include their antimicrobial and antifungal activities and their incorporation into various biopolymers, hydrogels or nanomaterial structures to reduce cytotoxicity [24]. PBA derivatives have the ability to transform from hydrophobic form to hydrophilic form by adjusting pH and diol concentration. This feature offers the ability to apply in many different areas, such as diabetes treatment [25]. Abid and colleagues investigated the antibacterial and wound healing effects of Quercetin-4-formyl phenylboronic acid (4FPBA−Q) against bacterial pathogens responsible for diabetic foot ulcers. 4FPBA−Q showed a significant effect on both gram-positive and gram-negative bacteria. In the experimental model, wound healing was observed to be increased after 10 days in diabetic rats [26]. Similar studies show the antimicrobial effects of

formyl phenylboronic acid and that it is beneficial for diabetic foot ulcers due to the presence of two hydroxyl groups [10]. In another study, a new boron-based compound was synthesized using PBA and quercetin, and its antioxidant, antibacterial, antiurease, anticholine esterase, antithyrosinase, and anticancer properties were investigated. This process was then tested dermatologically and biologically in an *in vivo* experiment to examine its effectiveness in cream formulation. The authors stated that the component synthesized using PBA-quercetin may have higher potential compared to the use of quercetin alone and suggested that the relevant component could be used in areas such as the food, pharmaceutical, or cosmetic industry [27].

Boron derivatives have important biological properties such as antimicrobial activity, keratinocyte migration, proliferation, vascularization, growth factor expression, and effectively accelerating the wound healing process [28]. It is also reported in the literature that boron derivatives improve extracellular matrix transformation, increase the release of proteoglycan, collagen, and proteins, which have important roles in the wound healing process, and also stimulate the synthesis of tumor necrosis factor (TNF-a) [29]. In a previous study, the effects of curcumin and PBA-linked hydrogel (GOHA-Cur) on diabetic wound healing were investigated, based on the dynamic interaction of hemoglobin and oxygen in red blood cells. *In vivo* data have shown that GOHA-Cur enhances wound healing by inhibiting inflammation [30]. Similarly, Demirci and colleagues developed a new antimicrobial carbopol-based hydrogel formulated with boron and pluronic block copolymers and examined the wound healing potential of this hydrogel on *in vitro* cell culture techniques and an experimental burn model. The authors reported that this formulation triggered wound healing through complex mechanisms by stimulating cell migration, growth factor expression, inflammatory response, and vascularization [16].

5. Conclusion

As a result, 2-formylphenylboronic acid and 3-chlorophenylboronic acid used in our study showed dose-dependent effects on L929 fibroblast cells and had a non-toxic effect unless very high concentrations were used. In fact, it has been observed that proliferation increases significantly at certain concentrations. In addition, according to the cell migration test results, which allow us to obtain rapid and preliminary information about the wound-closing feature, the effects of both PBA derivatives in terms of cell migration increased over time. In particular, the effect of 2-formylphenylboronic acid at the 24th hour was significantly increased compared to its effect at the 12th hour ($P<0.01$). The multiple comparison test showed that, there are significant differences between the groups, namely between the control and 2-formylphenylboronic acid, between 2-formylphenylboronic acid and 3-chlorophenylboronic acid, and between 3-chlorophenylboronic and the control group ($P<0.01$). The effect of 3-chlorophenylboronic acid also increased in a time-dependent manner ($P<0.01$), but the difference between the 12th and 24th hours was less than that observed in the 2-formylphenylboronic acid group. Our data support the concentration-dependent wound healing effects of both PBA derivatives. 2-formylphenylboronic acid exhibited more effective results in terms of cell migration, especially at the 24th hour, compared to 3-chlorophenylboronic acid. However, the concentration dose used here is extremely important, and if this dose is not taken into account, 2-formylphenylboronic acid may have a more toxic effect. Considering that boron is the most important strategic mineral of our country, the wound healing potential of boronic acid derivatives 2-formylphenylboronic acid and 3-chlorophenylboronic acid should be supported by detailed *in vitro* and *in vivo* studies. The data obtained may provide insight into the use of these components in the production of wound creams or dressings, but the possible toxic effects of high concentrations should also be carefully considered in the evaluation.

6. Acknowledgments

This work was studied at Eskisehir Osmangazi University Central Research Laboratory Application and Research Center (ARUM).

7. Authors' Contributions

Betül Yılmaz Öztürk: Conceptualization, data curation, formal analysis; methodology, writing-original draft, visualization, investigation, supervision, software, validation.

Bükay Yenice Gürsu: Writing-review and editing, supervision, project administration, formal analysis.

İlknur Dağ: Writing-original draft, conceptualization, formal analysis, methodology, supervision, writing-review and editing, resources.

References

[1]. Türkez, H., Yıldırım, Ö. Ç., Öner, S., Kadı, A., Mete, A., Arslan, M. E., ... & Mardinoğlu, A. (2022). Lipoic acid conjµgated boron hybrids enhance wound healing and antimicrobial processes. *Pharmaceutics*, *15*(1), 149. https://doi.org/10.3390/pharmaceutics15010149

[2] Lungu, R., Anisiei, A., Rosca, I., Sandu, A. I., Ailincai, D., & Marin, L. (2021). Double functionalization of chitosan based nanofibers towards biomaterials for wound healing. *Reactive and Functional Polymers*, *167*, 105028. https://doi.org/10.1016/j.reactfunctpolym.2021.105028

[3] Chebassier, N., Ouijja, E. H., Viegas, I., & Dreno, B. (2004). Stimulatory effect of boron and manganese salts on keratinocyte migration. *Acta Dermato-Venereologica*, *84*(3), 191-194 https://doi.org/10.1080/00015550410025273

[4] Demirci, S., Doğan, A., Karakuş, E., Halıcı, Z., Topçu, A., Demirci, E., & Sahin, F. (2015). Boron and poloxamer (F68 and F127) containing hydrogel formulation for burn wound healing. *Biological Trace Element Research*, *168*, 169-180. https://doi.org/10.1007/s12011-015-0338-z

[5] Hall, D. G. (2005). Structure, properties, and preparation of boronic acid derivatives. Overview of their reactions and applications. In D. G. Hall (Eds.), *Boronic acids: Preparation and applications in organic synthesis and medicine* (pp. 1-99). John Wiley & Sons. https://doi.org/10.1002/3527606548

[6] Jeelani, A., Muthu, S., Raajaraman, B. R., & Sevvanthi, S. (2020). Spectroscopic, quantum chemical calculations, and molecular docking analysis of 3-Chlorophenyl boronic acid. *Spectroscopy Letters*, *53*(10), 778-792. https://doi.org/10.1080/00387010.2020.1834410

[7] Trippier, P. C., & McGuigan, C. (2010). Boronic acids in medicinal chemistry: Anticancer, antibacterial and antiviral applications. *MedChemComm*, *1*(3), 183-198. https://doi.org/10.1039/C0MD00119H

[8] Bayraktutan, Z. (2022). 4 hidroksi fenilboronik asidin lipopolisakkarit ile indüklenmiş karaciğer hasarı üzerine muhtemel koruyucu etkilerinin incelenmesi. *Journal of Boron*, *7*(1), 430-439. https://doi.org/10.30728/boron.1057322

[9] Lu, C., Li, H., Wang, H., & Liu, Z. (2013). Probing the interactions between boronic acids and cis-diol-containing biomolecules by affinity capillary electrophoresis. *Analytical Chemistry*, *85*(4), 2361-2369. https://doi.org/10.1021/ac3033917

[10] Yang, P., Bam, M., Pageni, P., Zhu, T., Chen, Y. P., Nagarkatti, M., ... & Tang, C. (2017). Trio act of boronolectin with antibiotic-metal complexed macromolecules toward broad-spectrum antimicrobial efficacy. *ACS Infectious Diseases*, *3*(11), 845-853. https://doi.org/10.1021/acsinfecdis.7b00132

[11] Gozdalik, J. T., Adamczyk-Woźniak, A., & Sporzyński, A. (2018). Influence of fluorine substituents on the properties of phenylboronic compounds. *Pure and Applied Chemistry*, *90*(4), 677-702. https://doi.org/10.1515/pac-2017-1009

[12] Adamczyk-Woźniak, A., Gozdalik, J. T., Wieczorek, D., Madura, I. D., Kaczorowska, E., Brzezińska, E., ... & Lipok, J. (2020). Synthesis, properties and antimicrobial activity of 5-trifluoromethyl-2-formylphenylboronic acid. *Molecules*, *25*(4), 799. https://doi.org/10.3390/molecules25040799

[13] Borys, K. M., Wieczorek, D., Pecura, K., Lipok, J., & Adamczyk-Woźniak, A. (2019). Antifungal activity and tautomeric cyclization equilibria of formylphenylboronic acids. *Bioorganic Chemistry*, *91*, 103081. https://doi.org/10.1016/j.bioorg.2019.103081

[14] Ailincai, D., Cibotaru, S., Anisiei, A., Coman, C. G., Pasca, A. S., Rosca, I., ... & Marin, L. (2023). Mesoporous chitosan nanofibers loaded with norfloxacin and coated with phenylboronic acid perform as bioabsorbable active dressings to accelerate the healing of burn wounds. *Carbohydrate Polymers*, *318*, 121135. https://doi.org/10.1016/j.carbpol.2023.121135

[15] Miao, S., Ge, Y., Yi, Z., & Feng, Q. (2020). Screening of aptamer for breast cancer biomarker calreticulin and its application to detection of serum and recognition of breast cancer cell. *Chinese Journal of Analytical Chemistry*, *48*(5), 642-649. https://doi.org/10.1016/S1872-2040(20)60020-2

[16] Simsek, F., Inan, S., & Korkmaz, M. (2019). An *in vitro* study in which new boron derivatives maybe an option for breast cancer treatment. *Eurasian Journal of Medicine and Oncology*, *3*(1), 22–27. https://doi.org/10.14744/ejmo.2018.0020

[17] Kahraman, E., & Göker, E. (2022). Boric acid exert anti-cancer effect in poorly differentiated hepatocellular carcinoma cells via inhibition of AKT signaling pathway. *Journal of Trace Elements in Medicine and Biology*, *73*, 127043. https://doi.org/10.1016/j.jtemb.2022.127043

[18] Sevimli, M., Bayram, D., Özgöçmen, M., Armağan, I., & Sevimli, T. S. (2022). Boric acid suppresses cell proliferation by TNF signaling pathway mediated apoptosis in SW-480 human colon cancer line. *Journal of Trace Elements in Medicine and Biology*, *71*, 126958. https://doi.org/10.1016/j.jtemb.2022.126958

[19] Sevimli, T. S., Ghorbani, A., & Sevimli, M. (2023) Investigation of the anti-proliferative and anti-apoptotic effects of boric acid on human non-small cell lung cancer cells through the tgf-β signaling pathway. *Journal of Adnan Menderes University Health Sciences Faculty*, *7*(3), 553-564. https://doi.org/10.46237/amusbfd.1287877

[20] Psurski, M., Łupicka-Słowik, A., Adamczyk-Woźniak, A., Wietrzyk, J., & Sporzyński, A. (2019). Discovering simple phenylboronic acid and benzoxaborole derivatives for experimental oncology–phase cycle-specific inducers of apoptosis in A2780 ovarian cancer cells. *Investigational New Drugs*, *37*(1), 35-46. https://doi.org/10.1007/s10637-018-0611-z

[21] Kowalska, K., Adamczyk-Woźniak, A., Gajowiec, P., Gierczyk, B., Kaczorowska, E., Popenda, Ł., ... & Sporzyński, A. (2016). Fluoro-substituted 2-formylphenylboronic acids: Structures, properties and tautomeric equilibria. *Journal of Fluorine Chemistry*, *187*, 1-8. https://doi.org/10.1016/j.jfluchem.2016.05.001

[22] Cebeci, E., Yüksel, B., & Şahin, F. (2022). Anti-cancer effect of boron derivatives on small-cell lung cancer. *Journal of Trace Elements in Medicine and Biology*, *70*, 126923. https://doi.org/10.1016/j.jtemb.2022.126923

[23] Marasovic, M., Ivankovic, S., Stojkovic, R., Djermic, D., Galic, B., & Milos, M. (2017). *In vitro* and *in vivo* antitumour effects of phenylboronic acid against mouse mammary adenocarcinoma 4T1 and squamous carcinoma SCCVII cells. *Journal of Enzyme Inhibition and Medicinal Chemistry*, *32*(1), 1299-1304. https://doi.org/10.1080/14756366.2017.1384823

[24] Wang, R., Tian, Y., Wang, J., Song, W., Cong, Y., Wei, X., ... & Chen, Y. M. (2021). Biomimetic glucose trigger-insulin release system based on hydrogel loading bidentate β-cyclodextrin. *Advanced Functional Materials*, *31*(38), 2104488. https://doi.org/10.1002/adfm.202104488

[25] Wang, Q., Wang, H., Chen, Q., Guan, Y., & Zhang, Y. (2020). Glucose-triggered micellization of poly (ethylene glycol)-b-poly (N-isopropylacrylamide-co-2-(acrylamido)

phenylboronic acid) block copolymer. *ACS Applied Polymer Materials*, *2*(9), 3966-3976. https://doi.org/10.1021/acsapm.0c00635

[26] Abid, H. M. U., Hanif, M., Mahmood, K., Aziz, M., Abbas, G., & Latif, H. (2022). Wound-healing and antibacterial activity of the quercetin–4-formyl phenyl boronic acid complex against bacterial pathogens of diabetic foot ulcer. *ACS Omega*, *7*(28), 24415-24422. https://doi.org/10.1021/acsomega.2c01819

[27] Temel, H., Atlan, M., Ertas, A., Yener, I., Akdeniz, M., Yazan, Z., ... & Akyuz, E. (2022). Cream production and biological *in vivo*/*in vitro* activity assessment of a novel boron-based compound derived from quercetin and phenyl boronic acid. *Journal of Trace Elements in Medicine and Biology*, *74*, 127073. https://doi.org/10.1016/j.jtemb.2022.127073

[28] Beyranvand, S., Pourghobadi, Z., Sattari, S., Soleymani, K., Donskyi, I., Gharabaghi, M., ... & Adeli, M. (2020). Boronic acid functionalized graphene platforms for diabetic wound healing. *Carbon*, *158*, 327-336. https://doi.org/10.1016/j.carbon.2019.10.077

[29] Routray, I., & Ali, S. (2016). Boron induces lymphocyte proliferation and modulates the priming effects of lipopolysaccharide on macrophages. *PLOS ONE*, *11*(3), e0150607. https://doi.org/10.1371/journal.pone.0150607

[30] Zhao, B., Zhu, S., Liu, Y., Zhu, J., Luo, H., Li, M., ... & Cao, X. (2023). Enriching and smart releasing curcumin via phenylboronic acid-anchored bioinspired hydrogel for diabetic wound healing. *Advanced NanoBiomed Research*, *3*(5), 2200177. https://doi.org/10.1002/anbr.202200177

YAZAR KILAVUZU

GENEL BİLGİLER

• Makale başvurusu için Makale Metni Dosyası, Telif Hakkı Devir Dosyası ve Benzerlik Oran Dosyası olmak üzere üç ayrı formun doldurulması ve sisteme yüklenmesi gerekmektedir.
• Başvurularda iletişimde bulunulacak yazar ve diğer yazarların iletişim bilgileri bulunmalıdır.
• Makale metni içerisindeki makale kontrol listesi ve kapak sayfası eksiksiz olarak doldurulmalıdır.
• Makale metni dosyası içerisinde bulunan makale kontrol listesi ve kapak sayfası eksiksiz doldurulmalıdır.
• Derleme makalelerde başka yayınlara ait şekil ve tablolar kullanılacaksa, kaynak gösterilecek makalenin yayıncısından izin alınmalıdır. Yayıncıdan izin alındığı ve şekillerin uyarlanıp uyarlanmadığı veya doğrudan kullanılıp kullanılmadığı bilgisi şekil başlığında belirtilmelidir. İlgili izin yazısının journalofboron@tenmak.gov.tr adresine gönderilmesi gerekmektedir.
• Her makale, konusu ile ilgili en az iki hakeme gönderilerek şekil, içerik, özgün değer, uluslararası literatüre katkısı bakımından incelettirilir. Hakem görüşlerinde belirtilen eksikler tamamlandıktan sonra, son baskı formatına getirilir ve yazarlardan makalenin son halinin onayı alınır. Dergide basıldığı haliyle makale içinde bulunabilecek hataların sorumluluğu yazarlara aittir.

MAKALE METNİ DOSYASI

• Makale metninin yazımında yazım kurallarına uyulması gerekmektedir.
• Makale metninde kapsayıcı ve bilimsel bir dil kullanılmalıdır.
• Makale metni referanslar dahil araştırma makaleleri için 14.000 kelimeyi tarama makaleleri için ise 22.000 kelimeyi geçmemelidir.
• Makalenin metni, Times New Roman 12 punto ile Makale Metni Dosyası'nın sayfa düzeni değiştirilmeden yazılmalıdır.
• Makale metninin Microsoft Office Word 2010 ve üzeri bir kelime işlemci ile hazırlanması ve yazım hatalarının kontrol edilmesi ve düzeltilmesi gerekmektedir.
• Eğer makale Türkçe ise, Türkçe başlıklarla bire bir uyumlu olacak şekilde oluşturulmuş İngilizce başlıklar parantez içerisinde yazılmalıdır.
• Makale içerisinde kullanılan kısaltma ve sembollerin anlamları ilk kullanıldıklarında açıklanmalıdır.
• Makale metni içerisindeki alt başlıklar numaralandırılmalıdır. Numaralandırma işlemleri ana bölümler için 1.'den başlamalı ve tüm ana başlıklar (Özet, Teşekkür ve Kaynaklar ve Ekler bölümleri hariç) için devam etmelidir. İkincil başlıklar ana bölüm numaralandırmasına uygun olarak 1.1., 1.2., 1.3., ... şeklinde devam etmelidir. Üçüncü başlıklar ikinci başlıklara uygun olarak 1.1.1., 1.1.2., 1.1.3., ... şeklinde devam etmelidir.

TELİF HAKKI DEVİR DOSYASI

• İmzalı Telif Hakkı Devir Dosyası taranarak sisteme yüklenmelidir.
• İmzalı Telif Hakkı Devir Dosyası'nı göndermeyen yazarların başvuruları değerlendirmeye alınmaz.

BENZERLİK ORAN DOSYASI

• Makalenin referanslar bölümü hariç metni "iThenticate" veya "Turnitin" programları ile taranmalıdır.
• Benzerlik oranı raporunun PDF formatında sisteme yüklenmelidir.
• Benzerlik oranı %15'in üzerinde olmamalıdır.

GİZLİLİK POLİTİKASI

Journal of Boron gizliliğe saygı duymaktadır. Kişisel bilgiler, sadece derginin belirtilen amaçları doğrultusunda kullanılacak ve üçüncü kişilerle paylaşılmayacaktır.

YAZIM KURALLARI

MAKALE BAŞLIĞI
• Makale başlığı standart kısaltmalarla birlikte en çok 15 kelimeden oluşmalıdır.
• Eğer makale Türkçe ise, İngilizce başlıkla bire bir uyumlu olacak şekilde Türkçe makale başlığı da oluşturulmalıdır.

ÖZET
• Özet, 250 kelimeyi geçmemelidir.
• Standart olmayan kısaltmalar ilk kullanıldığında tam açıklamalarından sonra parantez içerisinde yazılmalıdır.
• Eğer makale Türkçe ise, İngilizce özetle bire bir uyumlu olacak şekilde Türkçe özet de oluşturulmalıdır.

ANAHTAR KELİMELER
• En fazla 5 anahtar kelime, alfabetik sıraya göre yazılmalıdır.
• Kısaltmalar anahtar kelime olarak kullanılmamalıdır.
• Eğer makale Türkçe ise, İngilizce anahtar kelimelerle bire bir uyumlu olacak şekilde Türkçe anahtar kelimelere de oluşturulmalıdır.

GİRİŞ
• İlgili literatürün özeti, çalışmanın amacı ve özgün değeri ve kurulmuş olan hipotezi içermelidir.
• Kaynaklar, toplu olarak ve aralıklı verilmemeli (örnek [1-5] veya [1, 2, 3, 5, 8]), her kaynağın çalışmaya katkısı irdelenmeli ve metin içerisinde belirtilmelidir.

MALZEMELER VE YÖNTEMLER
• Yürütülmüş olan çalışma deneysel bir çalışma ise deney prosedürü/metodu anlaşılır bir şekilde açıklanmalıdır.
• Teorik bir çalışma yürütülmüşse teorik metodu detaylı bir şekilde verilmelidir.
• Yapılan çalışmada kullanılan metot daha önce yayınlanmış bir metot ise diğer çalışmaya atıf yapılarak bu çalışmanın diğer çalışmadan farklı belirtilmelidir.

SONUÇLAR VE TARTIŞMA
• Elde edilen sonuçlar açık ve öz bir şekilde verilmelidir.
• Elde edilen tüm sonuçlar atıf yapılarak literatür ile karşılaştırılmalıdır.
• Tablolar numaralandırılmalıdır ve düzenlenebilir formatta olmalıdır. Eğer makale Türkçe ise, tablo üst yazılarının bire bir İngilizce çevirileri parantez içerisinde verilmelidir.
• Makale içerisindeki şekiller numaralandırılmalıdır ve en az 300 dpi çözünürlükte olmalıdır. Şekillerin üzerindeki yazılar okunabilir büyüklükte ve yazı tipinde olmalıdır. Kabul edilen şekil formatları TIFF, JPG ve JPEG'dir. Eğer makale Türkçe ise, şekil alt yazılarının bire bir İngilizce çevirileri parantez içerisinde verilmelidir.

SONUÇLAR
• Çalışmadan elde edilen ana sonuçlar ve çıkarımlar kısa ve öz bir şekilde verilmelidir.
• Çalışmaya ait gelecek perspektifleri bu bölümde verilir.

TEŞEKKÜRLER
• Çalışmanın gerçekleşmesi için sağlanan maddi kaynaklar ve kullanılan altyapı bu bölümde belirtilir.
Yazar Katkıları
• Her yazarın katkıları belirtilmelidir.
• Katkı rolleri şu şekildedir: kavramsallaştırma, veri analizi, veri iyileştirme, finansman sağlama, metodoloji, proje yönetimi, kaynak sağlama, yazılım analizi, denetim, doğrulama, görselleştirme, orijinal taslak yazma, inceleme yazma ve düzenleme.

YAZAR KATKILARI
• Her yazarın katkısı belirtilmelidir.
• Katkı rolleri şu şekildedir: kavramsallaştırma, veri analizi, veri iyileştirme, finansman sağlama, metodoloji, proje yönetimi, kaynak bulma, yazılım analizi, denetim, doğrulama, görselleştirme, orijinal taslak yazma, yazı inceleme ve düzenleme.

KAYNAKLAR
• Basılmış kaynakların DOI ve ISBN numarası belirtilmelidir.
• İnternet sitesi adresleri (URL) kaynak olarak verilmemelidir. Ancak metin içerisinde istatistiksel bir verinin geçtiği yerde veriden sonra belirtilebilir.
• Kaynaklar listesi metin içerisinden kullanılma sırasına uygun olarak numaralandırılmalıdır.
• Kaynaklar, "APA Publication Manual, Seventh Edition" kurallarına uygun olarak hazırlanmalıdır.
• Kaynaklar İngilizce olarak hazırlanmalıdır. Türkçe kaynakların İngilizce karşılıkları köşeli parantez içerisinde belirtilmelidir.
• APA formatı ve örneklere aşağıdaki bağlantıdan ulaşılabilir.
https://apastyle.apa.org/style-grammar-guidelines/references/examples

EKLER
• Makaledeki ekler EK A (Appendix A), EK B (Appendix B) ve EK C (Appendix C) vb. olarak adlandırılmalıdır.
• Ekler içerisindeki denklemler A1, A2, A3 vb. olarak adlandırılmalıdır, tablo ve şekiller Tablo A1, Tablo A2, Şekil A1, Şekil A2 vb. olarak adlandırılmalıdır.

AUTHOR'S GUIDE

GENERAL INFORMATION

• For article application, 3 individual files which are Manuscript File, Copyright Transfer File and Similarity Ratio File, must be filled in and uploaded to the system.
• Applications should include the contact information of the author and other authors to be contacted.
• The article checklist and cover page in the Manuscript File should be filled in completely.
• Each article is sent to at least two referees related to its subject and examined in terms of format, content, novelty, contribution to literature.
• If figures and tables from other publications are to be used in review articles, permission must be obtained from the publisher of the article to be cited. The information that permission has been granted from the publisher and whether the figures have been adapted or used directly should be mentioned in the figure caption. The relevant permission letter should be sent to journalofboron@tenmak.gov.tr.
• After the deficiencies stated in the referee's comments are completed, it is brought to the final print format and the approval of the final version of the article is obtained from the authors. The responsibility of errors that may be found in the article as it is published in the journal belongs to the authors.

MANUSCRIPT

• Writing rules must be followed, during writing of the manuscript.
• Inclusive and scientific language must be used in the manuscript.
• Manuscript should not exceed 14,000 words for research articles and 22,000 words for review articles, including references.
• The manuscript should be written in Times New Roman 12 points without changing the page layout of the Manuscript File.
• The manuscript should be prepared with a word processor of Microsoft Office Word 2010 and above, and spelling errors should be checked and corrected.
• Abbreviations and symbols used in the manuscript must be explained when used fort he first time.
• Subheadings in the article should be numbered. Numbering should start at 1 for the main section and continue for all main headings (except the Summary, Acknowledgments and References and Appendices sections). Secondary titles continue as 1.1., 1.2., 1.3., ... in accordance with the main chapter numbering. The third headings continue as 1.1.1., 1.1.2., 1.1.3., ... in accordance with the second headings.

COPYRIGHT TRANSFER FILE

• Signed Copyright Transfer File should be scanned and uploaded to the system.
• Applications of the authors who do not send the signed Copyright Transfer File will not be evaluated.

SIMILARITY RATIO FILE

• The manuscript should be scanned with "iThenticate" or "Turnitin" programs, except for the references section.
• The similarity ratio report should be uploaded to the system in PDF format.
• The similarity ratio should not exceed 15%.

PRIVACY POLICY

Journal of Boron respects privacy. Any personal information will only be used in line with the stated purposes of the journal and will not be shared with third parties.

WRITING RULES

TITLE
• The title of the manuscript should consist of a maximum of 15 words with standard abbreviations.

ABSTRACT
• The abstract should not exceed 250 words.
• Non-standard abbreviations should be written in parentheses after their full explanation, when they are used for the first time.

KEYWORDS
• A maximum of 5 keywords should be written in alphabetical order.
• Abbreviations should not be used as keywords.

INTRODUCTION
• The summary of the relevant literature, aim and novelty of the study, and the established hypothesis should be included.
• References should not be given in bulk and in intervals (example [1-5] or [1, 2, 3, 5, 8]), the contribution of each source to the study should be examined and stated in the text.

MATERIALS AND METHODS
• If the study carried out is an experimental study, the test procedure/method should be clearly explained.
• If a theoretical study has been carried out, the theoretical method should be given in detail.
• If the method used in the study is a previously published method, the other study should be mentioned by citing.

RESULTS AND DISCUSSION
• Obtained results should be given in a clear and concise manner.
• All of the results should be compared with the literature by citing.
• Tables should be numbered and in editable format.
• Figures in the manuscript should be numbered and have at least 300 dpi resolution. The texts on the figures should be in legible size and font. Accepted figure formats are TIFF, JPG, and JPEG.

CONCLUSIONS
• Main conclusions and inferences obtained from the study should be given concisely.
• Future perspectives of the study are given in this section.

ACKNOWLEDGEMENTS
• The financial resources provided and the infrastructure used during the study are specified in this section.

AUTHOR CONTRIBUTIONS
• Contributions of each author must be stated.
• Contribution roles are as follows: conceptualization, data analysis, data curation, funding acquisition, methodology, project administration, sourcing, software analysis, supervision, validation, visualization, writing original draft, writing review and editing.

REFERENCES
• DOI and ISBN numbers of printed sources should be specified.
• Website addresses (URLs) should not be given as a source. However, it can be specified after the data where a statistical data is mentioned in the text.
• The list of references should be numbered according to the order in which they are used in the text.
• References should be prepared in accordance with the rules of “APA Publication Manual, Seventh Edition”.
• References should be prepared in English. English equivalents of sources should be indicated in square brackets.
• APA format and examples can be found at the link below.
https://apastyle.apa.org/style-grammar-guidelines/references/examples

APPENDICES
• Appendices in the manuscript must be named as Appendix A (Appendix A), Appendix B (Appendix B) and Appendix C (Appendix C) etc.
• Equations in the appendices must be named as A1, A2, A3, etc., and table and figures numberings must be named as Table A1, Table A2, Figure A1, Figure A2 etc.

TENMAK BOREN BOR ARAŞTIRMA ENSTİTÜSÜ

BOR DERGİSİ

JOURNAL OF BORON

https://dergipark.org.tr/boron

İÇİNDEKİLER/CONTENTS

TENMAK Bor Araştırma Enstitüsü

Dumlupınar Bulvarı (Eskişehir Yolu 7. km), No:166, D Blok, 06530, Ankara
Tel: (0312) 201 36 00
Faks: (0312) 219 80 55
e-mail: boren.journal@tenmak.gov.tr
web:https://dergipark.org.tr/boron